Membrane fusion studies with solid state NMR : a new structural perspective on the interplay between biomimetic lipids and De Novo designed synthetic peptides

Agrawal, P.R.

Membrane Fusion Studies with Solid State NMR

A New Structural Perspective on the Interplay Between Biomimetic Lipids and *De Novo* Designed Synthetic Peptides

PROEFSCHRIFT

ter verkrijging van
de graad van Doctor aan de Universiteit Leiden,
op gezag van de Rector Magnificus Prof. Dr. P. F. van der Heijden,
volgens besluit van het College voor Promoties
te verdedigen op donderdag 1 maart 2007
klokke 13.45 uur

door

Prashant Radheshyam Agrawal

geboren te 5 september 1978

in Dhamangaon (Rly), India

Promotiecommissie

Promotor:	Prof. dr. H. J. M. de Groot
Co-promotor:	Dr. F. B. Hulsbergen
Referent:	Prof. dr. A. Killian, Utrecht University
Overige leden:	Prof. dr. J. Brouwer
	Prof. dr. Ir. J. Fraaije
	Dr. Ing. M. Overhand

To Bhawana and my Parents

Contents

Chapter 1

General Introduction

Chapter 2

Solid phase synthesis and purification of a set of uniformly ^{13}C, ^{15}N labeled *de novo* designed membrane fusogenic peptides.

Chapter 3

Solid State NMR Investigation of the Interaction between Biomimetic Lipid Bilayers and a de novo Designed Fusogenic Peptide.

Chapter 4

Contrasting biomimetic lipids rearrangements induced by low-complexity peptides involved in membrane fusion: extended cylindrical curvature regions versus toroidal pore signals.

Chapter 5

^{13}C and ^{15}N NMR of uniformly labeled fusogenic peptides incorporated in a biomimetic membrane: Additional support for the peripheral intercalation model and future outlook.

1

General introduction

Fusion allows cells to exchange contents. In order to maintain the individuality of each of the intracellular compartments and of the cell itself, membranes do not fuse easily under normal circumstances. Membrane fusion implies that two phospholipid bilayers are merging in an aqueous environment. Prior to fusion, the participating membranes are separate and more than 1000 Å from each other. The fusion process requires the action of specific proteins and their transmembrane fusion peptide segments, which trigger the lipid rearrangements. Upon activation, these peptides undergo spontaneous conformational changes and engage in mutual interactions in response to fusogenic conditions.[1] During fusion, aqueous fusion pores are formed that connect the compartments on the distal sides of the merging membranes. Formation of these fusion pores requires non-bilayer transition states of the fusing membranes. The repulsion between two opposing phospholipid membranes in an aqueous environment is very strong at atomic distances (100–200 Å). These forces need to be overcome in order to reach the meta-stable transition state that leads to fusion. The exact nature of the intermediate state and the involved molecular arrangements, in fusion mechanisms, is not yet understood.

1.1 Membrane fusion

In particular two classes of fusion processes have been investigated in detail, the synaptic membrane fusion involving the transmembrane segments and the peripheral interaction of the viral fusion. Both processes require action of specific proteins or peptides and are thought to proceed via the formation of stalks, hourglass-shaped intermediates, in which the proximal leaflets of the fusing membranes are merged (Fig. 1.1). Expansion of the stalk is believed to result in a hemifusion diaphragm where the contacting outer monolayers mix over an extended area while the distal monolayers stay intact, thus preserving the separation of both aqueous compartments before a fusion pore forms. However, the initiation of the two processes is different. Synaptic membrane fusion is preceded by Ca^{2+} influx while viral fusion is triggered by a change of the intracellular pH.

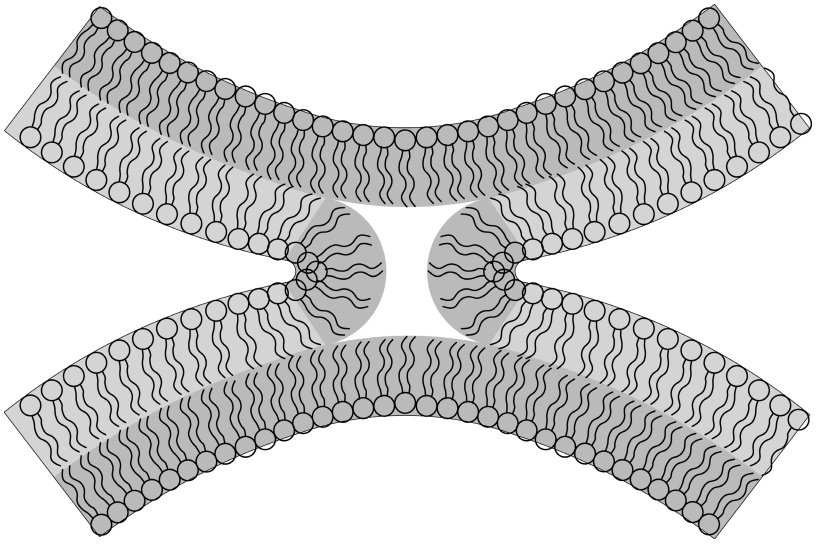

Figure 1.1: Lipid topology in stalk intermediates. *The schematic depicts hypothetical lipid arrangements in a stalk that is thought to be on-the pathway of the membrane fusion. The hourglass shaped stalk intermediate has negative curvature at the contact point of the two bilayers and this leads to the hemifusion diaphragm. Dark gray represents regions of negative curvature, while light grey corresponds to regions of positive curvature*

1.1.1 Synaptic membrane fusion

Among hundreds of activities happening in the mind, the most important are the signal transduction or neurotransmission processes. The power of the brain is based upon the extraordinary ability of nerve cells to communicate with each other at specialized intercellular junctions called synapses.[2] Signal transduction at the cellular level refers to the movement of signal molecules from outside the cell to inside or *vice versa*. In the nervous system, the information is transferred from one cell to another by the secretion of neurotransmitters at synapses. Prior to secretion, neurotransmitters are stored in synaptic vesicles, organelles that are found in large numbers in the nerve terminals. In resting nerve terminals, a subpopulation of synaptic vesicles containing neurotransmitters is stably docked at the active zone of the synapse (Fig. 1.2).[3] Under physiological conditions, synaptic vesicles docked at the active zone undergo membrane fusion, followed by neurotransmitter release. Synaptic membrane fusion involves the merger of two phospholipid bilayers in an aqueous environment. Such intracellular membrane fusion reactions are complex supramolecular events and involve various transition states. While the distal leaflets are still separate, fusion stalks can be formed, followed by the reversible opening of small aqueous fusion pores.

Each of the billions of synapses in a mammalian brain can release neurotransmitters. Although there is a broad spectrum of synapses, all share fundamental structural features that are responsible for specific functions. As transmission at synapses is highly modifiable, the architecture of synapses must also be very dynamic. Synaptic vesicle sizes vary and depend strongly on the type of the neurotransmitter.[2] Generally, vesicles containing fast-acting neurotransmitters are approximately 50 nm in diameter and appear to have clear centers. A second class of synaptic vesicles, which contain slower-acting transmitters and protein material, are usually larger in diameter, up to several hundred nanometers, and they have an electron-dense core.[2]

Synaptic fusion involves several protein families including SNAREs, Rab

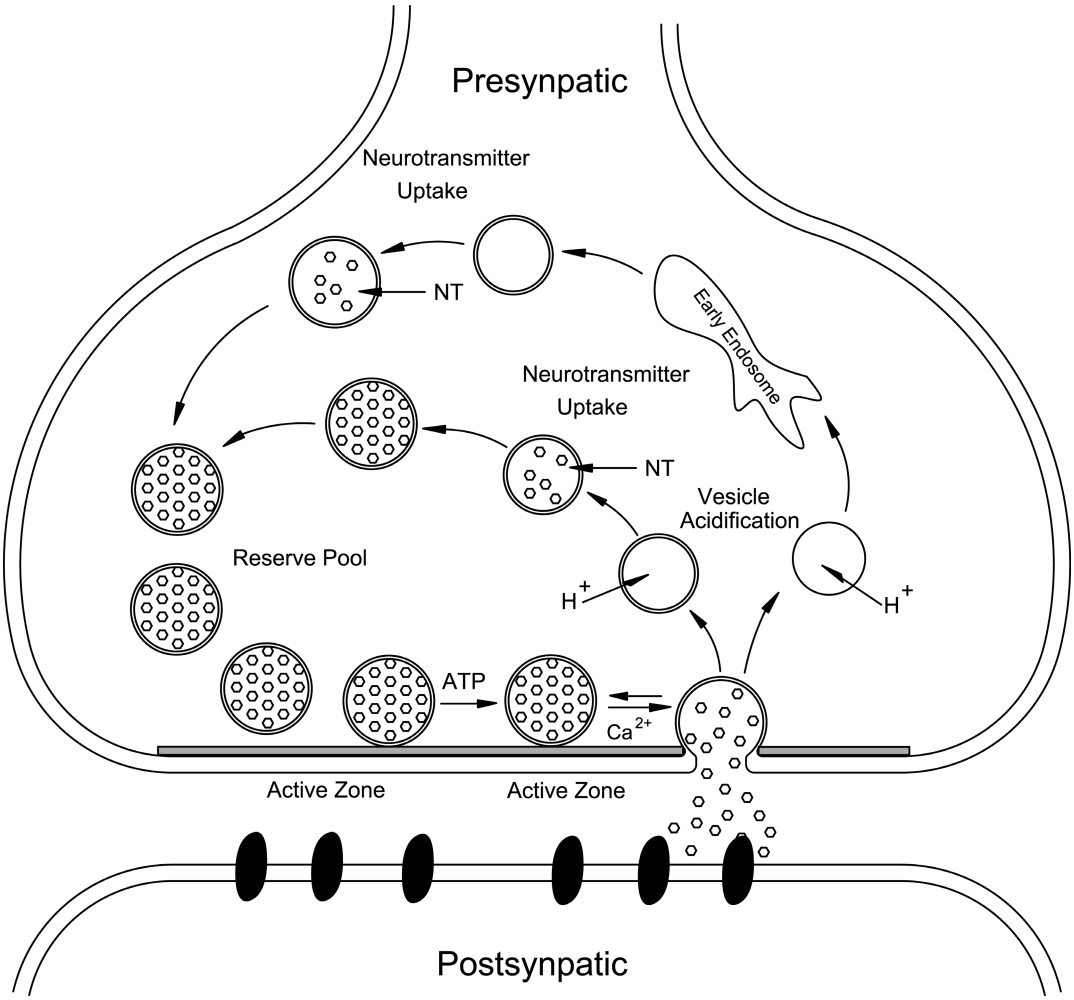

Figure 1.2: ***The synaptic vesicle cycle.*** *Synaptic vesicles are filled with neurotransmitters by active transport and form the vesicle clusters that represent the reserve pool. Filled vesicles dock at the active zone, where they undergo a priming reaction that makes them competent for Ca^{2+} triggered fusion-pore opening. After fusion-pore opening, synaptic vesicles undergo endocytosis and recycle via several routes: local reuse fast recycling without an endosomal intermediate, or clathrin-mediated endocytosis with recycling via endosomes. (Adapted from reference [3])*

proteins, and SM-proteins. SNAREs form a novel superfamily of small and mostly membrane-anchored proteins that share a common motif of about 60 amino-acid residues. SNAREs reversibly assemble into tightly packed helical bundles, the core complexes. Assembly is thought to pull the fusing membranes closely together, thus inducing fusion.

It was postulated that fusion proteins without transmembrane domains (TMD) are not able to catalyze the mixture of the distal lipid monolayers.[4] In contrast, TMD peptides alone are sufficient to drive fusion of liposomes, suggesting that they constitute autonomous fusogenic domains.[5] In the last decade, research on membrane fusion has been extensive, but it has not yet led to a coherent molecular picture. A central issue in neurobiology concerns the mechanism of membrane fusion, which is not only relevant for understanding vesicular trafficking but also for the concept of higher brain functions such as learning and memory.

1.1.2 Viral membrane fusion

During infection, the viral membrane fuses with the host cell membrane, thereby injecting the nucleocapsid into the cytoplasm. Some viruses, for example, influenza virus (HA), are endocytosed and only fuse after they have reached an endocytic acidic interior.[6] Other viruses, for example, the HIV, fuse with the plasma membrane directly after binding to the host cell receptor.[7] A fascinating aspect of viral infection is that in most cases binding of the virus to the host single protein, referred as the viral fusion protein, carries out fusion of the viral particles with this membrane. Viral fusion proteins such as influenza virus HA, or gp41 of the HIV assume flexible random conformations in an aqueous environment and upon insertion into phospholipid bilayers their secondary structure is altered.[8-10] Much is known about viral fusion proteins, although their mechanisms of action are still unknown. Evolutionarily unrelated viral fusion proteins share structural features that appear to be responsible for their fusogenic activities and that exhibit similarities with eukaryotic fusion proteins.[8,11,12]

Most viral fusion proteins contain a short amphiphilic peptide domain, the fusion peptide, which is essential for fusion. These fusion peptides typically encompass 20–30 amino acid residues. Their sequence is conserved within a family of proteins.[14] In the case of the paradigmatic fusion proteins of the HA and of the HIV, an amphiphilic fusion peptide is inserted into the target membrane. The exact

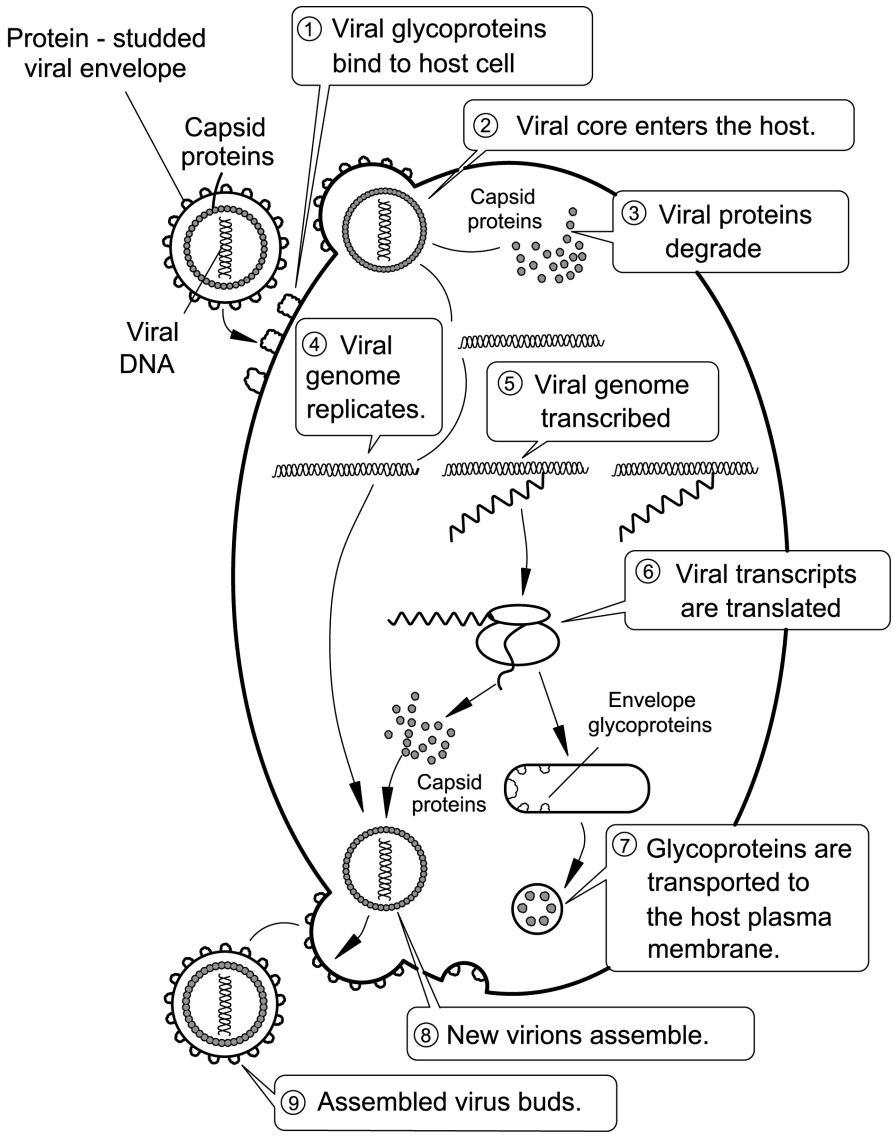

Figure 1.3: ***The Reproductive Cycle of the Influenza Virus.*** *The membrane-enclosed, or enveloped, influenza virus is taken into the host cell by endocytosis. Once inside, fusion of the vesicle and viral membranes releases the RNA genome, which replicates and assembles new virions.*[13]

conformation, assumed by a fusion peptide inserted into a phospholipid bilayer, is unclear, but at least some parts of the peptide form an amphiphilic α- helix.[8,15,16] Using hydrophobic photoactivatable cross-linkers, it has been demonstrated that during fusion the fusion peptide is the only sequence of the HA protein that inserts into the hydrophobic interior of the bilayer.[17] The protein then reorients itself, thus

forcing the fusing membranes together and inducing lipid mixing. The schematic diagram of the reproduction cycle of influenza HA is visualized in figure 1.3.[13]

In order to fuse an enveloped virus with the host cell, the viral fusion protein must overcome the energy barrier to separate two membranes to initiate the formation of fusion intermediates. Fusion therefore requires the generation of a mechanical force that brings the membranes closely together and bends the membranes as required for the initiation of fusion (Fig. 1.3). The key to understand the initialization of fusion of the influenza and HIV fusion proteins is that proteolytic processing generates a metastable fold that resembles a loaded spring. Activation triggers relaxation of the proteins, resulting in dramatic conformational changes that expose the previously buried fusion proteins. In the activated form, the N-terminally located fusion peptides reside on top of an extended, triple-stranded coil. Once activated, the fusion proteins become unusually stable.

The conformational changes during activation drive the fusion reaction, with the activated protein representing an end-stage condition that is inactive. It remains a challenge to clarify the precise role of the fusion protein during viral membrane fusion. Probably, the fusion protein injects the fusion peptide into the target membrane during activation and subsequently forces a reorientation of the phospholipid bilayers. Reorientation may be mediated by an alignment of oligomers of the fusion peptides and transmembrane regions that finally induce the formation of a fusion pore.

1.2 The architecture of a membrane

A membrane is composed of a lipid bilayer, which serves to separate different compartments of the cell, or in the case of lower organisms, the cell from its environment. In a lipid bilayer the hydrocarbons or acyl chains of two monolayers of lipids are fused together and form a single sheet with phosphate heads on both sides (Fig. 1.4). This effectively makes the membrane soluble, but not permeable. Lipid

bilayers are fluid, and individual phospholipids diffuse rapidly throughout the two-dimensional surface of the membrane. This is known as the fluid mosaic model of biological membranes. It is named mosaic because it includes proteins, cholesterol, and other types of molecules besides phospholipids. The phospholipid consists of a hydrophilic head, which points towards the outside environment and the cytoplasm.

The hydrophobic tails repel the water and point inward. Thus, the phospholipids form a bilayer that acts like a barrier between the cell and the environment. The presence of cholesterol makes the bilayer stronger, more flexible and permeable. Around 25 % of all protein types in a cell are membrane bound proteins, such as transporters, linkers, receptors and fusion proteins. Membrane proteins diffuse throughout the membrane in the same fashion as lipids, though at a slower pace because of their massive size. A phospholipid has average molecular weight of 800 Da and a medium sized protein can be 100 kDa.

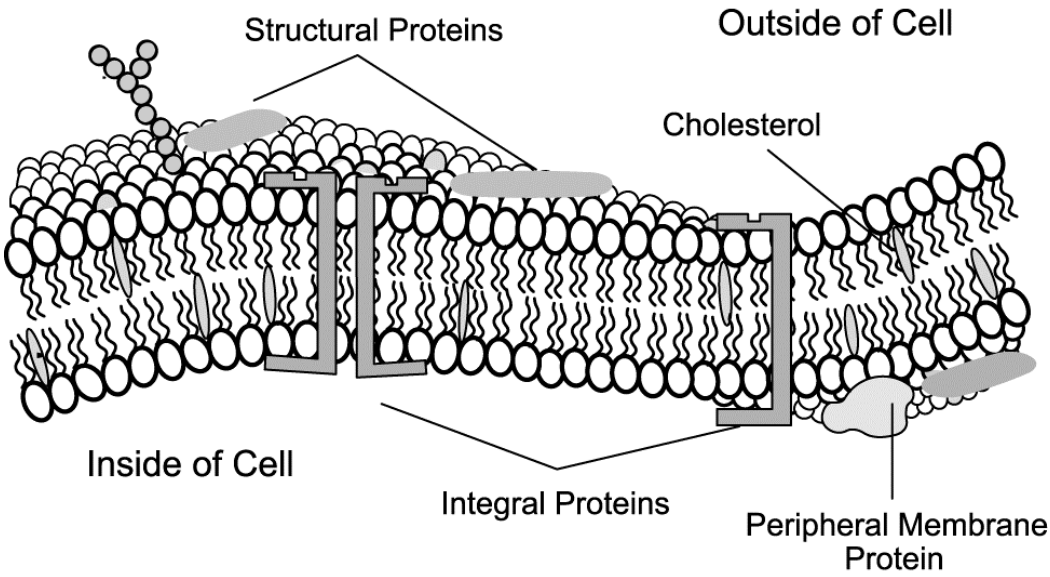

Figure 1.4: *The fluid mosaic model of cell membranes. The membrane is mainly made up of lipid molecules but also contains other molecules like membrane proteins, cholesterol and glycolipids. (Adapted from reference [21]) In this study the complex membrane of the synaptic vesicle is modeled with a mixture of its three most abundant components POPC, DOPE and DOPS.*

The membrane structural properties are known to depend critically on the nature of both acyl chains of phospholipids and the headgroup moiety.[18,19] The presence of phosphatidylethanolamine (PE) and phosphatidylserine (PS) in addition to phosphatidylcholine (PC) in the membranes significantly stimulates peptide-induced fusion.[5] These lipids represent the three major phospholipid species found in synaptic vesicles and the chemical structure is shown in Figure 1.5.[20] Pure PE bilayers are more rigid and more laterally compressed. Lipid phasestability depends primarily on the molecular shape of the constituents. Equal size heads and tails are needed for lamellar arrays.

PE is known to promote lipid hexagonal phases and membrane fusion due to its cone shape (Fig. 1.5).[22] The PS is negatively charged, it suppresses background fusion, and may favor membrane insertion of positively charged peptides or proteins (Fig. 1.5).[15] Using deuterium and phosphorus NMR, it was found that a PS headgroup has a relatively rigid structure as compared to both PC and PE.[23,24] It has been suggested that asymmetric distribution of PS over the inner and outer leaflet of cell membranes can moderate the interplay of the membrane with extrinsic membrane proteins.[24]

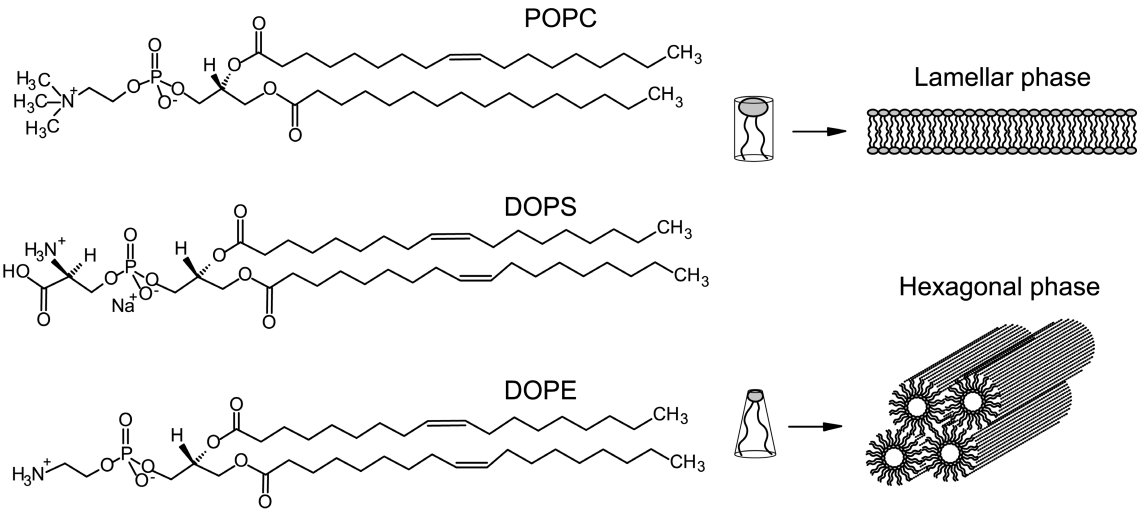

Figure 1.5: *Summary of lipid characteristics. Chemical structure and geometrical shape with the energetically preferred phases of the lipids used in this study. POPC and DOPS prefer the lamellar phase while DOPE prefers the hexagonal phase*

A delicate balance of forces in the headgroup and acyl-chain regions maintains the membrane bilayer structure. For a bilayer, since the two halves are hydrophobically coupled, a deformation of one side is restricted by the opposing monolayer. When both monolayers tend to adopt the negative curvature, the bilayer cannot lower its internal stress simply by bending. This state of balance, where the internal stresses across the whole bilayer stabilize a planar bilayer configuration, is an example of physical frustration.[25] Mismatches in packing in either region induce a tendency toward membrane curvature, which is offset by similar changes in the opposite leaflet.

The bilayer is a highly cooperative system. An acyl chain cannot change its direction without compensating changes in the neighboring chains. The methylenes located toward the middle of the bilayer show considerably more disorder than those near the surface, the order parameter is ~0.2.[26] The order parameter profile is not sensitive to the lipid chemical structure or membrane composition as long as the bilayer is in the liquid crystalline phase. The order parameter is relatively constant for C-2 through about C-8 or C-10 (~0.4).[26]

1.3 The molecular mechanism of biological membrane fusion

Among many different models and mechanisms that have been proposed for the initiation of membrane fusion, the formation of stalks has been put forward most frequently.[27,28] Stalk formation is estimated to lead to fusion intermediates with diameters of >4 nm and a lifetime <1 ms.[28] According to the stalk hypothesis model, fusion of pure lipid membranes requires at least four distinct steps: approach to small separation distances (Fig. 1.6A), local perturbation of the lipid structure and merger of proximal monolayers (Fig. 1.6B), stalk formation (Fig. 1.6C), stalk expansion leading to pore formation (Fig. 1.6D).

Originally, it was assumed that relaxation of the stalk would result in the formation of a central “unrestricted” hemifusion intermediate, which is a disk-

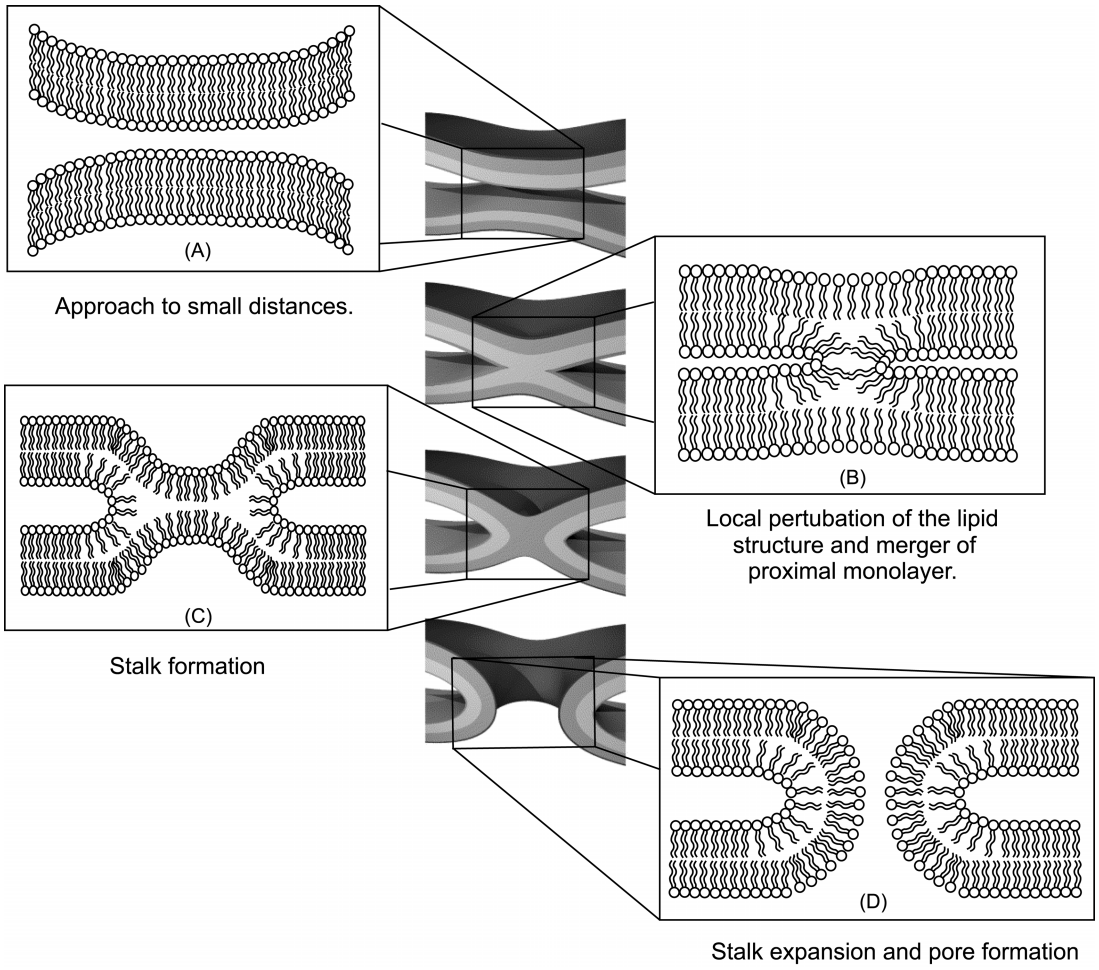

Figure 1.6: ***Transient conditions and curvature of lipids during vesicle fusion according to the stalk hypothesis.*** ***(A)*** *Approach to small distances.* ***(B)*** *Local perturbation of the lipid structure and merger of proximal monolayers, hemifusion. The outside lipids of spherical vesicles form a convex structure with positive curvature.* ***(C)*** *Stalk formation. The stalk develops with negative curvature at the contact area in the outer lipids.* ***(D)*** *Stalk expansion and pore formation. Complete fusion is effected via eruption of the stalk producing a mixing of the distal lipids. (Adapted from reference [29])*

shaped diaphragm consisting of a single bilayer derived from the two distal monolayers.[1,30] The diaphragm of the unrestricted hemifusion state was thought to expand until the accumulated tension destabilizes the structure, resulting in opening of single or multiple fusion pores. The stalk hypothesis is currently the only coherent concept that describes the transition states during membrane fusion.

Theoretical considerations and a variety of experimental approaches support this model and modeling indicates that the formation of stalks requires less energy than e.g. inverted micellar intermediates.[28,31]

Each membrane fusion event culminates in an organized assault on membrane integrity, rupturing two opposed bilayer surfaces in the process of fusing their lipid leaflets and mixing their respective contents. Such an event is in principle thermodynamically unfavorable, with the size of the energy barrier being in part a function of the intermediate structures sampled by the two membranes during the fusion event. Energy barriers may separate consecutive steps from each other. For fusion to proceed, every step needs to be driven by an energy gradient towards lower energies. This can be achieved by a low water content between the two merging bilayers and introduction of a high curvature.[32] Removal of water between two vesicles decreases the repulsive hydrophobic forces, which paves the way for vesicle collision and docking.[32]

1.4 Aim and scope of the thesis

In this thesis peptides are studied that are derived from the SNARE proteins, which are involved in synaptic fusion. A molecular understanding of the interaction of peptides and proteins with lipid bilayers requires experimental knowledge of the structure of the membrane bilayer, the trans-bilayer location of bound peptides, the structures the peptides adopt, and the changes that occur in the bilayer structure as a result of partitioning.

Following this introduction, **Chapter 2** describes the synthesis of *de novo* designed uniformly labeled artificial biomimetic peptides. The high yield synthesis of the peptides is done using only 3 equivalents of labeled amino acids in each coupling step. The optimized conditions used for the synthesis give less aggregation problems and better yield as compared to standard SPPS conditions and to pave the way for isotope labeling. The crude peptides are purified using modified RP-HPLC

methods. Finally, the purified peptides yield reproducible and reliable fusogenic assays, with intended functional design characteristics, from strongly fusogenic to almost non-fusogenic and this opens up a novel route to obtain valuable insight into the complex world of membrane fusion.

1.4.1 Fusion peptide design

TMDs of different SNARE proteins contain low complexity sequences with a majority of Ile, Leu and Val residues.[5] Also for viral fusion proteins, in the fusogenic species β-branched amino acids occur frequently.[1] The presence of β-branched amino acids into the predominantly helical TMD of both classes of fusogenic proteins suggests a connection between destabilization of helical structure and fusogenicity.[33]

This leads me to investigate a series of synthetic peptides with various lengths, L/V ratios and charged constituents (Table 1.1 and **Chapter 2**). The structural properties of the peptides are correlated with their capability to induce membrane fusion *in vitro*.[34] Detailed biophysical studies on these peptides lead towards a better understanding of their fusogenic activity and help to pave the way for the design of biomimetic systems for pharmaceutical applications. There have been several breakthroughs in elucidating mechanisms of function of membrane proteins and the principle focus of this thesis is on how solid-state NMR can provide information about mechanisms and structural detail of lipids, peptide-lipid interactions and peptides.

Table 1.1, set 1, shows the peptides with different lengths. They are based on an alternating Leu-Val sequence in the hydrophobic core. Studies on these peptides will help to determine the optimal hydrophobic length for fusogenicity. The effect of the Leu/Val ratio on fusogenicity and conformational flexibility is systematically examined in **Chapter 4**. The Lys is positively charged at physiological pH due to the protonation of the amino group (pKa ≈ 10.3) and can have electrostatic interactions with the lipid headgroups. In order to investigate the effect of the charges of the

Set 1: Length dependency	
LV12	K K K W **L V L V L V L V L V L V** K K K
LV16	K K K W **L V L V L V L V L V L V L V L V** K K K
LV20	K K K W **L V L V L V L V L V L V L V L V L V L V** K K K
LV24	K K K W **L V L V L V L V L V L V L V L V L V L V L V L V L V** K K K
Set 2: L/V ratio	
L16	K K K W **L L L L L L L L L L L L L L L L** K K K
LLV16	K K K W **L L V L L V L L V L L V L L V L** K K K
LV16	K K K W **L V L V L V L V L V L V L V L V** K K K
LV16G8P9	K K K W **L V L V L V L G P V L V L V L V** K K K
Set 3: Charge effect	
H-L16	H H H W **L L L L L L L L L L L L L L L L** H H H
H-LV16	H H H W **L V L V L V L V L V L V L V L V** H H H
H-LV16G8P9	H H H W **L V L V L V L G P V L V L V L V** H H H

Table 1.1: ***Sets of peptides that are used during this study. Set 1*** *consists of peptides with different lengths, varying between 19 to 31 residues.* ***Set 2*** *consists of peptides with the same hydrophobic length but different composition in the central hydrophobic core.* ***Set 3*** *consist of peptides with the same hydrophobic core and length as in set 2 but with His (H) substituted for the Lys (K) to trace the effect of charged residues.*

peptides on their fusogenic properties the Lys can be replaced by His (Table 1.1, set 3). The imidazole ring of His has a pKa ~ 6.0 and is neutral at physiological pH.

In **Chapter 3** the mechanism of membrane fusion is studied with ^{31}P SSNMR of a biomimetic three-lipid mixture loaded with the *de novo* designed synthetic hydrophobic peptides L16 and LV16G8P9. The peptides induce phase changes in the lipids that correlate with their fusogenic behavior in liposomes. The fusogenic

peptide induces pronounced stabilization of curvature at low humidity, probably by interacting with the outer layer and by inducing phase separation across the bilayer. The data are explained in terms of a release of physical frustration in the three-lipid system. Surprisingly, although the peptides are derived from the TMS of the membrane proteins, the mechanism of interaction with the lipids resembles the peripheral intercalation reported for viral proteins.[5] It transpires that the stabilization of curvature may be a prerequisite for fusogenic behavior.

Chapter 4 describes the effect of different series of peptides (Table 1.1) on a biomimetic lipid mixture at different conditions. This paves the way for finding a possible common denominator for their membrane fusion behaviour. The ageing effect as well as the structure of the lipid mixture in the presence of the fusogenic peptide LV16G8P9 is also studied. These studies help to provide insight into the changes of lipid systems over a period of time. The peptides stabilizing the aligned bilayer structure or introducing toroidal pores are non-fusogenic since they prevent the lipids to form a high curvature unoriented structure.

When functional fusogenicity correlates with a large degree of peptide structural flexibility, the dynamics of TMS peptides can become the rate limiting factor in the initiation of membrane fusion.[34] How the structural dynamics of these peptides is coupled to the lipid phase is still not known. In **Chapter 5** the peptide structure in the lyophilized form and in orientation studies of aligned bilayers and vesicles is addressed. By combining ^{15}N NMR investigations of the peptides with the ^{31}P NMR studies of peptide-membrane interactions, another view on the molecular mechanisms of fusion by peptides is obtained. 1D ^{15}N studies on peptides, with the bilayer normal parallel (0°) or perpendicular (90°) to the applied field, give information about the orientation of the peptides in the lipid membrane. Using ^{1}H spin diffusion experiments the topology of these uniformly labeled peptides in a biomimetic lipid mixture is characterized. Finally, the results and conclusions are summarized and are put in the perspective of recent results and interpretations of data in the field of membrane fusion. Possible future experiments and developments are also presented here.

References

1. Cleverley, D. Z.; Lenard, J., *Proc. Natl. Acad. Sci. U S A* **1998,** 95, 3425-3430.
2. Burns, M. E.; Augustine, G. J., *Cell,* **1995,** 83, 187-94.
3. Sudhof, T. C., *Annu. Rev. Neurosci.,* **2004,** 27, 509-547.
4. Grote, E.; Baba, M.; Ohsumi, Y.; Novick, P. J., *J. Cell Biol.,* **2000,** 151, 453-466.
5. Langosch, D.; Crane, J. M.; Brosig, B.; Hellwig, A.; Tamm, L. K.; Reed, J., *J. Mol. Bio.* **2001,** 311, 709-721.
6. Jahn, R.; Sudhof, T. C., *Annu Rev Biochem,* **1999,** 68, 863-911.
7. Laage, R.; Langosch, D., *European J. Biochemistry,* **1997,** 249, 540-546.
8. Cerpa, R.; Cohen, F. E.; Kuntz, I. D., *Folding and Design,* **1996,** 1, 91-101.
9. Epand, R. F.; Scheraga, H. A., *Biopolymers,* **1968,** 6, 1551-1571.
10. Szyperski, T.; Vandenbussche, G.; Curstedt, T.; Ruysschaert, J. M.; Wuthrich, K.; Johansson, J., *Protein Science,* **1998,** 7, 2533-2540.
11. Reed, J.; Kinzel, V., *Proc. Natl. Acad. Sci. U S A* **1993,** 90, 6761-6765.
12. Zhang, S. G.; Rich, A., *Proc. Natl. Acad. Sci. U S A* **1997,** 94, 23-28.
13. Sinauer Associates Inc. 1998, http://www.mie.utoronto.ca/labs/lcdlab/biopic/.
14. Li, S. C.; Deber, C. M., *Nature Structural Biology,* **1994,** 1, 368-373.
15. Liu, L. P.; Deber, C. M., *Biochemistry,* **1997,** 36, 5476-5482.
16. Struck, D. K.; Hoekstra, D.; Pagano, R. E., *Biochemistry,* **1981,** 20, 4093-4099.
17. Durrer, P.; Galli, C.; Hoenke, S.; Corti, C.; Gluck, R.; Vorherr, T.; Brunner, J., *J. Biol. Chem.* **1996,** 271, 13417-21.
18. Gawrisch, K.; Holte, L. L., *Chemistry and Physics of Lipids,* **1996,** 81, 105.
19. Nagle, J. F.; Tristram-Nagle, S., *Biochim Biophys Acta,* **2000,** 1469, 159-95.
20. Deutsch, J. W.; Kelly, R. B., *Biochemistry,* **1981,** 20, 378-385.
21. http://student.biology.arizona.edu/honors2002/group02/intro.htm. In.
22. Hamai, C.; Yang, T.; Kataoka, S.; Cremer, P. S.; Musser, S. M., *Biophys. J.,* **2006,** 90, 1241-1248.
23. Browning, J. L.; Seelig, J., *Biochemistry,* **1980,** 19, 1262-70.
24. de Kroon, A. I.; Timmermans, J. W.; Killian, J. A.; de Kruijff, B., *Chem Phys Lipids,* **1990,** 54, 33-42.
25. Seddon, J. M., *Biochim. Biophys. Acta,* **1990,** 1031, 1-69.

26. Gennis, R. B., *Biomembranes - Molecular-Structure And Function - Gennis,Rb*. Springer-Verlag: New York, 1989.
27. Siegel, D. P., *Biophys. J.* **1984,** 45, 399-420.
28. Siegel, D. P., *Biophys. J.* **1993,** 65, 2124-2140.
29. Jahn, R.; Grubmuller, H., *Curr Opin Cell Biol,* **2002,** 14, 488-95.
30. Nussler, F.; Clague, M. J.; Herrmann, A., *Biophys. J.,* **1997,** 73, 2280-2291.
31. Weber, T.; Zemelman, B. V.; McNew, J. A.; Westermann, B.; Gmachl, M.; Parlati, F.; Sollner, T. H.; Rothman, J. E., *Cell,* **1998,** 92, 759-772.
32. Yang, L.; Huang, H. W., *Science,* **2002,** 297, 1877-1879.
33. Minor, D. L.; Kim, P. S., *Nature,* **1994,** 367, 660.
34. Hofmann, M.; Weise, K.; Ollesch, J.; Agrawal, P.; Stalz, H.; Stelzer, W.; Hulsbergen, F.; de Groot, H.; Gerwert, K.; Reed, J.; Langosch, D., *Proc. Natl. Acad. Sci. U S A* **2004,** 101, 14776 - 14781.

2

Solid phase synthesis and purification of a set of uniformly ^{13}C, ^{15}N labeled *de novo* designed membrane fusogenic peptides.*

The transmembrane segments of SNARE proteins or viral envelope proteins drive membrane fusion, which suggests that simple synthetic biology constructs for fusion exist and can be evaluated. This chapter describes the high yield synthesis of a set of *de novo* designed fusogenic peptides that are isotopically enriched in ^{13}C and ^{15}N nuclei using 3 equivalents of labeled amino acids and optimized reaction conditions minimizing aggregation. The biomimetic peptides have a high purity >90% and show reproducible and fusogenic activity that correlates well with the intended functional design characteristics, from strongly fusogenic to almost non-fusogenic.

* ***Journal of Peptide Science,*** 13, 75-80, (2007).

2.1 Introduction

Synaptic transmission is initiated when an action potential triggers neurotransmitter release from a presynaptic nerve terminal.[1] All the presynaptic functions, directly or indirectly, involve synaptic vesicles. Synaptic vesicles undergo a trafficking cycle in the nerve terminal and deliver their load.[1] A major goal in neurobiology in recent years has been to gain insight into the molecular machinery that mediates neurotransmitter release. More than 1000 proteins function in the presynaptic nerve terminal and hundreds are thought to participate in exocytosis.[1] In this protein zoo, which proteins are actually important and which are only bystanders, is difficult to answer. However, the integral membrane proteins such as soluble SNAREs are essential for fusion of cargo vesicles.[2,3] A direct role of their transmembrane segments in fusion is supported by recent *in vitro* studies.[4-7] For instance, TMDs of presynaptic SNAREs or of the VSV G-protein, represented by synthetic peptides, were shown to drive fusion of liposomal membranes. In addition, evidence has been obtained that transmembrane segments of fusogenic membrane proteins display conformational flexibility and that this enhances the fusogenicity.[7-9] It is possible to mimic these transmembrane segments with *de novo* designed synthetic peptides.[8] In addition, it was proposed that sheet formation by the fusogenic peptides *in vitro* reflects a structural flexibility of the original helices that is rather unusual for transmembrane segments of other membrane proteins and may be essential for their fusogenicity.[9]

For decades, the question of how a protein's amino acid sequence dictates its conformation has captivated the attention of many chemists, biophysicists, and biochemists. In the past TMbase 25 is assessed to see whether SNARE transmembrane segments exhibit an unusual amino acid composition by comparing the average amino acid compositions of the TMDs of different isoforms of synaptobrevin and syntaxin to that of a large database of unrelated TMDs.[9,10] An analysis of amino acid composition revealed that isoleucine and valine are strongly present in transmembrane segments from different SNARE subtypes and

orthologues as compared to a large database of unrelated Transmembrane segments.[9] Isoleucine and valine rank among those residues with the highest propensities to form β-sheet structures.[11-13] This property was ascribed to steric interference of their β-branched side-chain with the local polypeptide backbone that may destabilize the α-helical conformation. The previous data shows that the fusogenic peptides with mixed Leu and Val sequences in the hydrophobic core exhibit a higher degree of conformational plasticity than non-fusogenic peptides with oligo-Leu or oligo-Val cores.[9] Since fusogenicity correlates with structural flexibility for this class of peptides, the dynamics of the secondary structure apparently controls membrane fusogenic properties.[8] The helix-destabilizing residues enhance fusion protein function via transmembrane conformational dynamics and the structural rationale behind this is that Gly does not support the packing of side-chains along a helix backbone whereas Pro cannot form a hydrogen bond to the i+4 residue.[8] Both residues caused destabilization of transmembrane helices in membrane-mimetic environments and organic solvents.[14,15] Pro residues in transmembrane-helices are frequently associated with local kinks, especially when a Gly residue is present in the vicinity and it has been argued that these kinks may function as 'molecular hinges', i.e. sites of increased local flexibility.[16] These non-natural polymers present a new system, which provides an excellent medium for the design of biomimetic structures with practical applications in the areas of pharmaceutical and material science.

Although the structural flexibility of the fusogenic LV variants manifested itself as helix to sheet transition in isotropic solution, how this transition takes place in the low dielectric environment of a membrane is still unclear. ^{31}P solid-state NMR spectra of the lipids in the presence of these peptides show drastic changes and it transpires that the rearrangements of lipid phases drive membrane fusion (Chapter 3). The corresponding phase changes may be related to the conformationally flexible behavior of these peptides, in a sense that they locally unwind in the bilayer and impose a structural frustration facilitating lipid mixing. The interplay of flexibility and other features such as hydrophobic length and the nature of flanking residues

with lipids will have to be studied in the future for a more complete understanding of membrane fusion.

To pave the way for in dept analysis of these phenomena by NMR spectroscopy, a set of uniformly labeled peptides that show different fusogenic activities is prepared. This chapter describes the high yield synthesis and purification of a *de novo* designed set of synthetic hydrophobic peptides containing uniformly ^{13}C, ^{15}N isotopically labeled 16-residue cores. These peptide hydrophobic cores mimic transmembrane sequences in the sense that they contain helix- or sheet-promoting residues. Such peptides will tend to aggregate due to interchain association involving hydrogen bonding between the secondary amide groups of the peptide chain that leads to β-sheet formation and helix-destabilizing residues like Gly and Pro are introduced in the middle of the core to hinder aggregation. The chosen peptides have 23 residues consisting of a central (Leu and/or Val)$_n$ repeating unit with n=8 or 16. This unit is flanked on both sides by 3 Lys to enhance peptide incorporation in lipid bilayers and contains a Trp residue at one end for quantification. Below the sequences of these peptides are given where the amino acids, which are underlined, are uniformly ^{13}C and ^{15}N labeled.

L16 : K K K W <u>L L L L L L L L L L L L L L L L</u> K K K

LV16 : K K K W <u>L V L V L V L V L V L V L V L V</u> K K K

LV16G$_8$P$_9$: K K K W <u>L V L V L V L G P V L V L V L V</u> K K K

The peptides are synthesized using Fmoc solid phase peptide synthesis (SPPS). Fmoc SPPS is a rapid, efficient and reliable method for the synthesis of peptides and proteins.[17,18] In addition, for SSNMR spectroscopic studies on peptides in biomimetic lipid bilayers, they have to be isotopically labeled in both ^{13}C and ^{15}N to enhance the signals and this puts additional constraints on the possible synthetic routes and purification. To pave the way for isotope labeling the conditions used for the synthesis are optimized to give less aggregation problems and better yields as compared to standard SPPS conditions. The crude peptides are purified using

modified RP-HPLC methods. This results to high cost efficiency for very expensive uniform labeling of these peptides. Finally, the purified peptides show reproducible and reliable fusogenic assay data sets, opening up a novel route to obtain valuable insight into the complex world of membrane fusion.

2.2 Materials and Methods

All reagents were purchased from Acros Chemicals and used without further purification unless otherwise stated. Solvents and reagents used in the peptide synthesis are all of peptide synthesis grade and purchased from Biosolve, except for HATU, which was from Applied Biosystems. TIS is supplied by Aldrich Chemical Co. All amino acids used are the naturally occurring L-amino acids. Fmoc-Lys(Boc) preloaded TentaGel S resin was bought from Rapp Polymere. The two isotope-labeled Fmoc protected amino acids, Fmoc-[U-^{13}C,^{15}N]-Leu-OH and Fmoc-[U-^{13}C,^{15}N]-Val-OH, were purchased from Cambridge Isotope Laboratories. Fmoc protection of [U-^{13}C,^{15}N]-Pro-OH, and [U-^{13}C,^{15}N]-Gly-OH was carried out as described.[18,19] Synthesis of the peptides is performed on an automated CS336 (CS Bio, US) peptide synthesizer. Finally MALDI-TOF spectra of purified peptides are recorded using on a Voyager-DE PRO mass spectrometer (Perseptive Biosystems, Inc.). POPC lipid is purified from fresh hen egg yolk; DOPE and DOPS are purchased form Avanti Polar Lipids, US. The liposome-liposome fusion assay was measured at a temperature of 37°C.

2.2.1 Synthesis of the Peptides

Selected uniformly ^{13}C, ^{15}N-labeled peptides were prepared via the solid-phase Fmoc method on a commercially available preloaded Fmoc-Lys(Boc) TentaGel S PHB resin (265 mg, 0.25 mmol/g NH_2). The consecutive steps in the solid phase peptide synthesis performed in each cycle were: (i) Deprotection of the Fmoc-group

with 20% piperidine in 20% DMSO/NMP for 5×2 min. (ii) Coupling by applying a three-fold excess of the appropriate amino acid. The amino acid (0.25 mmol) and HATU (0.225 mmol) were dissolved in 20% DMSO/NMP (1 ml) and subsequently 0.5 ml of 1 M DIPEA in NMP was added. After 1 min preactivation time the mixture was transferred to a reaction vessel, which was shaken for 2 h. (iii) The unreacted amino functions are capped by acetylation with 0.5 M acetic anhydride and 0.125 M DIPEA in NMP. (iv) The free peptides are obtained after treatment of the resin with a mixture of 95% TFA / 2.5% TIS /2.5% H_2O. The synthesized peptide is filtered in cold diethyl ether and the precipitate is collected after centrifugation.

2.2.2 Purification of the Peptides

Purifications were conducted on a BioCAD "Vision" automated HPLC system (PerSeptive Biosystems, inc.), supplied with a semipreparative Alltima (Alltech) columns (250 mm x 10 mm, running at 4ml/min). The buffer gradient used for purification contains, A: 25% methanol + 75% water, B: 100% CH_3CN and C: 1% TFA + 99% methanol. Linear gradients of B with 10% C were applied over 3 CV unless stated otherwise. The purification of peptides LV16 and L16 was performed with an Alltima CN phase column and for LV16G8P9; a Prosphere C_{18} column was used. Detection was done by UV spectroscopy at 214 and 294 nm. The final peptide purity was confirmed by MALDI-TOF. The peptides were lyophilized from a 10% acetic acid and water mixture. The lyophilized peptides were stored at – 20°C until used for the fusion assays.

2.2.3 Preparation of small unilamellar liposomes

Liposomes are prepared from mixtures of egg PC /brain PE /brain PS at a ratio of 3:1:1 (w/w/w) with or without 0.8% (w/w) of NBD-PE and Rh-PE (Molecular Probes).[9] Lipid solutions in chloroform, with or without transmembrane-peptides first dissolved in TFE, are dried under a stream of nitrogen as a thin film and rehydrated with a fusion buffer (25 mM Tris-HCl, pH 7.4, 150 mM NaCl, 0.1 mM

EDTA, 5 mM DTT). Liposomes are formed using sonication (Bransonic Sonifier W450 cup horn) for 8 min and cooling with ice. The sample was centrifuged at 16000 × *g* for 20 min to remove lipid aggregates. Peptide/lipid ratios were determined after separating peptides from proteoliposomes by density gradient centrifugation.[6] The liposomes were lyophilized with 1% (wt/vol) SDS and the amounts of lipid-associated peptide were determined using the Trp fluorescence of the top fractions.

2.2.4 Fusion assays

Fusion assays were performed using the fluorescence dequenching method.[9] Briefly, 'donor' liposomes containing fluorescence labels and unlabeled 'acceptor' liposomes (2.5 mg/ml phospholipid) were mixed at a ratio of 1:4 (v/v) on ice, transferred to 96-well white Corning non-binding plates with translucent bottoms and heated for 2 min by floating the plates on a 37°C water bath. NBD fluorescence is immediately assayed at 1 min intervals for 60 min at 37°C. Initial rates of fusion were obtained by fitting the first 10 minutes of the kinetics using ORIGIN software (OriginLab Corporation, Northampton, MA) with a polynomial function and determining its first derivative. All values are corrected for detergent quenching which was below 4%. The peptide-independent, spontaneous fusion of pure liposomes was routinely determined in parallel and subtracted from the values obtained with peptide-containing liposomes.

2.3 Results

The MALDI-TOF spectrum of L16 ($M + H^+ = 2895$), with a uniformly labeled inner 16 residue core (Fig. 2.1) shows a peak at m/z value of 2896.23 and other peaks with sodium and potassium clusters 2918.25 $(M+Na)^+$, 2935 $(M+ K)^+$ and 2940 $(M+2Na)^{2+}$. Similarly, $LV16G_8P_9$ ($M + H^+ = 2715$), with a uniformly labeled inner 16

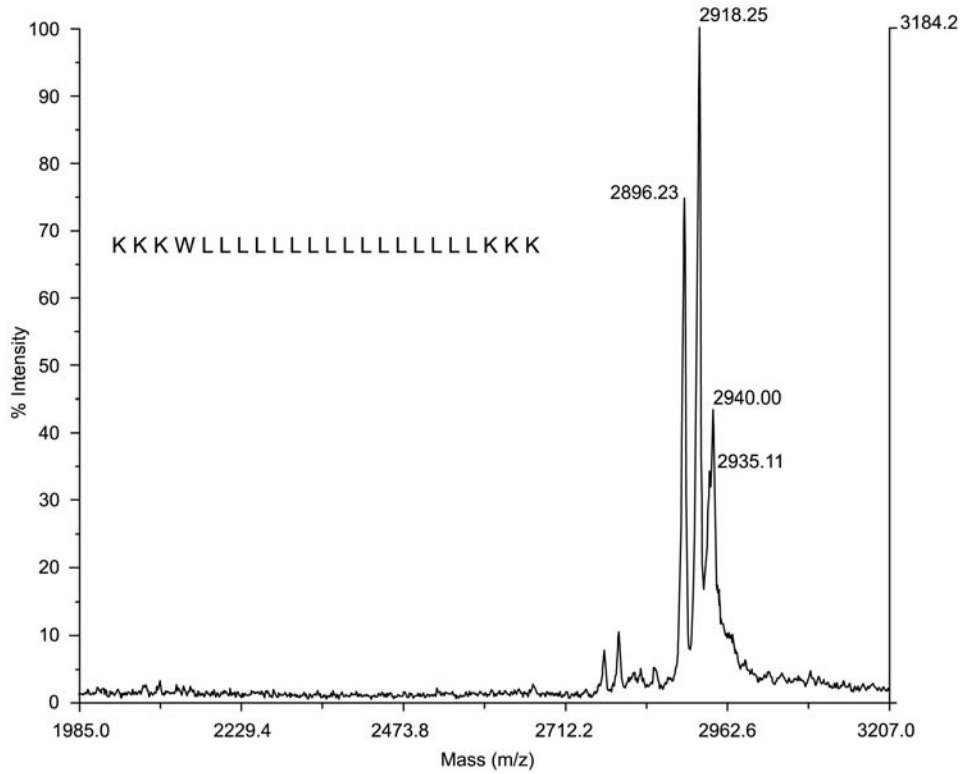

Figure 2.1: *MALDI-TOF spectrum of the peptide **L16** ($M + H^+ = 2895$), with uniformly labeled inner 16-residue core, obtained after purification. Beside the main peak at 2896.23 there are sodium and potassium clusters of the main peak present.*

residue core (Fig. 2.2) gave a major peak at m/z value of 2714.76 and other peaks with sodium and potassium clusters 2736.65 $(M+Na)^+$, 2753.41 $(M+ K)^+$ and 2758.64 $(M+2Na)^{2+}$. In addition to these major peaks there are some small peaks present that are difficult to separate which makes these peptides > 90% pure.

Peptide LV16 ($M + H^+ = 2775$), with a uniformly labeled inner 16-residue core (Fig. 2.3) gave two clusters of peaks. The major peak at m/z values of 2776.21 and other peaks associated with these peak are sodium and potassium clusters 2796.84 $(M+Na)^+$ and 2820.27 $(M+2Na)^{2+}$. The other minor cluster of peaks is from the fragment with an amino acid short, 2670.88 (LV16-K) and its sodium cluster 2692.47. In addition, there are some small peaks of the fragmented peptide that are difficult to separate using the modified purification method. The purity in this case is about 90%.

The peptides were incorporated into liposomal membranes by sonication at different peptide/lipid (P/L) ratios. Liposome-liposome fusion was examined by a standard fluorescence-dequenching assay upon rapidly shifting the temperature to 37°C. This assay is based upon fluorescence resonance energy transfer from NBD-PE to Rh-PE being present at quenching concentrations in 'donor' liposomes. Upon fusion of labeled liposomes with unlabeled liposomes that hold the peptides, the average distance between the fluorophores, and thus NBD-fluorescence, increases over time; this is taken as a measure of lipid mixing. Fusion kinetics of peptides are compared in Fig. 2.4, which indicates membrane fusogenicity of these peptides. These values were correlated with the fusion extents observed after 1 h of incubation.

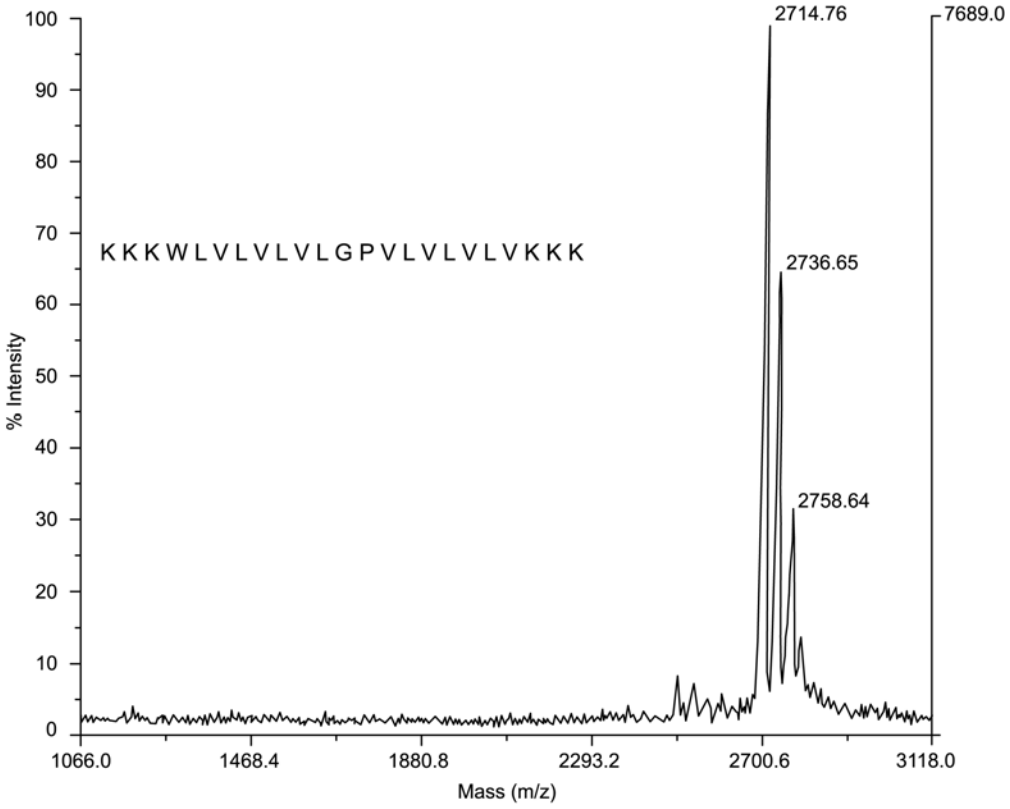

Figure 2.2: *MALDI-TOF spectrum of the peptide* ***LV16G$_8$P$_9$*** *(M + H$^+$ = 2715), with uniformly labeled inner 16-residue core, obtained after purification. Beside the main peak at 2714.96 there are sodium and potassium clusters of the main peak present.*

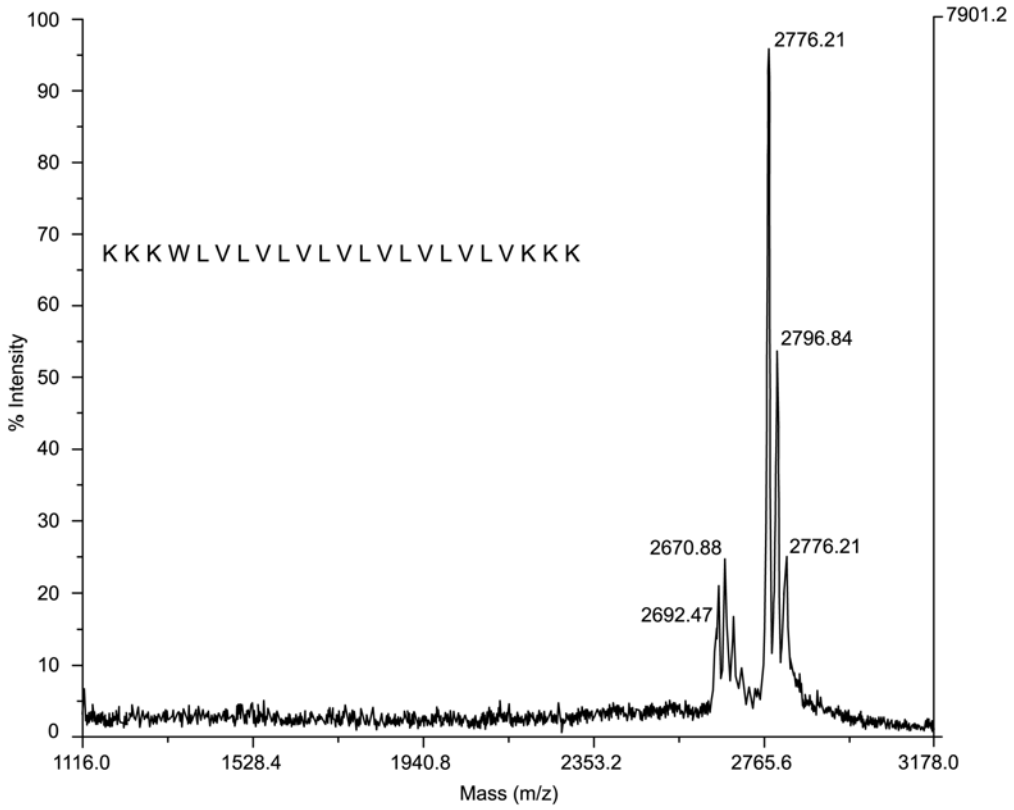

Figure 2.3: *MALDI-TOF spectrum of the peptide* ***LV16*** *($M + H^+ = 2775$), with uniformly labeled inner 16-residue core, obtained after purification. Beside the main peak at 2776.21 there is another peak at 2670.88, which is assigned to the one amino acid (Lys) short impurity that is difficult to separate. The clusters of sodium and potassium of main and side peak are present.*

2.4 Discussion

The incorporation of synthetic peptides representing the transmembrane segments of membrane fusion proteins into the membranes of synaptic liposomes strongly increases their ability to fuse.[8] This *in vitro* fusion system consisting of only lipids and transmembrane peptides appears to display characteristic hallmarks of biological membrane fusion, which is a complex process. The structure-function correlation studies on these peptides will help to understand the complexity of this process. The peptides in the chosen *de novo* set are hydrophobic sequences with the

repetitive units of amino acid residues, which tend to aggregate. Aggregation of hydrophobic peptides on resins generally leads to low coupling yields and an accumulation of single amino acid deletions, which are difficult to separate from the target peptide.[18,20] During Fmoc-SPPS, aggregation through interchain association of the growing resin-bound peptides is known to contribute to the difficulty of synthesis.[21,22] Aggregation typically results in a decrease in rates of acylation and deprotection, and consequently leads to the production of deletion products of varying length and composition. Such a decrease in the purity of the crude material often results in subsequent difficult purification. To overcome the difficulties of decreased coupling efficiency, low yield and aggregation, a modified Fmoc SPPS method is implemented. The onset of internal aggregation in SPPS is usually indicated by slow acylation and/or by shrinkage of the swollen gel resin. The TentaGel S resin with low loading (0. 26 mmol/g) is used, which is known to provide the best conditions for reducing aggregation.[18]

To synthesize these hydrophobic peptides using conventional SPPS (PyBOP/DIPEA) and double coupling requires 10 equivalents of amino acids per coupling step (twice 5 eq.). Out of those 10 equivalents used, 9 go to waste, which is unacceptable for isotope labeling. To overcome this hurdle, a strong activator, increased the coupling time, and different solvent mixtures are used. In particular, HATU reagent does not require double coupling and thus allows to reduce the consumption of Fmoc amino acids in the synthesis of hydrophobic peptides.[23,24] Use of HATU doubles the yield of the peptide as compared with PyBOP

	L16	**LV16**	**LV16G$_8$P$_9$**
Column	C4	CN	C18
Gradient	15-90 Acetonitrile	10-90 Acetonitrile	20-90 Acetonitrile
Yield	4.15 µmol	4.32 µmol	4.79 µmol

Table 2.1: *Purification and characterization of transmembrane peptides prepared in this study. Different solvent systems and gradient profiles used for the respective columns are mentioned in detail (see text) and purity is determined by using both HPLC and MS.*

or HBTU and eliminates double couplings. In this way we have decreased the consumption of uniformly labeled amino acids to only 5 equivalents at each coupling step.

The advantages of DMSO as a valuable disaggregating solvent in SPPS have been known for some time, both as a neat coupling solvent and mixed with polar (e.g. DMF, NMP) and non-polar (e.g., THF, toluene) co-solvents.[25-29] In addition, DMSO is a powerful co-solvent for the dissolution of poorly soluble amino acid derivatives and reagents. By using a solvent mixture containing 20% DMSO and increasing the coupling time from 1 hour to 2 hours, the consumption of amino acids was further reduced to 3 equivalents at each coupling step. This implies that only 2 equivalents of amino acids go to waste, allowing the synthesis of uniformly labeled peptides in a cost effective manner.

Previous experience using unlabeled commercial peptides has shown that the purity of these peptides plays an important role in obtaining reproducible and consistent data sets. However, hydrophobic peptides have a tendency to stick to the standard RP columns like C_8 or C_{18}, particularly if elution is performed with the standard acetonitrile-water system. This commonly leads to increased back pressure and low yields of the purified peptides. So to purify these hydrophobic peptides to high level is a major challenge. Purification of L16 and LV16 peptides is found to be most efficient and reproducible using a CN phase polar column, while for the $LV16G_8P_9$ a C_{18} wide pore column is sufficient. It proved to be essential to include 25% methanol in the HPLC buffer to eliminate the back pressure problem. This purification method gives both high purities and high yields (Table 2.1).

To test whether the synthesized peptides give reproducible and consistent fusion in liposomes the fusion kinetics of unlabeled L16, LV16, and $LV16G_8P_9$ peptides were analyzed (Fig. 2.4A). Although the LV16 sample contains minor impurities, this does not change its fusogenic activity. In line with earlier literature results using peptides synthesized by Boc-chemistry, the assays show that L16 is non-fusogenic and $LV16G_8P_9$ is the most fusogenic peptide, while LV16 shows intermediate fusogenic activity.[8]

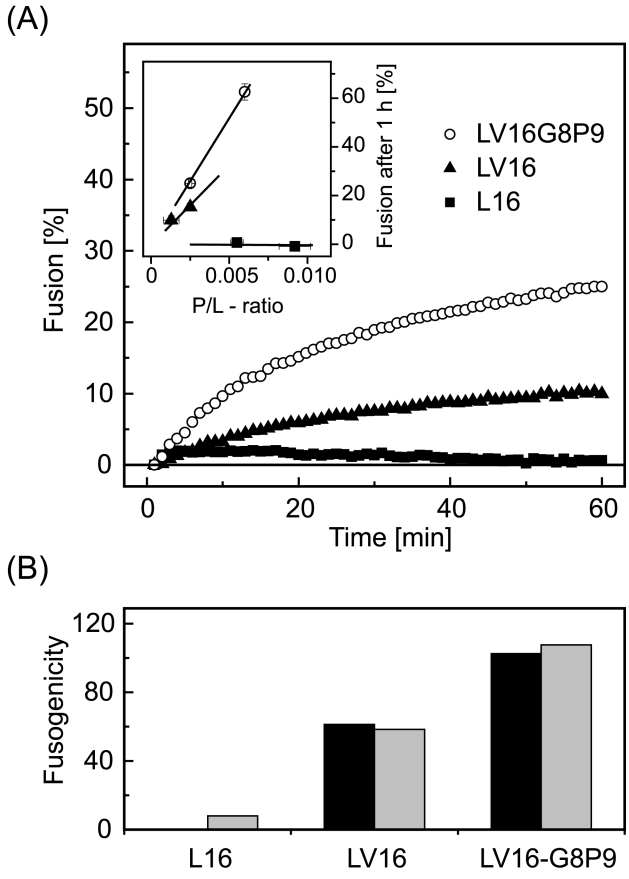

Figure 2.4: *Fusogenic activities of labeled peptides.* ***(A)*** *Original fusion kinetics of* ***L16***, ***LV16*** *and* ***LV16G8P9*** *(n = 6). The values were corrected for spontaneous fusion of liposomes without peptide, as measured in parallel. The incorporation of these peptides in liposomes was determined experimentally by measuring the P/L-ratios. These values were correlated with the fusion extents seen after 1 h of incubation (Inset). The incorporation of LV16 was somewhat less efficient than for L16 or LV16G8P9.* ***(B)*** *Labeled peptides (black bars) show similar fusogenicity as unlabeled peptides (gray bars[8]).*

2.5 Conclusion

The cost effective strategy described in this chapter for these *de novo* designed peptides is efficient and promising for the synthesis and purification of other hydrophobic peptides. The functionality of these peptides paves the way for in detail

structural and dynamic interactions studies of these uniformly labeled peptides in lipid bilayers and also for the effects of these peptides on lipid behavior. In future, spectroscopic studies on these labeled peptides, incorporated in lipid bilayers, will also contribute to the elucidation of the mechanism by which these peptides fuse lipid bilayers and thus will provide valuable information on membrane fusion.

References

1. Sudhof, T. C., *Annu. Rev. Neurosci.,* **2004,** 27, 509-547.
2. Jahn, R.; Lang, T.; Sudhof, T. C., *Cell,* **2003,** 112, 519-533.
3. Ungermann, C.; Langosch, D., *J. Cell Sci.* **2005,** 118, 3819-3828.
4. Rohde, J.; Dietrich, L.; Langosch, D.; Ungermann, C., *J. Bio. Chem.* **2003,** 278, 1656-1662.
5. Schuette, C. G.; Hatsuzawa, K.; Margittai, M.; Stein, A.; Riedel, D.; Kuster, P.; Konig, M.; Seidel, C.; Jahn, R., *Proc. Natl. Acad. Sci. U.S.A.* **2004,** 101, 2858-2863.
6. Langosch, D.; Brosig, B.; Pipkorn, R., *J. Bio. Chem.* **2001,** 276, 32016-32021.
7. Dennison, S. M.; Greenfield, N.; Lenard, J.; Lentz, B. R., *Biochemistry,* **2002,** 41, 14925-14934.
8. Hofmann, M.; Weise, K.; Ollesch, J.; Agrawal, P.; Stalz, H.; Stelzer, W.; Hulsbergen, F.; de Groot, H.; Gerwert, K.; Reed, J.; Langosch, D., *Proc. Natl. Acad. Sci. U.S.A.* **2004,** 101, 14776 - 14781.
9. Langosch, D.; Crane, J. M.; Brosig, B.; Hellwig, A.; Tamm, L. K.; Reed, J., *J. Mol. Bio.* **2001,** 311, 709-721.
10. Hofmann, K.; Stoffel, W., *Biological Chemistry Hoppe-Seyler,* **1993,** 374, 166.
11. Minor, D. L.; Kim, P. S., *Nature,* **1994,** 367, 660-663.
12. Smith, C. K.; Withka, J. M.; Regan, L., *Biochemistry,* **1994,** 33, 5510-5517.
13. Street, A. G.; Mayo, S. L., *Proc. Natl. Acad. Sci. U.S.A.* **1999,** 96, 9074-9076.
14. Li, S. C.; Deber, C. M., *FEBS Letters,* **1992,** 311, 217-220.
15. Liu, L.-P.; Deber, C. M., *J. Biol. Chem.,* **1998,** 273, 23645-23648.
16. Cordes, F. S.; Bright, J. N.; Sansom, M. S. P., *J. Mol. Bio.* **2002,** 323, 951-60.
17. Fields, G. B.; Colowick, S. P., *Methods in Enzymology*. Academic Press: 1997; Vol. 289, p 3-336.
18. Chan, W. C.; White, P. D., *Fmoc Solid Phase Peptide Synthesis: A Practical Approach*. Oxford University Press, New York: 2000; p 115–117.
19. Dener, J. M.; Fantauzzi, P. P.; Kshirsagar, T. A.; Kelly, D. E.; Wolfe, A. B., *Organic Process Research & Development,* **2001,** 5, 445-449.
20. Miranda, L. P.; Meutermans, W. D. F.; Smythe, M. L.; Alewood, P. F., *J. Org. Chem.* **2000,** 65, 5460-5468.

21. Hyde, C.; Johnson, T.; Owen, D.; Quibell, M.; Sheppard, R. C., *International J. Peptide And Protein Research,* **1994,** 43, 431-440.
22. Bedford, J.; Hyde, C.; Johnson, T.; Jun, W.; Owen, D.; Quibell, M.; Sheppard, R. C., *International Journal Of Peptide And Protein Research,* **1992,** 40, 300-307.
23. Carpino, L. A., *J. American Chem. Soc.* **1993,** 115, 4397-4398.
24. Carpino, L. A.; Elfaham, A.; Minor, C. A.; Albericio, F., *J. Chem. Soc.-Chem. Comm.* **1994**, 201-203.
25. Pugh, K. C.; York, E. J.; Stewart, J. M., *International Journal Of Peptide And Protein Research,* **1992,** 40, 208-213.
26. Hyde, C.; Johnson, T.; Sheppard, R. C., *J. Chem. Soc.-Chem. Comm.* **1992**, 1573-1575.
27. Miranda, L. P.; Alewood, P. F., *Proc. Natl. Acad. Sci. U.S.A.* **1999,** 96, 1181-1186.
28. Hendrix, J. C.; Jarrett, J. T.; Anisfeld, S. T.; Lansbury, P. T., *J. Org. Chem.* **1992,** 57, 3414-3420.
29. Fields, G. B.; Fields, C. G., *J. Am. Chem. Soc.* **1991,** 113, 4202-4207.

3

Solid state NMR investigation of the interaction between a biomimetic lipid bilayers and a *de novo* designed fusogenic peptide.*

In this chapter established ^{31}P solid-state NMR methods are used to probe the interactions of peptides with lipid bilayers. The system undergoes changes in orientation and conformation that help to induce fusion events. Membrane fusion requires drastic and transient changes of bilayer curvature.[1] Here, the interaction of two *de novo* designed synthetic hydrophobic peptides with a biomimetic three-lipid mixture is studied by ^{31}P solid state NMR. The peptides induce phase changes in the lipids that correlate with their fusogenic behavior in liposomes. The fusogenic peptide induces pronounced stabilization of curvature at low humidity, probably by interacting with the outer layer and by inducing phase separation across the bilayer. The data are explained in terms of a release of physical frustration in the three-lipid system. The stabilization of curvature may be a prerequisite for fusogenic behavior of a peptide.

---

* ***ChemBioChem*** (in press)

3.1 Introduction

Regulated fusion of biological membranes can be induced by membrane-associated peptides with low-complexity sequences.[2] Such peptides can drive fusion depending on their structural flexibility, and how the peptide couples into the lipid phase is still unknown. Recent membrane fusion studies suggest that the major energy barrier for fusion involves bringing membranes close together by removal of water in conjunction with increases in curvature.[1] Here the study of the interaction of *de novo* designed synthetic peptides with a biomimetic lipid mixture by ^{31}P solid-state NMR spectroscopy of oriented phospholipid bilayers is described. It has been used previously to investigate the structural and dynamic properties of membrane bound peptides, proteins and the microscopic phase properties of membranes.[3,4] Two peptides are investigated in this chapter: one previously shown to be rigid and non-fusogenic, L16, and one flexible and highly fusogenic, LV16G8P9.[2] A mixture of phosphatidylethanolamine (PE), phospatidylserine (PS), and phosphatidylcholine (PC) in 60:20:20 ratio is used to mimic the biological membrane composition of synaptic vesicles.[5] This chapter shows how such peptides can alter biomimetic lipid bilayers dramatically, even at peptide to lipid ratios of 1:100. The data reveal a subtle balance between bilayer and vesicle type behavior. A high curvature is favored upon addition of the fusogenic peptide. The obtained data are explained in terms of a release of physical frustration in the three-lipid biomimetic system by phase separation across the lipid bilayer, induced by the cylindrical PC and cone-shaped PE lipid fraction. This produces an excess curvature at low water context, which is a prerequisite for fusogenic behavior.

L16 : K K K W L L L L L L L L L L L L L L L L K K K

LV16G8P9 : K K K W L V L V L V L G P V L V L V L V K K K

3.2 Experimental

Samples for solid state NMR studies were prepared by dissolving 1-palmitoyl-2-oleoyl-sn-glycero-3-phosphocholine (POPC), 1,2-dioleoyl-sn-glycero-3-[phospho-L-serine] (DOPS) and 1,2-dioleoyl-sn-glycero-3-phosphoethano- lamine (DOPE) (Avanti Polar Lipids, Birmingham, AL) in chloroform in a 3:1:1 ratio. The peptide, dissolved in trifluoroethanol, was added at a peptide:lipid molar ratio of 1:100. In case of POPC lipid bilayer studies, the peptide dissolved in TFE is mixed with POPC in chloroform at the desired peptide to lipid ratio. The mixtures were applied onto 15 ultra thin cover glass plates (6.2 X 20 mm^2; Paul Marienfeld GmbH & Co. KG, Lauda-Konigshofen, Germany), first dried under a dry stream of nitrogen, and kept overnight under high vacuum. Subsequently the plates were hydrated by spraying them with fusion buffer of 150 mM NaCl, 20 mM Tris, and 0.2 mM EDTA, pH 7.4. The plates with peptide–lipid films were equilibrated at 4°C for 72 hours. Stacks of plates were stabilized and sealed with Teflon tape and plastic wrappings. The samples were inserted into a multichannel flat coil solid-state NMR probe head and placed in a Bruker AV750 spectrometer with the membrane normal oriented parallel to the magnetic field direction. Proton-decoupled ^{31}P solid-state NMR spectra were recorded using a Hahn echo pulse sequence with a 90° pulse length of 7.8 μs, an echo delay of 40 μs, 6K scans of 1K data points with a spectral width of 94.339 kHz, and a recycle delay of 3 s. A line broadening of 10 Hz was applied before Fourier transformation.[6] The spectra were processed without first order phase correction and referenced relative to $(NH_4)_2HPO_4$ at 0 ppm chemical shift. All the simulations reported herein are performed using IGOR 4.0 (Wavemetrics. Lake Oswego, Oregon) and the procedures used were received from the University of Michigan, USA and are slightly modified.[7] The modified procedures are shown in Appendix.

3.3 Results

With ^{31}P SSNMR, the orientational states of lipids can be probed since the observed line shape reflects the symmetry of the dynamic order of lipid molecules in a very characteristic manner.[8] This property can be used to analyze the effect of the peptides on the membrane system. Every headgroup of a glycerophospolipid contains a single ^{31}P nucleus with 100% natural abundance and good sensitivity. Lipids rotate at the ns timescale, which is fast relative to the NMR time scale set by the shift anisotropy in hydrated lipid bilayers. The CSA tensor is partially averaged, to an effective tensor that is axially symmetric about the rotation axis and has principal axis values $\sigma_{II} \sim 28$ ppm and $\sigma_{\perp} \sim -19$ ppm, for 0° orientation parallel to the rotation axis and for 90° orientation perpendicular to the rotation axis, respectively. These values vary somewhat with lipid types and also depend on the exact orientation of the headgroup with respect to axis of the rotation.[9] The isotropic ^{31}P chemical shifts of lipids in a buffer with pH = 7.4 and at a temperature T = 310 K are –2.7 ppm for POPC, –1.7 ppm for DOPE and –2.5 ppm for DOPS.

It has been proposed in the past that during the membrane fusion lipids go through various lipid phases.[10] Figure 3.1 shows the simulated NMR responses for various lipid phases, starting with a powder pattern for multi-lamellar vesicles that are large in diameter and with lipid diffusion across the surface that is slow on the NMR shift anisotropy time scale (Fig. 3.1A). In contrast, aligned lipid bilayers, on glass plates, parallel to the magnetic field with a 0^{o} orientation, yield a single peak with $\sigma \approx \sigma_{II}$ (Fig. 3.1B).[8] The aligned lipid bilayers perpendicular to the magnetic field with a 90° orientation also yield a single peak with $\sigma \approx \sigma_{\perp}$ but at the other extreme of the powder pattern. The orientations that are between these extremes lead to the signals with intermediate chemical shifts, reflecting the tilting of the lipid molecules.

Figure 3.1C shows the simulated response for a cylindrical distribution of orientations with the long axis of the cylinder perpendicular to the field and a diameter of 1 μm.[3] In contrast, for an inverted hexagonal phase, where single

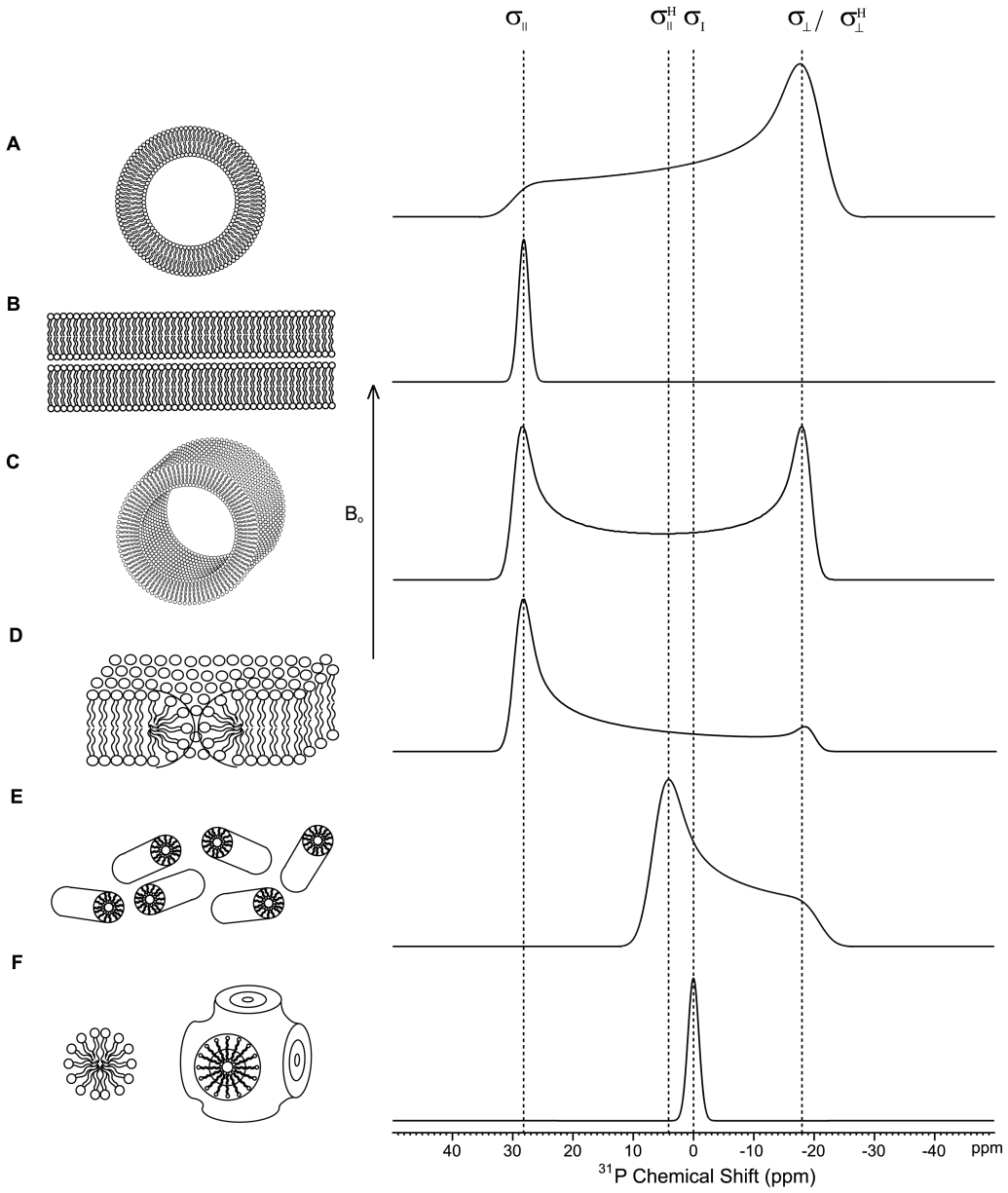

Figure 3.1: ***^{31}P chemical shift anisotropy patterns for lipid phases (schematic).*** *(**A**) Unoriented lamellar phase (MLVs) – lamellar powder pattern. (**B**) Oriented lamellar phase with 0° orientation of lipids and the bilayer normal parallel to the main magnetic field. (**C**) The cylindrical distribution of orientations in which the long axis of the cylinder is perpendicular to the field. (**D**) Toroidal pore where the surface of a pore has a non-lamellar and non-spherical distribution of lipids and the pore is static. (**E**) Hexagonal phase and (**F**) Cubic, Q_{II} or isotropic phase. σ_{II}, σ_I and $\sigma_\perp$ indicate chemical shifts characteristic of the full powder pattern $\sigma_{BPII}{}^H$ and $\sigma_\perp{}^H$ indicate the CSA extremes of the hexagonal powder pattern.*

cylindrical rods have a diameter of only two lipid molecules, lateral diffusion of lipids over the curved surface gives rise to more pronounced averaging of the NMR anisotropy.[11] The toroidal pore has a non-lamellar and non-spherical distribution of lipids where the pore is stabilized by peptides (Fig. 3.1D).[8] Such a static pore would result in a ^{31}P spectrum similar to a reversed powder pattern where the high intensity peak is at the parallel edge and the low intensity maximum is at the perpendicular edge (Fig. 3.1D).[8] Alternatively complicated forms of thermodynamically stable micelle Q_{II} or cubic phases with highly curved surfaces can be formed.[10,12] It is generally assumed that rapid lipid diffusion over these surfaces results in isotropic averaging as shown in Figure 3.1F. Pure cone-shaped lipids give rise to a thermodynamically stable hexagonal (H_{II}) phase (Fig. 3.1E).[12,13]

The ^{31}P NMR line shape of the pure lipid mixture is dominated by signals that are characteristic of oriented and cylindrical type phospholipid phases (Fig. 3.2A).[3] Three narrow signals at 21.3 ppm, 22.5 ppm, and 32 ppm are assigned to 0° oriented PC, PE, and PS in the bilayer phase, respectively, by comparison with values known for the pure lipids.[4,8,9] The broad signal at – 20 ppm and the shoulder at – 24 ppm reveal a cylindrical distribution of orientations in the unaligned phase, with the long axis of the cylinder perpendicular to the field.[3] The other extremes of the cylindrical signals are hidden under the bilayer signals. When the unoriented response is simulated and combined with a set of narrow lines representing the bilayer signal, a remarkably good reproduction of the experimental data is obtained (Fig. 3.2D). With 60% PC and 20% of both PE and PS in the sample, the simulated curves that are generated for different phases of lipids in Figure 3.2D indicate that ~ 64% of the ^{31}P signal is in the unoriented response in a ratio PC:PE:PS ~ 9:3:4, while the analysis of the intensities of the narrow signals translate into relative fractions PC:PE:PS ~ 3:1:1 for the aligned bilayer component (Fig. 3.3). Provided the underlying model of aligned bilayers and cylindrical defects is correct, the composition analysis is accurate to about 5%.

Upon incorporation of the non-fusogenic L16 peptide, which forms stable α-helices[1], the spectrum shows minor, but reproducible, changes (Fig. 3.2B). The PC

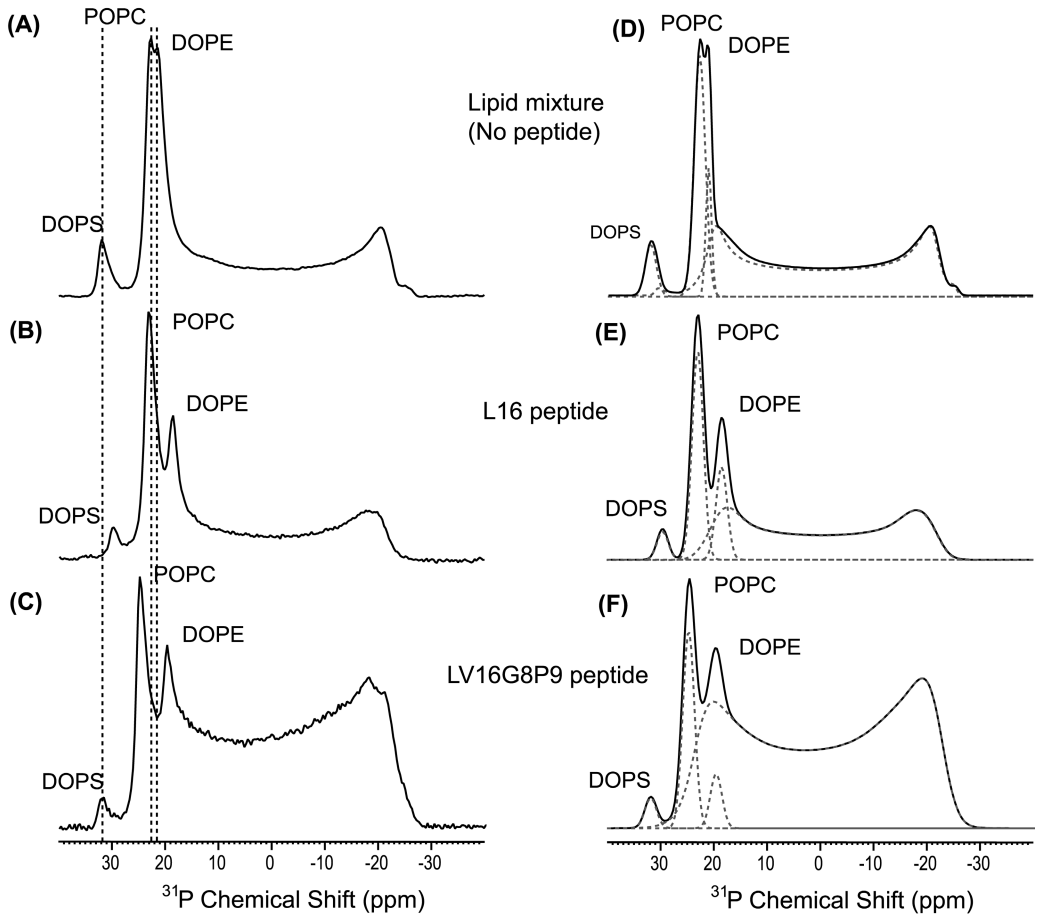

Figure 3.2: *^{31}P spectra of oriented bilayer samples, with the bilayer normal parallel to the magnetic field (left panels). The simulated spectra are shown in the right panels, and are generated by calculating the responses of various lipid species, shown as dotted lines. (**A**) For the lipid mixture spectrum the aligned bilayer component representing ordered lipid molecules has a composition PC:PE:PS ~ 3:1:1 and the cylindrical type response has a composition PC:PE:PS ~9:3:4 (based on the relative amount of each lipid species used in the sample, in a ratio of 60% POPC, 20% DOPS and 20% DOPE). (**B**) Spectrum for the lipid mixture + non-fusogenic peptide L16. The aligned bilayer component, representing ordered lipid molecules, has relative intensities PC:PE:PS ~ 9:3:1 and the cylindrical response has composition PC:PE:PS ~ 7:2:3. (**C**) Lipid mixture + fusogenic peptide LV16G8P9 spectrum. Here the unaligned phase has a major cylindrical component with a small but significant fraction of vesicle type signal, ~ 15%, possibly due to end lipids (F). The relative intensities of PC:PE:PS are ~ 4:1:1 for the aligned and ~ 3:1:1 for the unaligned signals. The Dotted vertical lines are to guide the eye.*

response shifts to 23.2 ppm and a PE peak is present at 18.6 ppm. In addition, the weak PS signal at 32 ppm in Fig. 3.2A shifts to 29.5 ppm in Fig. 3.2B. The broad signal that peaks at –18 ppm again reflects a cylindrical distribution in the unaligned phase and comprises ~ 60% of the lipids (Fig. 3.2 and 3.3). The data can be simulated with a signal ratio PC:PE:PS ~ 9:3:1 for the aligned region and PC:PE:PS ~ 7:2:3 for the unaligned region (Figs. 3.2E and 3.3). Interestingly, when the lipid mixture is loaded with fusogenic LV16G8P9 peptide, strikingly different results are obtained (Fig. 3.2C). The 0° oriented signal has a PC component resonating with $\sigma_{II} \approx 24.5$ ppm while the PE response is shifted to $\sigma_{II} \approx 19.5$ ppm. Here the increased curvature phase has a significant fraction of vesicle type signal, ~ 15%, which is reflected by an anisotropic component in the signal, perturbing the symmetric cylinder line shape (Fig. 3.2F). The asymmetric component may correspond to an increased fraction of end lipids covering the hydrophobic edges of the bilayer. This suggests that cylindrical domains are short and more vesicle-type

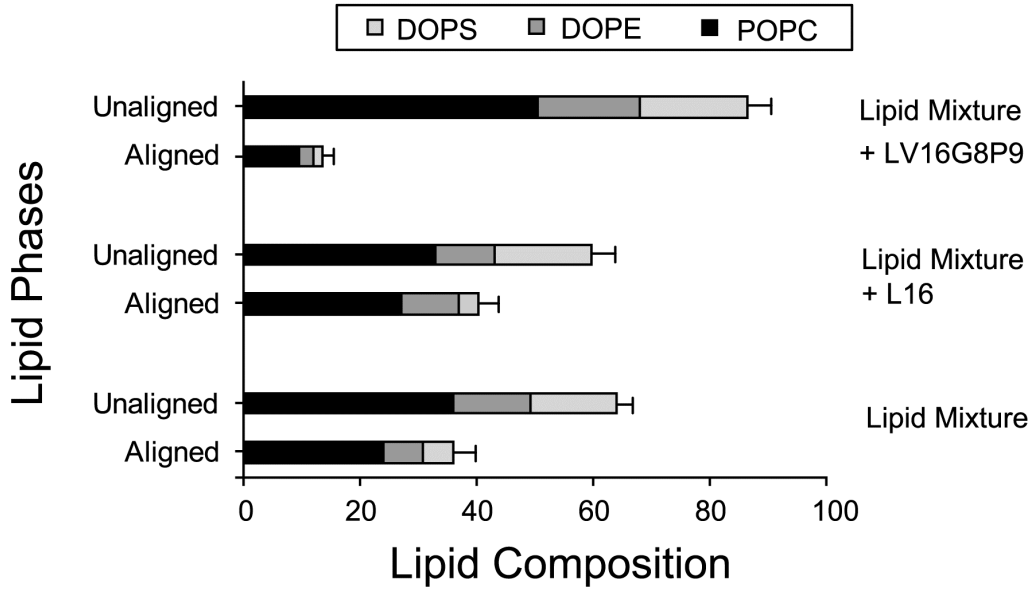

Figure 3.3: *Graphical representation of the lipid composition in the lipid mixture without peptide, the lipid mixture with non-fusogenic peptide L16 (1mol %), and the lipid mixture with fusogenic peptide LV16G8P9 (1mol %). The error bars are based on estimates for the lipid compositions of two independently prepared samples.*

in the presence of the fusogenic peptide (Fig. 3.2F). It is clear that LV16G8P9 stabilizes the high curvature phase relative to the flat bilayer phase. The data are simulated with relative intensities PC:PE:PS ~ 4:1:1 for the flat membrane fraction and PC:PE:PS ~ 3:1:1 for the high curvature component (Figs. 3.2F and 3.3).

To test the effect of peptides on POPC, which is the major component in the lipid mixture, the POPC bilayers are prepared at a peptide:lipid molar ratio of 1:100 (calculated with respect to POPC). Figure 3.4 shows the ^{31}P spectra of POPC bilayers with and without peptides. In the absence of peptide, the POPC bilayers are

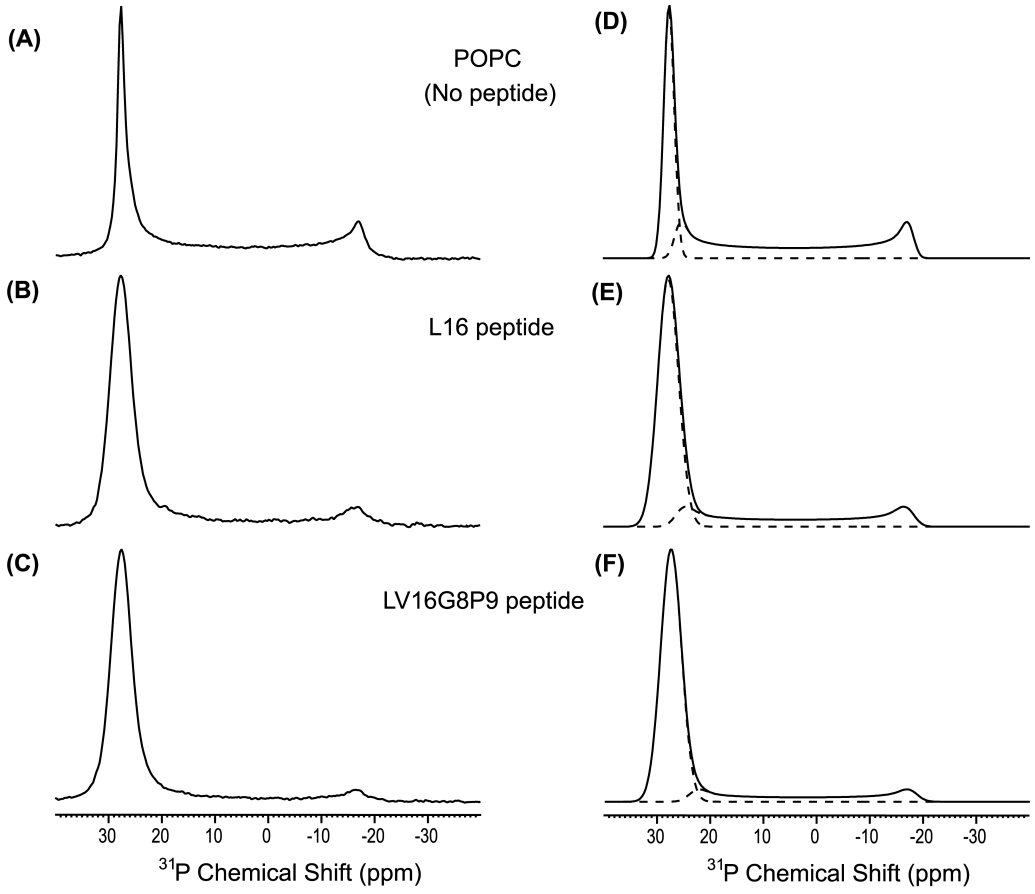

Figure 3.4: *Proton-decoupled Hahn-echo ^{31}P spectra of oriented POPC bilayer, with the bilayer normal parallel to the magnetic field (left panels). The simulated spectra are shown in the right panels, and are generated by calculating the responses of various lipid line shapes, shown as dotted lines. (**A** and **D**) POPC without peptide, (**B** and **E**) POPC loaded with 1% non-fusogenic L16 peptide, (**C** and **F**) POPC with 1% fusogenic LV16G8P9 peptide.*

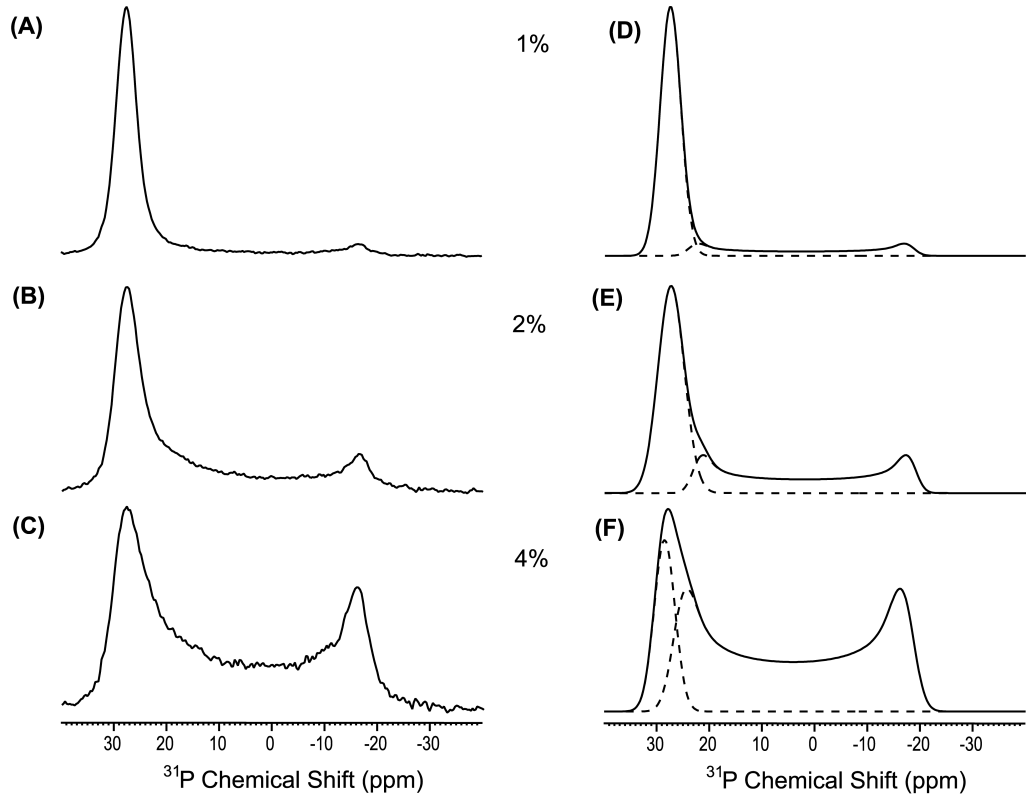

Figure 3.5: *Proton-decoupled Hahn-echo ^{31}P spectra of oriented POPC bilayer loaded with the fusogenic peptide LV16G8P9. The bilayer normal is parallel to the magnetic field (left panels). The simulated spectra are shown in the right panels, and are generated by calculating the responses of various chemical shift anisotropy patterns for lipid phases, shown as dotted lines.* ***(A)*** *POPC loaded with 1% fusogenic LV16G8P9 peptide, the integrated intensities of the simulated ^{31}P signals in* ***(D)*** *translate into ~ 80% for the aligned phase and ~ 20% for the unoriented cylindrical response.* ***(B)*** *POPC with 2% non-fusogenic LV16G8P9 peptide, where the aligned phase has ~ 60% and the unoriented cylindrical response has ~ 20% of lipids. (**C**) POPC with 4% fusogenic LV16G8P9 peptide, the simulated ^{31}P signals in* ***(F)*** *translate into ~ 20% for the aligned phase and ~ 80% for the unoriented cylindrical response.*

aligned, exhibiting a 0° oriented signal at 27 ppm and a broad signal at –18 ppm. The simulated curves in Figure 3.4D indicate that ~ 50% of the ^{31}P signal accounts for the cylindrical response. The addition of non-fusogenic peptide, L16, moderately increases the order in the POPC bilayer where the aligned component represents ~ 70% of the lipids (Figs. 3.4B and E). After addition of the fusogenic peptide,

LV16G8P9, the POPC bilayers becomes well aligned and the cylindrical response accounts only for ~ 20% of lipids (Figs. 3.4C and F).

Figure 3.5 shows the ^{31}P spectra of POPC bilayers with 1-4% LV16G8P9 (calculated with respect to POPC). The increased addition of LV16G8P9 moderately increases the cylindrical response. At 4% LV16G8P9 the spectrum is manifested mainly as a cylindrical line shape which accounts for ~ 80% of the lipids (Figs. 3.5C and E). The broader signal of POPC has been ascribed in the past to wobbling of molecules. Alternatively, it may be related to bulk susceptibility effect. All observations were confirmed by measuring duplicate samples.

3.4 Discussion

Fusion peptides of viral fusogens are thought to catalyze membrane fusion by disturbing the lipid bilayer structure and inducing curvature by peripheral intercalation with lipids.[14] In particular, the fusion peptide of influenza hemagglutinin has been shown to associate laterally with membranes in a mixture of conformations, β-sheet as well as α-helix.[15,16] It can assume a V-shaped form that is thought to be critical for fusion initiation.[15] Finally, molecular dynamic simulations have provided evidence that fusion peptides can promote formation of a convex bulge, which may facilitate close initial contacts of hydrated repulsive membranes and promote exchange of lipids at an early stage of fusion.[17]

According to the data presented here, the biomimetic lipid mixture used is able to form different fluid phases. One phase component is the aligned bilayer, representing ordered lipid molecules, while the other phase produces a cylindrical type ^{31}P response representing unordered lipids. The lipid cylindrical type domains that form the high curvature fraction are likely to be formed from multilamellar bilayers and may have some water in the center.[3] These curved domains are expected to have diameters in the range of 500-1000 nm large, compared to the length scale of ~10 nm of lipid lateral diffusion.[3] At a characteristic diffusion rate of

~10^{-11} m^2/s, small cylinders would give rise to line narrowing of the ^{31}P chemical shift anisotropy.[3] In particular, for an inverted hexagonal phase, the single cylindrical rods have a diameter of about two lipid molecules, and lateral diffusion of lipids over the curved surface gives rise to partial averaging of the NMR anisotropy.[11]

Small vesicles composed of two differently shaped lipids, such as PC and PE, are known to exhibit strong compositional asymmetry between the two monolayers of the highly curved bilayer.[18] This asymmetry reduces the frustration between the two monolayers.[19] According to the analysis of Figure 3.3 the high curvature phase appears to contain less PC, while the flat membrane phase is PC enriched relative to the overall composition PC:PE:PS of 3:1:1. In the unoriented cylindrical fraction, the PE lipid molecules that prefer negative curvature may favor the inner layer while PS lipids that prefer zero to positive curvature in the hydrated state may predominate in the outer layer. On the other hand, PC is thought to have neither strong preference for the positively curved (outer) nor for the negatively curved (inner) monolayer.[12]

Thus, it appears that the fusogenic LV16G8P9 peptide strongly induces increased curvature, relative to either the pure or the L16-containing lipid mixtures. Obviously the fusogenic peptide can induce excess membrane curvature provided that the bilayer contains PE and/or PS in addition to POPC. Thus the data indicate an intimate interplay between the fusogenic peptide and lipid component(s) that is required for a phase change to occur. In particular, the cone-shaped PE is known to favor membrane fusion, which is attributed to its ability to support negative bilayer curvature in fusion intermediates. Both, PE and PS have indeed been shown to enhance liposome fusion that is driven by peptides that correspond to SNARE transmembrane domains. Recently, enhanced stabilization of cylinder type structures has also been observed for antimicrobial peptides in interaction with a two component POPC/POPG model system.[3] Peptide-induced lipid tubule formation has been reported for a *de novo* designed 18-residue amphipathic helical peptide[20] and for gramicidin D.[21] Further, the unoriented phase of the sample with peptide

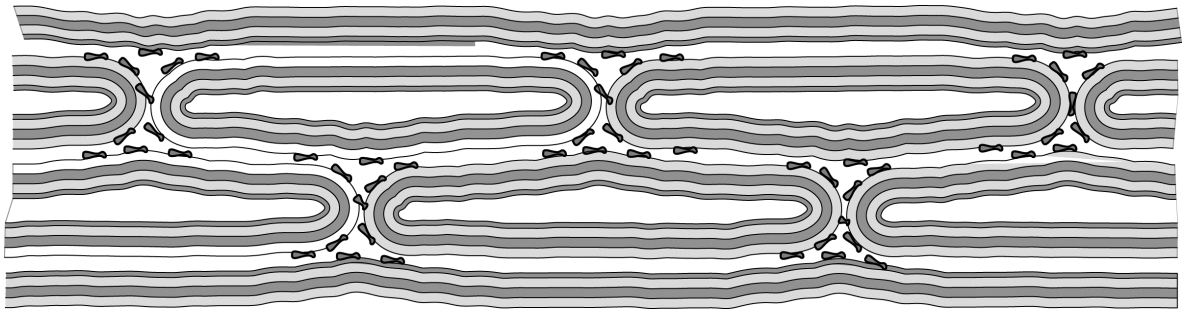

Figure 3.6: *Graphical representation of defects in a lipid multilayer system induced by the fusogenic peptide LV16G8P9 (1mol %). In this model the peptide is thought to interact with the positive curvature of the outer layers of cylindrical type lipid arrangements (schematic). The multilayer thickness is most probably less than 1 μm.*

LV16G8P9 also contains less PC than the aligned phase but the ratio PC:PE:PS ~ 50:18:18 appears somewhat closer to 3:1:1 than for the pure lipid system.

Fusogenic LV16G8P9, with its structural instability due to the presence of the GP, might alter the balance of stresses by promoting positive curvature while intercalating with lipid headgroups of the outer layer (Fig. 3.6). A positive curvature of the outer layer can be accommodated by a partial release of lateral stresses and interfacial tensions due to accumulation of the PE in the inner layer to promote negative curvature on the inside. Circular dichroism measurements indicate that LV16G8P9 exists mainly in β-sheet and turn conformation in liposomes which would be consistent with inducing curvature by peripheral association with the outer layer.[22] Hence, the LV16G8P9 peptide may induce membrane fusion by induction of local positive curvature as proposed for natural viral fusion peptides. In case of fusogenic peptides the proposed architecture of the lipid/peptide arrangement is like pancakes that may give rise to cylinder-type edges (Fig. 3.6). The growing stalks shown in Figure 3.6 are in a way two multilamellar half-cylinders that can give rise to a cylindrical type ^{31}P response.

In the model system, the water fraction in the sample is too small to stabilize intact vesicles that can undergo fusion.[19] Yet the anisotropic NMR response reveals excess curvature at low water content, which is considered a prerequisite for

fusion.[1,23] This is interesting in terms of the *stalk hypothesis,* a widely accepted model for fusion, which derives from the original proposal that two bilayers brought into close contact can merge their contacting (*cis*) monolayers in a "stalk" that joins the adjacent components of the two original bilayers while distal (*trans*) monolayers of this structure are not merged. For instance, a recent observation of the formation of stalk structures shows that lipid systems that promote negative curvature at low humidity can also reduce the energy barrier for a close approach of the bilayers.[1,23] It has been shown that during membrane fusion lipids go through various phases and lipidic rearrangement proceeds to the formation of a hemifusion intermediate, which precedes the membrane fusion.[10] How exactly the fusogenic peptide does this is a matter of further investigation.

In summary, solid state NMR studies on mechanically aligned bilayers made up of a biomimetic three-lipid mixture show that a strong perturbation of the lipid bilayer can be induced by a small fraction of a synthetic peptide, which suggests that this is an important marker for fusogenic peptide behavior. Considering the complexity of a three lipid system and the role of the peptides in interaction with the inner and outer monolayers of the membrane, the experimental data are of surprisingly high quality and can be analyzed in a consistent manner. The data lead to the conclusion that small changes in the peptide content or character can cause significant and cooperative changes in membrane conformation, which is consistent with the picture of peptide-regulated fusion events. This may be of use in future assays of the interaction of low complexity peptides with membranes, for instance in the study of low complexity protein fragments involved in misfolding diseases like Alzheimer.

References

1. Yang, L.; Huang, H. W., *Science,* **2002,** 297, 1877-79.
2. Hofmann, M.; Weise, K.; Ollesch, J.; Agrawal, P.; Stalz, H.; Stelzer, W.; Hulsbergen, F.; de Groot, H.; Gerwert, K.; Reed, J.; Langosch, D., *Proc. Natl. Acad. Sci. U.S.A.,* **2004,** 101, 14776 - 81.
3. Buffy, J. J.; McCormick, M. J.; Wi, S.; Waring, A.; Lehrer, R. I.; Hong, M., *Biochemistry,* **2004,** 43, 9800-12.
4. Hallock, K. J.; Lee, D. K.; Ramamoorthy, A., *Biophys. J.,* **2003,** 84, 3052-60.
5. Deutsch, J. W.; Kelly, R. B., *Biochemistry,* **1981,** 20, 378-85.
6. Rance, M.; Byrd, R. A., *J. Mag. Reso.,* **1983,** 52, 221-40.
7. Wildman, K. A. H. The Mechanism of Lipid Bilayer Disruption by the Human Antimicrobial Peptide, LL-37. University of Michigan, Ann Arbor, 2003.
8. Wildman, K. A. H.; Lee, D. K.; Ramamoorthy, A., *Biochemistry,* **2003,** 42, 6545-58.
9. Pearce, J. M.; Komoroski, R. A., *Magn. Reson. Med.,* **1993,** 29, 724-31.
10. Siegel, D. P., *Biophys. J.,* **1999,** 76, 291-313.
11. Picard, F.; Paquet, M. J.; Dufourc, E. J.; Auger, M., *Biophys. J.,* **1998,** 74, 857-68.
12. Killian, J. A.; de Planque, M. R. R.; van der WeI, P. C. A.; Salemink, I.; de Kniijff, B.; Greathonse, D. V.; Koeppe II, R. E., *Pure Appl. Chem.,* **1998,** 70, 75-82.
13. Seddon, J. M., *Biochim. Biophys. Acta,* **1990,** 1031, 1-69.
14. Wasniewski, C. M.; Parkanzky, P. D.; Bodner, M. L.; Weliky, D. P., *Chem. Phys. Lipids,* **2004,** 132, 89-100.
15. Li, Y.; Han, X.; Lai, A. L.; Bushweller, J. H.; Cafiso, D. S.; Tamm, L. K., *J. Virol.,* **2005,** 79, 12065-76.
16. Huang, Q.; Chen, C. L.; Herrmann, A., *Biophys J,* **2004,** 87, 14-22.
17. Lague, P.; Roux, B.; Pastor, R. W., *J. Mol. Biol.,* **2005,** 354, 1129-41.
18. Lipowsky, R., *Curr. Opin. Struc. Biol. ,* **1995,** 5, 531-40.
19. Safran, S. A.; Pincus, P. A.; Andelman, D.; Mackintosh, F. C., *Phys. Rev. A,* **1991,** 43, 1071-78.
20. Lee, S.; Furuya, T.; Kiyota, T.; Takami, N.; Murata, K.; Niidome, Y.; Bredesen, D. E.; Ellerby, H. M.; Sugihara, G., *J. Biol. Chem.,* **2001,** 276, 41224-8.
21. Moll, F., 3rd; Cross, T. A., *Biophys. J.,* **1990,** 57, 351-62.

22. Langosch, D.; *et. al.*, **Manuscript Submitted**.

23. Yang, L.; Ding, L.; Huang, H. W., *Biochemistry,* **2003,** 42, 6631-35.

4

Contrasting biomimetic lipids rearrangements induced by low-complexity peptides involved in membrane fusion: extended cylindrical curvature regions versus toroidal pore signals.*

Membrane fusion requires restructuring of lipid bilayers mediated by fusogenic membrane proteins. Evidence has been obtained that peptides mimicking the transmembrane part of these proteins can drive membrane fusion by disturbing the lipid bilayer structure and by inducing curvature. Here, a direct approach is taken to test this hypothesis using the hydrophobic model TMS sequences that were prepared as mentioned in chapter 2. The hydrophobic sequences that are made up of mixtures of helix- and sheet-promoting residues plus helix-destabilizing residues with a length of 23 amino acids are most fusogenic, which is paralleled by a large degree of phase separation across the lipid bilayer as observed in the ^{31}P 2D spectrum. ^{31}P 1D spectra of oriented samples show that the peptides induce different phases in bilayers, which correlates with their fusogenic behavior. The data confirm that the stabilization of curved bilayers by a peptide due to phase separation *across* the lipid bilayer is a prerequisite for the fusogenic behavior. In contrast, non-fusogenic peptides appear to stabilize aligned bilayer structures or possibly toroidal pores.

---

* Manuscript is submitted for publication

4.1. Introduction

It is now known that membranes are heterogeneous mosaics of lipid domains with distinct and malleable identities, which have active roles in dynamic vesicle trafficking, signaling, and protein localization and function.[1] In order to maintain the structural integrity of intracellular compartments and of the cell itself, membranes do not fuse easily under normal circumstances. Membrane fusion implies that two phospholipid bilayers are merging in an aqueous environment and can be triggered by a variety of integral membrane proteins such as SNAREs and viral fusion proteins.[2-4] The TMSs of these proteins play a direct role in fusion as indicated by recent *in vivo* studies.[5-7] Further, *in vitro* studies show that membrane-embedded synthetic model TMS-peptides with low-complexity sequences derived from the natural system can drive liposome-liposome fusion depending on the structural flexibility of their secondary structure. Thus fusion does not necessarily involve many proteins interacting in complex ways.[8]

During fusion major rearrangements of lipid structures occur in a confined region of inter bilayer contact. It has been proposed that lipids go through various phase changes, starting with multi-lamellar vesicles to thermodynamically highly stable cubic phases or hexagonal tubes.[9,10] Fusion can be regarded as primarily mediated by phospholipids, with the role of the proteins restricted to reducing the activation energy and spatially organizing the fusion site.[11] This model assumes that lipids line the fusion pore. A recent review on the role of non-bilayer-forming lipids in biological fusion concludes that the lipid composition affects the fusion downstream to the activation of the fusion proteins and upstream to fusion pore formation and that the ability of fusion-promoting lipids is strongly correlated with their geometrical shape.[11] In addition, there is converging experimental evidence that the major energy barrier for fusion is due to bringing membranes close together by removal of water, in conjunction with the formation of high curvature necessary to reach the stalk intermediate stage that leads to hemifusion.[12]

Nature uses specialized peptides to achieve fusion, and how these peptides manage to fuse lipid membranes is one of the fundamental questions in cell biology. Recent studies on membrane fusion provide useful insight into the membrane fusion intermediates but they did not address the interaction of peptides with lipids.[10] To investigate this, a direct approach is taken to study *de novo* designed hydrophobic model TMS peptides, which are analyzed with respect to their membrane fusogenicity and secondary structures (Table 4.1).[8] All peptides have a central hydrophobic core, consisting of a (Leu and/or Val)$_n$ repeating unit, where n= 6 or 16. Each peptide is flanked on either side by 3 Lys or His to enhance the peptide incorporation in the lipid bilayer and terminated by one Trp residue for the quantification (Chapter 2).

The peptides are divided into two sets; one is based on the length of the hydrophobic core and the other class has different composition within the hydrophobic core. For the first set the hydrophobic core length varies between 12 residues in the LV12 peptide to 24 residues in the LV24 peptide (Table 4.1).

Set 1: Length dependency	
LV12	K K K W **L V L V L V L V L V L V** K K K
LV16	K K K W **L V L V L V L V L V L V L V L V** K K K
LV20	K K K W **L V L V L V L V L V L V L V L V L V L V L V** K K K
LV24	K K K W **L V L V L V L V L V L V L V L V L V L V L V L V L V L V** K K K
Set 2: L/V ratio	
L16	K K K W **L L L L L L L L L L L L L L L L** K K K
LV16	K K K W **L V L V L V L V L V L V L V L V** K K K
LLV16	K K K W **L L V L L V L L V L L V L L V L L V** K K K
LV16G8P9	K K K W **L V L V L V L G P V L V L V L V** K K K

Table 4.1: *The chosen sets of peptides that are used in this study.* ***Set 1*** *comprises the peptides with lengths between 19 residues and 31 residues.* ***Set 2*** *consists of peptides with the same hydrophobic length but with different composition of the inner hydrophobic core.*

This variation in length can provide insight into the effect of the length of the TMS part of peptides on their fusogenicity. The most fusogenic peptide in this series, LV16, has a strong tendency to aggregate, which can strongly quench the fusogenic activity. The aggregation problem can be partially overcome with the second set of peptides with various Leu-to-Val ratios. The hydrophobic core contains a secondary structure breaking GP pair, LV16G8P9 (Table 4.1).

Solid state NMR is a powerful tool for determining the structure and dynamics of membranes and their interaction with proteins or peptides. In addition, the microscopic phase properties of membranes can be investigated by ^{31}P solid state NMR.[13-17] Oriented bilayers can be prepared from a variety of lipid mixtures to mimic specific biomembranes, including bacterial, mammalian and myelin cell membranes.[14] The spectral line shapes of proton-decoupled ^{31}P spectra of phospholipid membranes have been used to analyze the orientational order of the phospholipid head group.[18] By using macroscopically oriented membranes, which have much better resolved ^{31}P resonances than unoriented powder samples, lipid domains with different mobilities and morphologies can be distinguished (See Chapter 3, Fig. 3.1). The principle advantage of ^{31}P NMR studies on this system is in the similarity of the conditions used for sample preparation with the functional fusion assays, by using a synthetic lipid mixture mimicking the natural system. In addition, earlier described solid state NMR studies on mechanically aligned bilayers made up of a biomimetic three-lipid mixture already showed that a strong perturbation of the lipid bilayer can be induced by a small fraction of a synthetic peptide, which suggests that this is an important marker for fusogenic peptide behavior (Chapter 3).

In nature, membranes are made up of multiple constituents and very little is known about them. Modeling of the mechanism of membrane fusion mainly by simple model systems composed of one lipid species or with binary mixtures, such as pure PS, pure PC, PC/PE or PC/PS, is not sufficient. The lipid compositions and phase behavior of natural membranes can be very complex, with different lipids likely having different roles in membrane function. Phosphatidylcholine (PC), one of

the major lipid species of mammalian membranes, forms a stable bilayer (See Fig. 1.4, Chapter 1). Phosphatidylethanolamine (PE), a second major component of mammalian membranes, has a cone-shaped molecular structure and the ability to promote the bilayer-to-hexagonal phase transition that is thought to facilitate membrane fusion (See Fig. 1.4, Chapter 1).[11] The role of PS in biomembrane fusion may be in binding or activating some of the several proteins that facilitate assembly of fusion complexes and facilitate the lipid rearrangements required during the fusion process.

Hence fusion induced by peptides is a multifactorial process and synthetic control over the peptide primary structure, combined with an assay of peptide fusogenicity can help to resolve mechanisms of membrane fusion. Fusion is strongly related to the intrinsic phase behavior and high curvature induction in a multi-component lipid system. The aim of the studies in this chapter is to address the effect of *de novo* designed peptides on structural changes of the biomimetic lipid membrane, which will contribute to better understanding of how the phase behavior of lipids is involved in membrane fusion.

4.2 Materials and methods

POPC, DOPS and DOPE were purchased from Avanti Polar Lipids, Birmingham, AL. Peptides were either synthesized according to the procedures mentioned in chapter 2 or commercially obtained from PSL, Heidelberg, Germany, and purified to >90% by high-performance liquid chromatography, as determined by mass spectrometry. Concentrations of peptide solutions were determined via tryptophan absorbance at 294 nm in a 1:1 (v/v) mixture of trifluoroethanol and dimethyl sulfoxide using an extinction coefficient of 5600 $M^{-1}cm^{-1}$.

4.2.1 Preparation and fusion of small unilamellar liposomes.

Liposomes were prepared from mixtures of egg PC /brain PE /brain PS at a ratio of 3:1:1 (w/w/w) with or without 0.8% (w/w) of NBD-PE and Rh-PE (Molecular Probes).[19] Lipid solutions in chloroform, with or without TMS-peptides, which were first dissolved in trifluoroethanol, were dried under a stream of nitrogen to a thin film and rehydrated with a fusion buffer (25 mM Tris-HCl, pH 7.4, 150 mM NaCl, 0.1 mM EDTA, 5 mM DTT). Liposomes were formed using sonicated (Bransonic Sonifier W450 cup horn) for 8 min while cooling with ice. The sample was centrifuged at 16000 × *g* for 20 min to remove lipid aggregates. Peptide/lipid ratios were determined after separation of peptides from proteoliposomes by density-gradient centrifugation.[7] The liposomes were lyzed with 1% (wt/vol) SDS and the amount of lipid-associated peptide was determined using the Trp fluorescence at λ_{ex} = 294 nm of the top fractions.

4.2.2 Fusion assay.

Fusion assays were performed using the fluorescence dequenching method.[19] Briefly, 'donor' liposomes containing fluorescence labels and unlabeled 'acceptor' liposomes (2.5 mg/ml phospholipid) were mixed at a ratio of 1:4 (v/v) on ice, transferred to 96-well white Corning non-binding plates with translucent bottoms and heated for 2 min by floating the plates on water at 310 K using a water bath. NBD fluorescence is immediately assayed at 1 min intervals for 60 min at 310 K. Initial rates of fusion were obtained by fitting the first 10 minutes of the kinetics using ORIGIN software (OriginLab Corporation, Northampton, MA) with a polynomial function and determining its first derivative. All values are corrected for detergent quenching, which was below 4%. The peptide-independent, spontaneous fusion of pure liposomes was routinely determined in parallel and subtracted from the values obtained with peptide-containing liposomes.

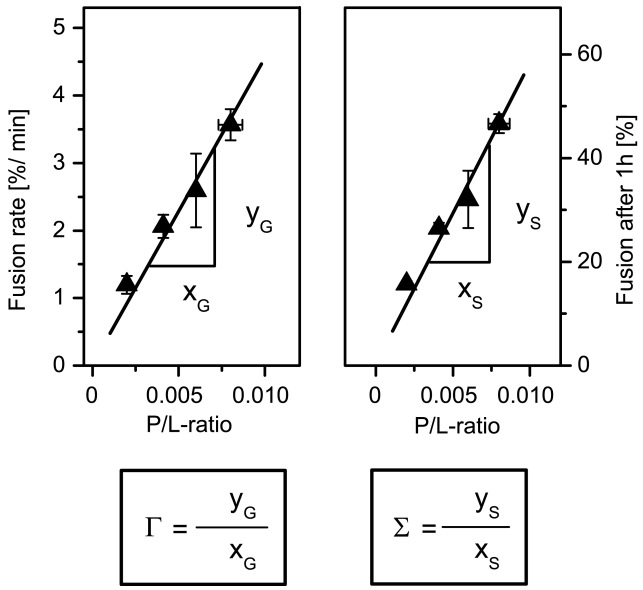

Figure 4.1: *Parameters of fusogenicity generated through the slopes of the linear regressions. Γ is the slope obtained after plotting the fusion rate against the P/L-ratio and Σ is the slope obtained after plotting fusion extent against the P/L-ratio.*

Fusogenicity assays can be obtained in two ways that are mutually consistent. To obtain a parameter that is independent of the P/L ratio, we calculated the slopes, Γ and Σ, of the dose/response relationships. In this way a general dimensionless measure for initial rates and extents of fusion for each peptide can be extracted from the data. Γ represents here the fusogenicity derived from the fusion rate and Σ measures the extent of fusion after 1 hour.[8] Background fusion of the liposomes without peptide was subtracted prior to performing the analysis.

4.2.3 Sample preparation

Samples for solid-state NMR studies were prepared by dissolving POPC, DOPE and DOPS in chloroform in a 3:1:1 ratio. A peptide dissolved in trifluoroethanol was added in a 1:100, peptide: lipid molar ratio. The mixtures were applied onto 15 ultra thin cover glasses (6.2 × 20 mm²; Paul Marienfeld GmbH and Co. KG, Lauda-Konigshofen, Germany), first dried under a stream of nitrogen, and

kept overnight in high vacuum. Subsequently, the plates were hydrated by spraying with fusion buffer containing 150 mM NaCl, 20 mM Tris, and 0.2 mM EDTA (pH 7.4). The plates with peptide–lipid films were equilibrated at 4°C for 72 hours and then stacked on top of each other. The stacks were stabilized at 4°C for 6 hours and sealed with Teflon tape and plastic wrappings to prevent dehydration.

4.2.4 NMR spectroscopy

The samples were inserted into a multichannel flat coil probe head and placed in a Bruker AV750 spectrometer with the membrane normal oriented parallel to the magnetic field direction. Proton-decoupled ^{31}P solid-state NMR 1D spectra were recorded using a Hahn echo pulse sequence with a 90° pulse length of 7.8 μs, an echo delay of 40 μs, 6K scans of 1K data points with a spectral width of 94.339 kHz, and a recycle delay of 3 s.[20] For the oriented lipid mixture without peptide, a sample ^{31}P 1D spectrum was recorded with the alignment axis at 90°, i.e. perpendicular to the magnetic field direction. A line broadening of 10 Hz was applied before Fourier transformation. The spectra were processed without first order phase correction and calibrated to $(NH_4)_2HPO_4$ at 0 ppm chemical shift. The NMR measurements were performed using similar conditions of pH 7.4, at a temperature of 310K and with ~ 30 min of equilibration time in the spectrometer before recording the data. Spectra were collected over 30 min intervals to monitor changes. Proton-decoupled ^{31}P-^{31}P 2D NOESY solid-state NMR spectra were recorded using various mixing times τ_m ranging from 250ms to 500ms and with an acquisition time of 12h.

4.3. Results

The series of peptides with different length and composition were studied for fusogenic activity by standard fluorescence dequenching assays.[8,21] This assay is based upon fluorescence resonance energy transfer from NBD-PE to Rh-PE present

at quenching concentrations in donor liposomes. Upon fusion of labeled with unlabeled liposomes the average distance between the fluorophores, and thus NBD-fluorescence, increases over time and is taken as a measure of fusion. Figure 4.1 and 4.2 compare the membrane fusogenicity of different peptides where initial fusion rates Γ reflect the probability by which a random liposome-liposome collision turns into a productive fusion event. Fusion as seen after 1 h of incubation reflects the sum of all fusion events within this time period.

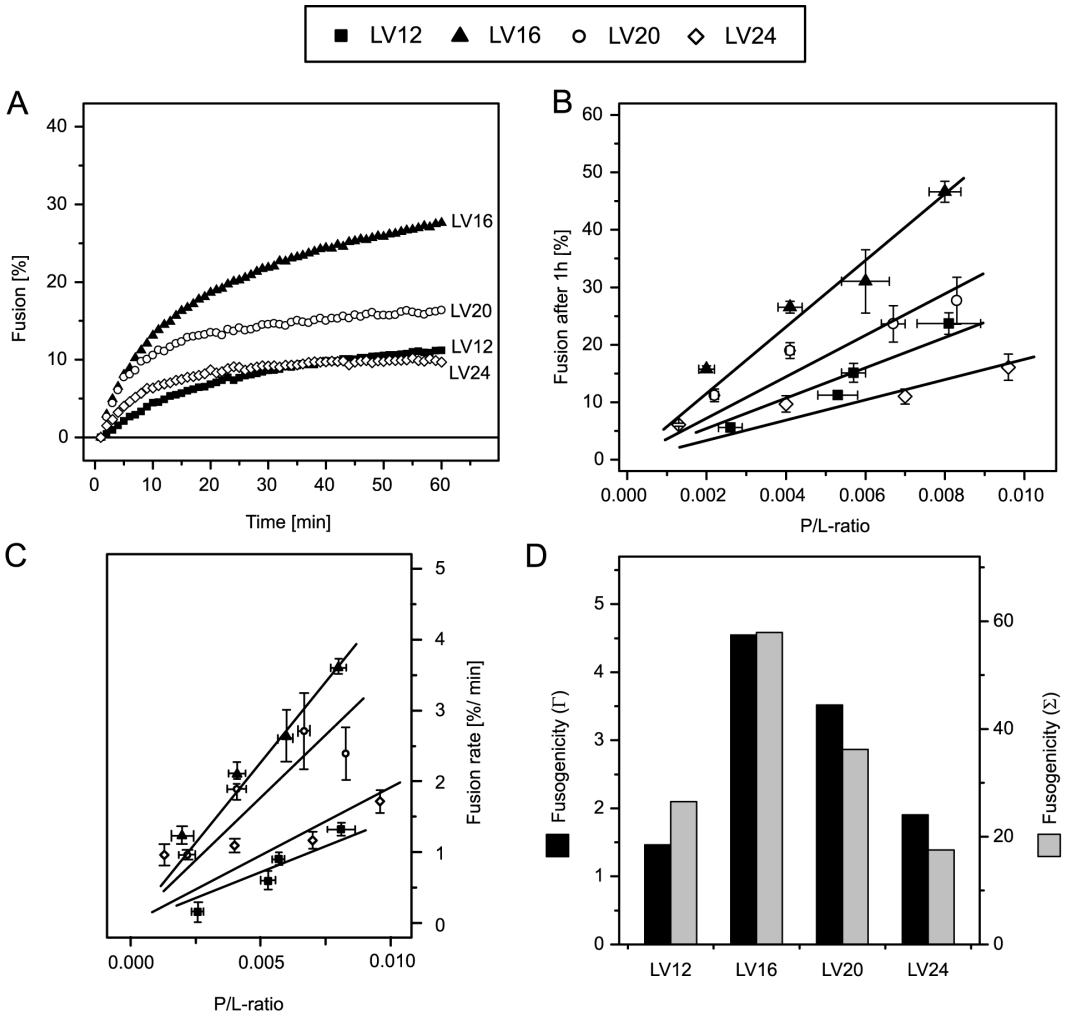

Figure 4.2: *Fusogenic activity of peptides of different hydrophobic length.* ***(A)*** *Typical fusion kinetics at P/L = 0.005.* ***(B)*** *The fusion values after one hour (Σ) and* ***(C)*** *the initial fusion rates from kinetics (Γ) both correlate linearly with the experimentally determined P/L-values.* ***(D)*** *Comparison of fusogenicities of peptides with the same hydrophobic length, determined as described in Fig. 4.1.*

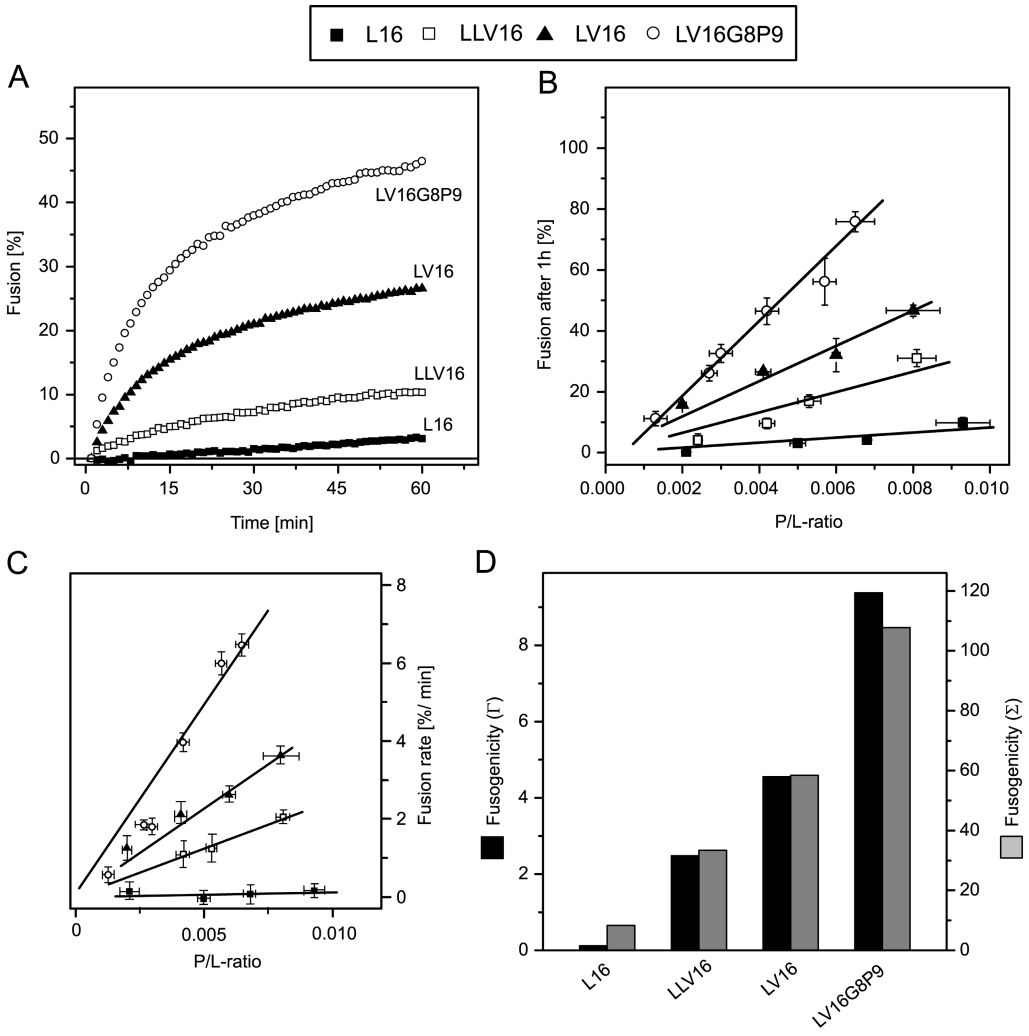

Figure 4.3: *Fusogenic activity of peptides with the same hydrophobic length having different core sequences.* ***(A)*** *The fusion kinetics is recorded at P/L = 0.005 and fusion values after one hour (Σ) at different P/L ratio is shown in* ***(B).*** *The initial fusion rates (Γ) from kinetics correlate linearly with the experimentally determined P/L-values shown in* ***(C)****. The comparison of fusogenicities for peptides with the same hydrophobic length is shown in* ***(D)****.*

The membrane phase behavior can be monitored using ^{31}P NMR spectroscopy since the chemical shift tensor properties reflect the symmetry of the dynamic order of lipid molecules in a very characteristic manner.[14] This property can be used to analyze the effect of the peptides on the membrane system. The isotropic ^{31}P chemical shifts of lipids at pH = 7.4 and at a temperature T = 310 K are –2.7 ppm for POPC, –1.7 ppm for DOPE and –2.5 ppm for DOPS. Here, the distribution of lipid

phases without peptides or upon incorporation of the peptides is compared at a molar peptide/lipid ratio of 0.01 as previously used in fusion assays.[8]

The ^{31}P NMR line shape of the biomimetic pure three-lipid mixture in fusion buffer is dominated by signals that are characteristic for oriented and unoriented phospholipid bilayers (Fig. 3.2A).[22] Three narrow signals at 21.3 ppm, 22.5 ppm, and 32 ppm are assigned to 0° oriented PC, PE, and PS in the bilayer phase, respectively, by comparison with values known for the pure lipids.[14,23,24] The broad signal at –20 ppm and the shoulder at –24 ppm indicate the presence of cylindrical type lipid arrangements in the unoriented phase, with the long axis of the cylinder perpendicular to the field.[22] Figure 3.2D shows how the relative fractions PC:PE:PS ~ 24:7:5 can be estimated using simulated curves generated for different phases of lipids, as in the aligned region, leading to a PC:PE:PS ~ 36:13:15 ratio in the lipid cylinder phase. To confirm that the –20 ppm signal in the spectrum does not have residual anisotropy, the ^{31}P spectra of the same samples rotated by 90° with the glass plate normal perpendicular to B_0 were measured (Fig. 4.4). The narrow signal consists of 35% of the lipids while the broad signal reflects a cylindrical and vesicle type distribution in the unoriented phase, which comprises ~ 65% of the lipids.

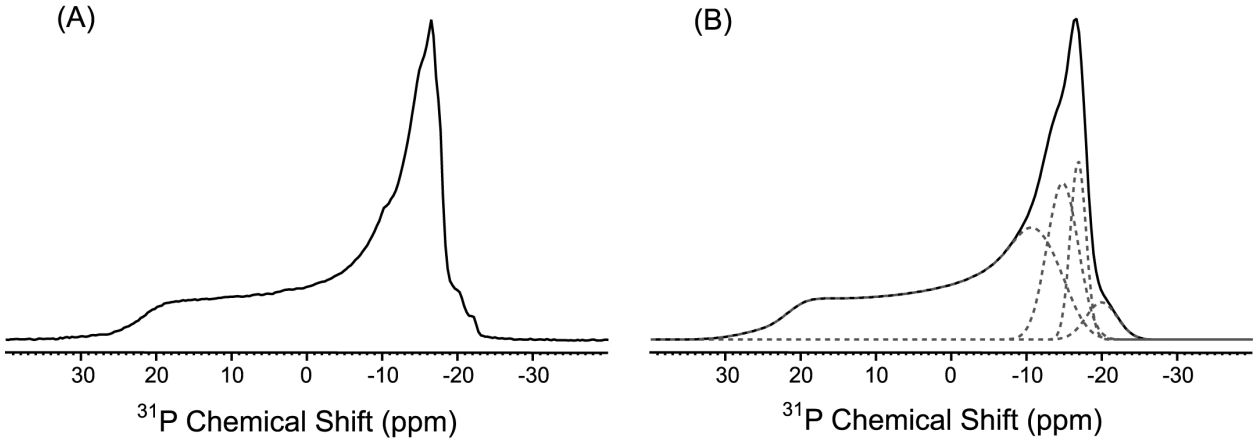

Figure 4.4: ***(A)*** *^{31}P spectrum of the oriented lipid mixture, with the bilayer normal perpendicular to the magnetic field B_0.* ***(B)*** *The simulated spectrum is generated by calculating the responses of various lipid species, shown as dotted lines. The data were recorded at 310 K and pH = 7.4 with 6 K scans.*

4.3.1. Fusogenic activities and membrane phase behavior of different lengths of peptides

The length of the TMS in a fusion protein is an important factor determining its functionality and the first *de novo* set of synthetic mimics comprises middle cores of alternate Leu and Val with different lengths (Table 4.1, Set 1).[5-7] Figure 4.3 compares the membrane fusogenicity of peptides with a middle core of 12 residues (LV12), 16 residues (LV16), 20 residues (LV20) or 24 residues (LV24). The resulting dose/response relationships, Γ and Σ reveal that both the rate and the extent of fusion increase linearly with the P/L ratios. Interestingly, the fusogenicity depends strongly on the length of the hydrophobic core. While peptides with a hydrophobic core containing 20 or 24 amino acids are virtually non-fusogenic, the peptide with the 12-residue hydrophobic core, LV12, exhibits intermediate fusogenicity and the peptide with the 16-residue hydrophobic core, LV16, shows strong fusogenicity (Fig. 4.2).

Oriented bilayers show reproducible changes upon incorporation of the peptides with different lengths (Fig. 4.5). After addition of non-fusogenic peptides LV12 and LV20, the 0° orientation signal of the POPC response shifts to $\sigma_{B//}$ = ~ 21 ppm and a DOPE peak is present under this peak. In case of LV24, the POPC response shifts to 25.11 ppm with a DOPE component resonating with $\sigma_{B//} \approx 20.86$ ppm. In addition, a weak DOPS signal is observed at 32 ppm for the lipid bilayer (See Fig. 3.2A). This signal shifts to ~ 38 ppm upon loading with LV24 and for LV12 it shifts to ~ 31.4 ppm (Figs 4.5A and D). The broad signal at ~ –18 ppm is less intense than for the pure lipid system, indicating a stabilization of the bilayer and a toroidal pore component for LV12 and LV20 samples (Fig. 4.5). For LV24 the broad signal that peaks at –18 ppm reflects a cylindrical distribution in the unoriented phase, which comprises ~ 60% of the lipids (Figs 4.5H and 4.6). The data can be simulated for the LV24 sample signal ratios PC:PE:PS ~ 7:2:1 for the aligned region and PC:PE:PS ~ 8:3:4 for the unoriented region (Figs 4.5H and 4.6). In case of LV12 the relative intensities of PC:PE:PS are ~ 10:2:1 in the aligned region, while the toroidal pore fraction represents ~ 74% of the lipids with relative

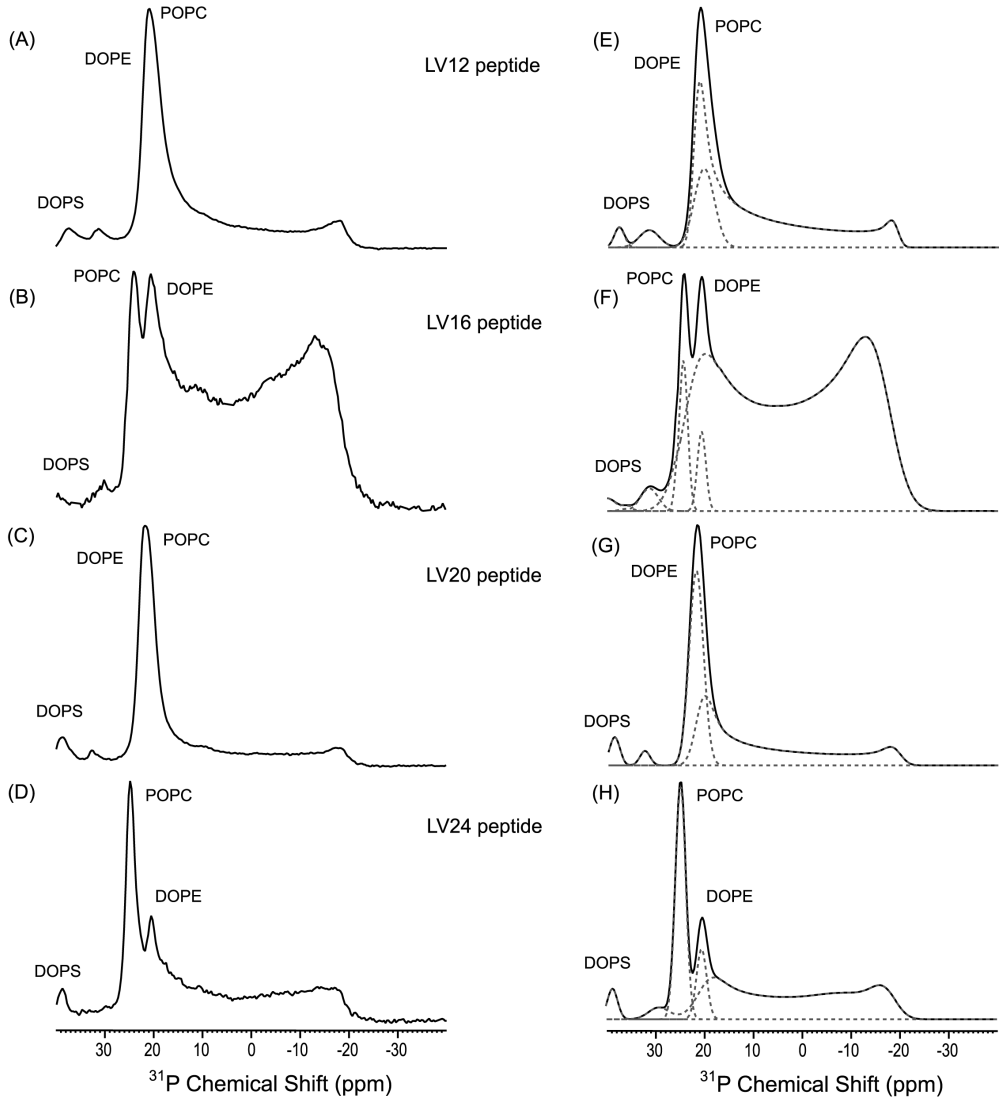

Figure 4.5: *^{31}P spectra of oriented bilayer samples loaded with peptides of different hydrophobic length and with the bilayer normal parallel to the B_0 are shown in the left panel. The right panel contains the simulated spectra that are generated by calculating the responses of various lipid species, shown as dotted lines. The spectrum for the lipid mixture loaded with non-fusogenic peptide LV12 is shown in* ***(A)****, while* ***(B)*** *shows the data for the lipid mixture containing the fusogenic peptide LV16. Spectra of lipid mixtures with non-fusogenic peptides LV20 or LV24 are shown in* ***(C)*** *and* ***(D)****, respectively.*

intensities PC:PE:PS ~ 5:2:2 (Figs. 4.5E and 4.6). On the other hand LV20 has PC:PE:PS ~ 20:1:2 in the aligned region and ~ 54% of lipids in the toroidal pore lipid component representing PC:PE:PS in a ~ 5:4:4 ratio (Figs. 4.5G and 4.6).

In contrast, when the peptide LV16 is incorporated in the lipid bilayer the 0° orientation signal of DOPE is shifted to $\sigma_{BII} \approx 20.6$ ppm with a POPC component resonating with $\sigma_{BII} \approx 24.08$ ppm (Fig. 4.3B and 4.5B). Here the high curvature phase has a significant fraction of vesicle type signal, ~ 11%, which is reflected by an anisotropic component in the signal, perturbing the symmetric cylinder line shape (Fig. 4.5F). The anisotropic component may correspond to an increased fraction of end lipids covering the hydrophobic edges of the bilayer. This suggests that the cylindrical structures become more vesicle-type in the presence of the fusogenic peptide (Fig. 4.5F). It is clear that LV16 stabilizes the high curvature phase relative to the flat bilayer phase. The data are simulated with relative intensities PC:PE:PS ~ 6:3:1 for the flat membrane fraction and PC:PE:PS ~ 3:1:1 for the high curvature component (Figs. 4.5F and 4.6).

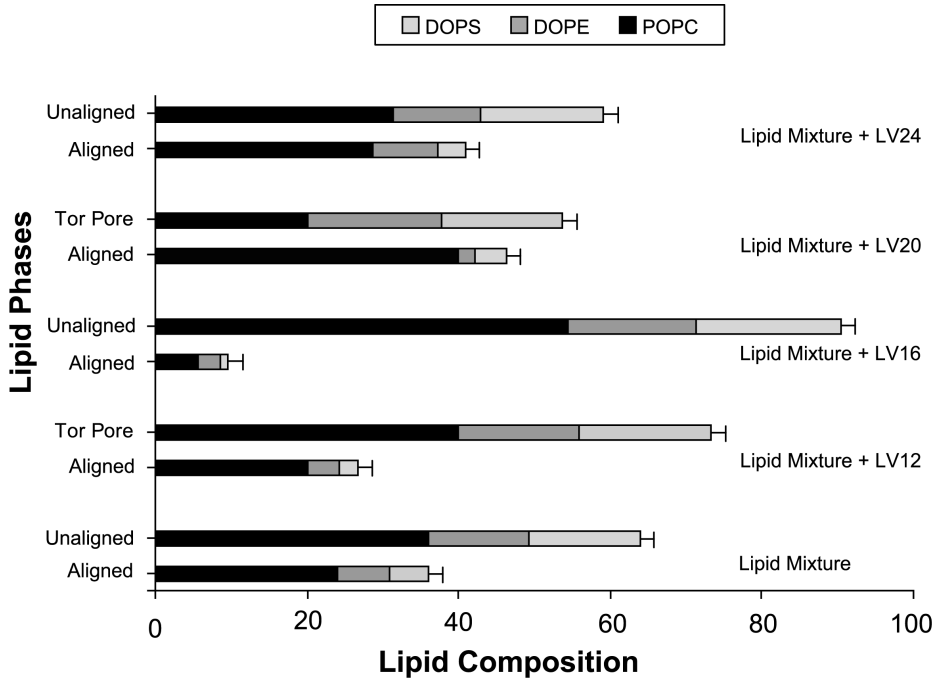

Figure 4.6: *The compositions of PC, PE and PS in the two phases in a lipid mixture without peptide, in the lipid mixture containing non-fusogenic peptides LV12, LV20 or LV24 (1mol %), and in the lipid mixture with the fusogenic peptide LV16 (1mol %). The error bars are based on estimates for the lipid compositions of two independently prepared samples.*

4.3.2. Peptide-induced fusogenic activity and membrane phase behavior

Interestingly, the fusogenicity strongly depends on the Leu/Val ratio (Fig. 4.3). A Leu-based peptide (L16) is virtually non-fusogenic, while mixing both Leu and Val residues yields intermediate (LLV16) to strong (LV16) fusogenic activity (Fig. 4.3). Placing either a Gly or a Pro residue at the center of the peptide (LV16-G8 and LV16-P8) has little effect on the fusogenicity.[8] However, a Gly-Pro in the middle of the hydrophobic core (LV16-G8P9) significantly enhances the fusion. Figure 4.2 summarizes fusogenicities for all peptides. Accordingly, fusion extents and rates increase up to ~10-fold and ~80-fold, respectively, in the following order: L16 < LLV16 < LV16 < LV16G8P9.

The peptides with different composition (Table 4.1, Set 2) were incorporated in oriented bilayers and the changes were monitored (Fig. 4.7). After addition of the non-fusogenic LLV16, a toroidal pore fraction forms, representing ~ 52% of the lipids with relative intensities PC:PE:PS ~ 1:1:1, while the aligned region has relative intensities PC:PE:PS ~ 21:1:2 (Figs 4.7B, 4.7F and 4.8). The POPC 0° orientation signal resonates with $\sigma_{B||}$ = ~ 21.33 ppm and a DOPE peak appears under this peak (Fig. 4.7B). In case of L16, the broad signal that peaks at –18 ppm reflects a cylindrical distribution in the unaligned phase and comprises ~ 60% of the ^{31}P signal (Figs. 4.7E and 4.8). The data can be simulated with a signal ratio PC:PE:PS ~ 9:3:1 for the aligned region and PC:PE:PS ~ 11:3:6 for the unaligned region (Figs. 4.7E and 4.8).

Interestingly, when the lipid mixture is loaded with fusogenic LV16G8P9 peptide, strikingly different results are obtained. The 0° oriented signal of a PC component resonates with $\sigma_{B||} \approx$ 24.5 ppm while the PE response is shifted to $\sigma_{B||} \approx$ 19.5 ppm. Here the high curvature phase has a significant fraction of vesicle type signal, ~ 16%, which is reflected by an anisotropic component in the signal, perturbing the symmetric cylinder line shape (Fig. 4.7H). It is clear that LV16G8P9 stabilizes the enhanced curvature phase relative to the flat bilayer phase. The data are simulated with relative intensities PC:PE:PS ~ 10:2:2 for the flat membrane

fraction and PC:PE:PS ~ 50:18:18 for the increased curvature component (Figs. 4.7H and 4.8). All observations were confirmed by measuring duplicate samples.

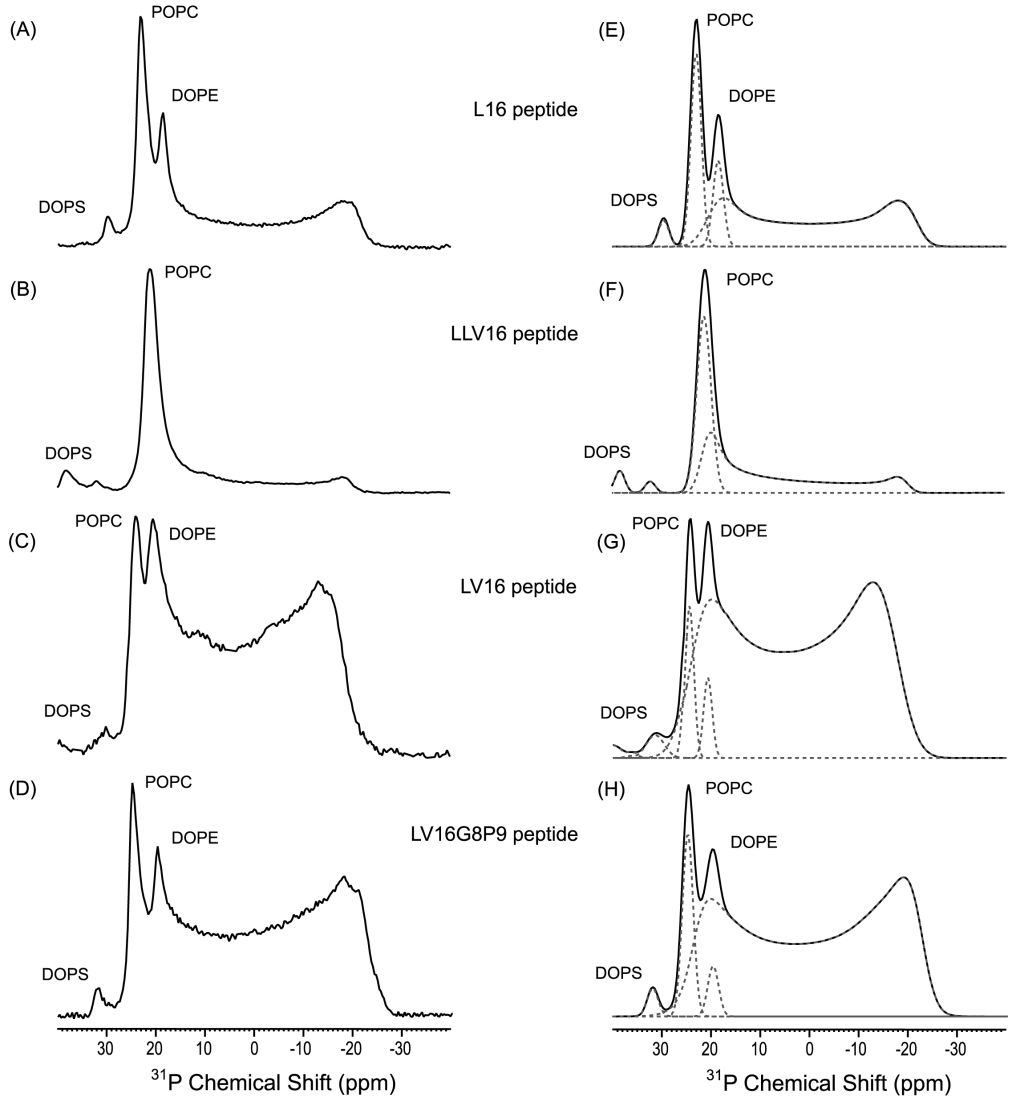

Figure 4.7: *^{31}P spectra of oriented bilayer samples, with the bilayer normal parallel to the B_0 are shown in left panel. The simulated spectra generated by calculating the responses of various lipid species, shown as dotted lines, are shown in the right panel.* ***(A)*** *Spectrum for the lipid mixture with the non-fusogenic peptide L16.* ***(B)*** *Spectrum for the lipid mixture with the non-fusogenic peptide LLV16.* ***(C)*** *Lipid mixture with the fusogenic peptide LV16 spectrum.* ***(D)*** *Lipid mixture with the fusogenic peptide LV16G8P9 spectrum. The data are recorded with 6 K scans at 310 K and pH 7.4.*

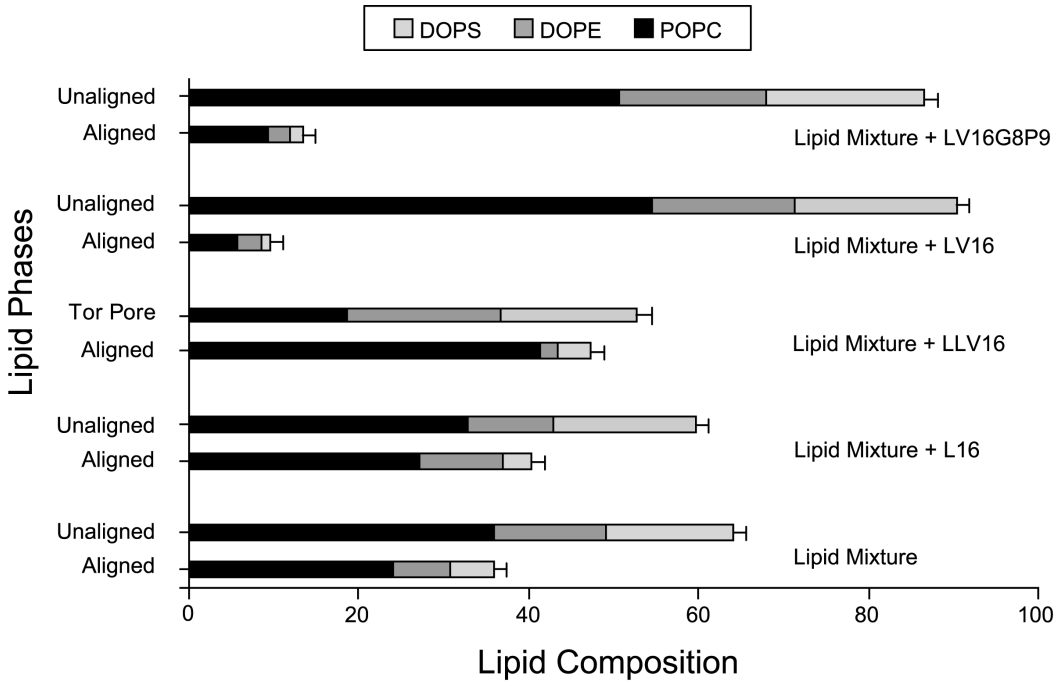

Figure 4.8: *Graphical representation of the PC, PE and PS composition of the biomimetic lipid mixture without peptide, the lipid mixture with non-fusogenic peptide L16 or LLV16 (1% mol), and the lipid mixture containing fusogenic peptide LV16 or LV16G8P9 (1% mol) in two different phases. The error bars are based on estimates for the lipid compositions of two independently prepared samples.*

4.3.3. Time-dependent phase changes in the biomimetic lipid bilayer loaded with LV16G8P9

Lipids show dramatic phase changes after addition of LV16G8P9 (Fig. 4.7D). When the sample is measured over larger times, additional changes are observed. In the spectrum of a sample measured after three weeks, a single oriented bilayer response with $\sigma_{B||} \approx 23$ ppm is observed that represents ~ 7% of the lipids and consists mainly of POPC (Fig. 4.9H). In addition, a pronounced anisotropic signal is present in the centre of the spectrum with a broad maximum at $\sigma_{BP||}{}^{H} \approx 3$ ppm and with $\sigma_{\perp}{}^{H} \approx -14$ ppm. A minor shoulder at $\sigma_{BP||}{}^{H} \approx 8.6$ ppm can be attributed to DOPS (Fig. 4.9H). The broad signal comprises the response from all DOPE and DOPS. It reveals a large fraction of unoriented hexagonal tubes, which can be attributed to DOPE and accounts for ~ 31% of the total NMR signal. The resonance line shape of

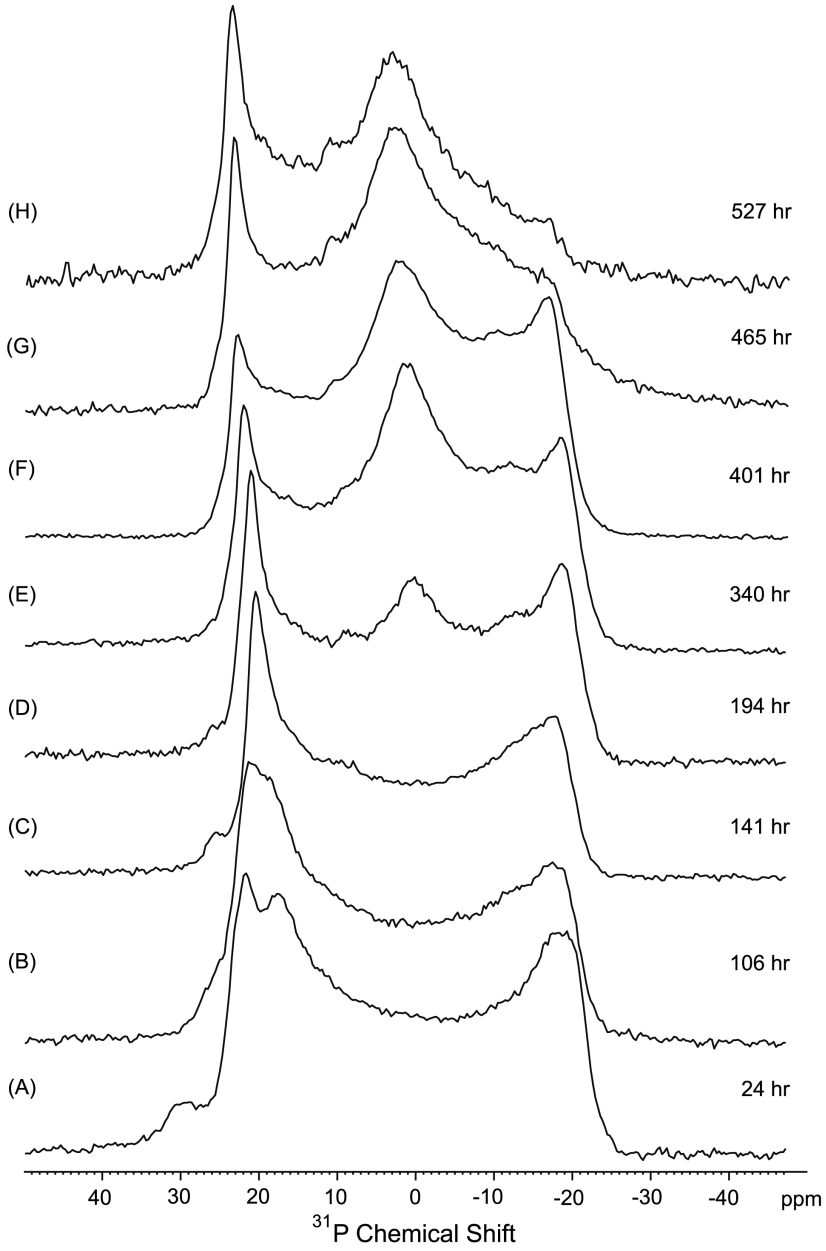

Figure 4.9: ***GP phase changes as a function of time.*** *Proton-decoupled Hahn-echo ^{31}P 1D solid-state NMR spectra of the POPC:DOPE:DOPS = 3:1:1 lipid mixture loaded with the fusogenic peptide LV16G8P9. The data were recorded at 310 K and pH 7.4 in 6 K scans with the bilayer normal parallel to the magnetic field. Spectra were recorded over an extended period up to three weeks to monitor the long-term changes in the biomimetic lipid mixture after addition of the fusogenic peptide.*

the remainder of the lipids, ~ 62%, still has cylindrical lipids consisting of ~ 50% POPC and ~ 12% DOPS. The broadening of the aligned signals has been attributed

in the past to wobbling of headgroups and increased mobility.[14] All observations were confirmed by measuring duplicate samples.

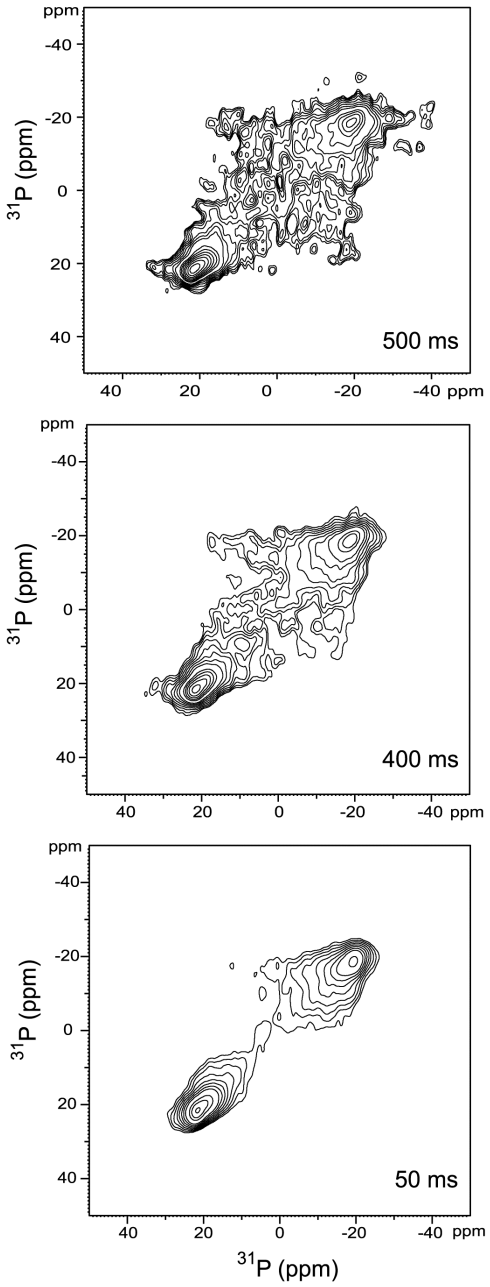

Figure 4.10: *2D ^{31}P exchange NOESY solid-state NMR spectra of oriented lipid membranes with 1% LV16G8P9. The exchange mixing times are 250, 400 and 500 ms. The spectra are recorded at 310 K and pH 7.4 with a total acquisition time of 12h.*

4.3.4. Structure of the biomimetic lipid bilayer in the presence of LV16G8P9

To further elucidate if the lipid phases in lipid membranes containing LV16G8P9 are spatially separate from or a part of the residual lamellar bilayer, 2D ^{31}P exchange experiments were measured. Lipids undergo lateral diffusion with diffusion coefficients of 10^{-7}–10^{-8} cm^2/s.[25,26]. If the isotropic lipids are contiguous with the residual oriented lipids, and if a typical radius of curvature of ~1 μm is assumed for the membrane, then the lipid reorientation induced by lateral diffusion is expected to change the ^{31}P frequency on time scales of 10-100 ms. This should give rise to cross-peaks in the 2D exchange spectra. Figure 4.10 displays the 2D ^{31}P spectrum of the lipid mixture containing the LV16G8P9 peptide, acquired with mixing times of 250 ms, 400 ms and 500 ms. Even at this longer mixing time only weak cross peaks between the 0° and the 90° peak are observed, despite their strong diagonal intensities.

Finally, the effect of the charge of the Lys residues on lipids may interfere with the lipid phase changes, which can be crosschecked by the peptides with His replacing a Lys residue (Data not shown). The effect of the His-peptides on the lipids is similar at pH 7.4 and pH 4, indicating that for the fusogenic peptide the charge on the peptides does not affect the lipid morphology.

4.4 Discussion

Figure 4.11 illustrates schematically how lipids in a monolayer are subject to different tensions and stress.[27] The lateral stress, F_h, in the headgroup region arises from steric, hydrational and electrostatic effects, and is usually repulsive. The interfacial tension or hydrophobic effect, F_Y, tending to minimize the interfacial area, arises from unfavorable hydrocarbon-water contacts. The repulsive lateral stress F_c, in the mobile chain region, is due to thermally activated trans-gauche rotations that can give rise to cone shaped molecules with lipids that have small head groups.[28] In general the first two forces do not vary considerably among lipids.

However, the repulsive chain force can vary largely between lipids due to differences in conformational flexibility.

When repulsion between the headgroups is reduced due to charge neutralization and/or dehydration, the packing pressure within the hydrocarbon interior will increase.[29,30] The lateral pressure within the membrane interior can be first relieved by chain reversal provided that the membrane free volume distribution is such that there is space in the interfacial region. At this point it is relevant also to consider the relationship between membrane fusion and membrane negative spontaneous curvature. The largest relief in packing within the hydrocarbon region is achieved when the chains extend into the two opposing leaflets forming the contact site between two adhering bilayers.[27] Here the projected interfacial area for the acyl chains is halved and the free energy can be lowered upon lipids adopting the extended conformation at the contact site of adhering vesicles.

For an isolated flat monolayer the lateral interactions need to be properly balanced across a single monolayer, to allow for zero mean curvature (Fig. 4.12). If the lateral pressure in the headgroup region outweighs the lateral forces in the chain region, there will be a tendency for the layer to curl towards the chain region and this will lead to positive mean curvature (Fig. 4.12). For the opposite case when the pressure in the chain region is dominant, the curvature will tend to develop towards the aqueous region, which corresponds to negative mean curvature (Fig. 4.12). However, for a bilayer, since the two halves are hydrophobically coupled, a deformation of one side is restricted by the opposing monolayer. For instance, when both monolayers tend to adopt a negative curvature, the bilayer cannot lower its internal stress simply by bending. This state of balance, in which the internal stresses across the whole bilayer stabilize a planar bilayer configuration is an example of a state of physical frustration.[31] Mismatches in packing in either region induce a tendency toward membrane curvature, which is offset by similar changes in the apposed leaflet; consequently, the curvature is not expressed, but is stored as

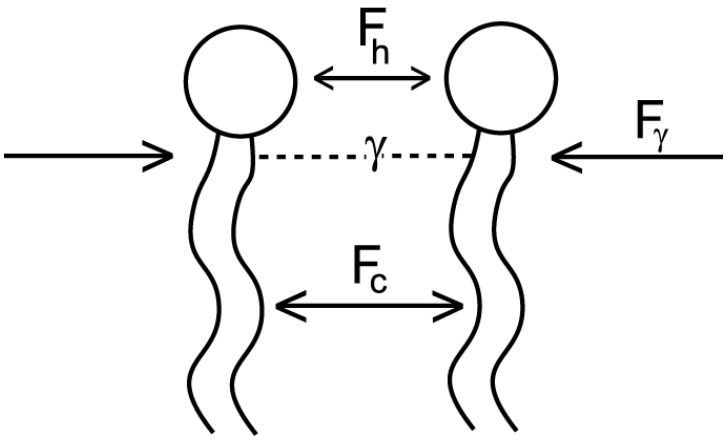

Figure 4.11: *Schematic diagram showing the principle forces acting upon molecules in a lipid monolayer.*

potential energy with a latent ability to destabilize the bilayer structure.

When a lipid bilayer forms toroidal pores, it bends back on itself like the inside of a torus and causes the top and bottom monolayers to be continuous (see Fig. 3.1D).[14] There is an energy cost for such a membrane deformation, mainly due to the bending in the toroidal area. The bending can be viewed as a lateral expansion of the head group region relative to the chains. The key feature of the model is the role of curvature strain in inducing the pore formation.[32,33] Curvature strain describes the situation where a bilayer contains some lipids that prefer a nonlamellar phase, resulting in a strained and less stable bilayer.

Non-bilayer lipids prefer nonlamellar phases due to a mismatch in the preferred cross-sectional area of the headgroups and acyl chains.[14] Toroidal pores have positive curvature through the pore and negative curvature around the pore, suggesting that the peptide orientation in the pore itself may depend on the type of curvature induced by the peptide.[34] The lipids in these openings then tilt from the lamellar normal and connect the two leaflets of the membrane, forming a continuous bend from the top to the bottom in the fashion of a toroidal hole; the pore is lined by the lipid head groups, which are stabilized by the peptides (Fig. 3.1D).[14]

Neglecting the area taken up by peptide and assuming that lipids cover the

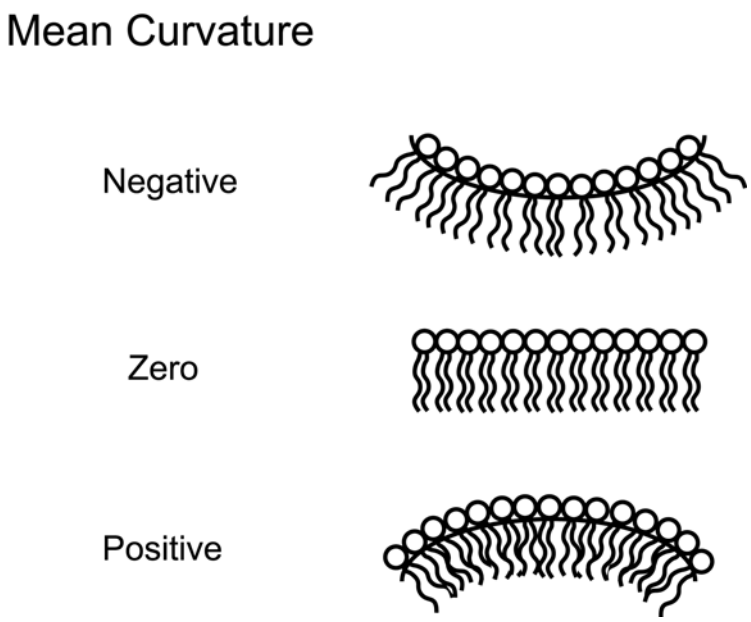

Figure 4.12: *Tendency for spontaneous curvature of a lipid monolayer due to an imbalance in the distribution of lateral forces across the layer.*

entire pore surface, a toroidal pore yields a ^{31}P spectrum similar to a reversed powder pattern where the high intensity peak is at the parallel edge and the low intensity maximum is at the perpendicular edge (Fig. 3.1D). The details of the pattern depend on the pore size. However, lipid diffusion is usually as rapid in the presence of small peptides as it is in pure lipid bilayers.[14] If the lipids diffuse rapidly through the pore, a response with a chemical shift between 10 and 25 ppm would be observed in the ^{31}P spectrum depending on the size of the pore.[14] Intermediate timescale motion may occur if the lipid diffusion through the pore is slowed or stabilized by the interaction with peptide in the pore. This would yield a signal pattern similar to the ^{31}P response detected for static toroidal pores since laterally diffusing lipid molecules spend more time in a perpendicular orientation at the center of the pore (Fig. 3.1D). Depending on the pore radius the intensity at the perpendicular edge (~ –18 ppm) will vary.[35]

For the pure lipid mixture there is a significant difference in lipid composition between the two fractions (Fig. 3.2A). The aligned bilayer phase has a composition of

34%, while on the other hand the unoriented high curvature phase consists 64% of the lipids similar to the composition of the natural lipid mixture. Figure 4.4 shows the spectrum of the biomimetic lipid mixture at 90° orientation.

It has been known for a long time that small vesicles that are composed of two different lipids, such as PC and PE, exhibit a strong asymmetry in the composition of the two monolayers of the bilayer.[36] This compositional asymmetry reduces the mismatch, or frustration, between the spontaneous curvatures of the two monolayers as has been recently discussed for surfactant vesicles.[31] The data presented here demonstrate that small amounts of the peptide can give rise to pronounced macroscopic rearrangements. This indicates that the interactions between hydrophobic sequences and the phospholipid bilayers can have remarkably strong control over the suprastructure of a multilamellar system.

4.4.1 The length of a peptide affects its fusogenicity

The synthetic peptides with different lengths show different fusogenic properties (Fig. 4.2). The ^{31}P line shapes indicate phase separation across the lipid bilayer that correlates with the fusogenicity of these peptides. When peptide LV12 is incorporated in the lipid bilayer, the unoriented fraction is reduced and the spectrum comprises a toroidal pore type response within the lipid bilayer (Figs 4.5A and E). Similar behavior is observed when a long length non-fusogenic peptide, LV20, is incorporated in the lipid bilayer (Fig. 4.5C). However, when the non-fusogenic peptide LV24 is incorporated in the lipid bilayer system, the cylindrical unoriented fragment is reduced compared to the pure lipid mixture (Figs 4.3D, H and 4.4). This indicates a stabilization of the aligned bilayer component. In contrast, when the fusogenic peptide LV16 is added the oriented signals broaden and the unoriented fraction represents 78% of the lipid response.

The increased stability of the lipid bilayers and the formation of toroidal pores may help to explain the non-fusogenic behavior of LV12, LV20 and LV24 (Figs 4.5 A, C and D). In case of LV20 and LV24 the peptides are too long to disturb the bilayer. On the other hand, in case of shorter LV12, the peptides may fit in bilayer either by

stretching itself or by compressing the bilayer, which promotes pore formation.[8] In both cases the fraction of high curvature unoriented component will be reduced. The peptide LV16 can protrude through the lipid bilayer, which may promote an initial destabilization of the bilayer, while peripheral interaction of LV16 with the lipid headgroups may support the formation of a high curvature cylindrical component. This could give rise to hemifusion, which explains the enhanced fusogenic behavior of LV16 as compared to the other peptides with different lengths (Table 4.1).

4.4.2 Introduction of a GP pair enhances fusion

The peptide with the oligo leucine middle core sequence shows a preference for a stationary secondary structure and corresponding non-fusogenic behavior (Chapter 3). Similarly the LLV16 peptide also prefers to be in a stable secondary structure and shows less fusogenicity (Fig. 4.3).[8] The peptide LV16, with an alternating Leu/Val sequence shows more fusogenicity than LV12 and LLV16. Apparently the introduction of the GP pair in the middle of the peptide sequence, LV16G8P9, produces the strongest fusogenicity, which suggests that increased conformational flexibility can enhance fusion (Fig. 4.3).[8]

When L16 is incorporated in lipid bilayers, the unoriented fragment is reduced compared to the pure lipid system (Fig. 4.7A and E). However, when the non-fusogenic peptide LLV16 is incorporated, the spectrum reveals the formation of toroidal pore structures within the lipid bilayers (Figs 4.7B and F). This suggests that incorporation of a peptide with a stationary conformation enhances the alignment of the lipids.[22] Again the data show that the fraction of unoriented component is larger in case of lipid mixtures containing fusogenic peptides and smaller in the case of a lipid mixture containing non-fusogenic peptides. In contrast, for the fusogenic peptide LV16 and the highly fusogenic peptide LV16G8P9 the oriented peaks are broad, indicating the wobbling of lipid headgroups and increased mobility (Fig. 4.7C and D).

4.4.3 Time-dependent phase changes in the biomimetic lipid bilayer induced by LV16G8P9

When a sample containing LV16G8P9 is measured over a period of time, pronounced phase separation of the lipids is observed in a few weeks (Fig. 4.9). The appearance of an anisotropic response, of the type shown in Figure 3.1E, reveals the presence of unoriented hexagonal tubes due to relaxation of strain at a much larger time scale. This is not observed for the lipid mixture without peptide and the lipid mixture containing the non-fusogenic L16 (data not shown). A hexagonal pattern is very characteristic since it requires partial averaging of the chemical shift by rapid self-diffusion over the radius of the tubes and it is clear from Figure 4.9 that the hexagonal phase is only important at the longer time period of several weeks. The normal and inverted hexagonal phase cannot be distinguished using ^{31}P NMR because they have the same symmetry, which is not occurring immediately after the addition of peptide. Over time, lipid separation will still occur, and the system will reach equilibrium and the time required is reduced by peptides that facilitate domains of high curvatures. It thus transpires that over a longer period of time forming hexagonal tubes can further stabilize the lipid system after addition of LV16G8P9.

4.4.4 Structure of the biomimetic lipid membrane loaded with fusogenic peptide LV16G8P9

One-dimensional ^{31}P spectra of 0° aligned samples indicate that there is phase separation when the biomimetic model membrane preparation is loaded with the fusogenic peptide LV16G8P9. At 50 ms, only diagonal intensities are observed, including prominent 0° and 90° peaks (Fig. 4.10). The weak cross peaks between the 0° peak and the 90° peak at 400 ms mixing time strongly suggest that the unoriented lipids reside in separate domains from the residual lamellar bilayer (Fig. 4.10). The lack of exchange between the lamellar and nonlamellar phases that was deduced from the NOESY spectra is well in line with data collected from lipid membranes without any peptide that also reveal a spatial separation of lamellar and

nonlamellar lipids.[2,37] 2D ^{31}P exchange spectra of the lipid mixture with fusogenic peptide LV16G8P9 show that the unoriented domain is spatially well separated from the oriented bilayers, since even after a mixing time of 500 ms the cross-peak between the 0˚ peak and the 90° peak is weak (Fig. 4.10).

Membrane fusion can be divided into early and late steps. Initially, membranes are brought into close proximity by the action of membrane-extrinsic fusion protein domains.[38-41] TMSs may support this early step by enhancing the stability and/or multimerization of viral or SNARE-based fusion complexes.[8] Actual lipids mixing occurs in a subsequent step and may be facilitated by structurally flexible TMSs.[8] Although structural flexibility of the fusogenic LV variants manifests itself as helix to sheet transitions in an isotropic solution, it does not necessarily mean that this transition takes place in the low dielectric environment of a membrane.[42] Rather, the corresponding helical structures may be conformationally flexible in a sense that they locally unwind in the bilayer and thus facilitate lipid mixing. In addition the possibility of peptide aggregation contributing to the lipid mixing cannot be ruled out.

Viral fusion peptides exert a variety of effects on the bilayer structure of membranes that are not fully understood yet. One effect that has been seen with fusion peptides from several viruses is their ability to alter the phase behavior of lipids that are prone to form hexagonal phases at elevated temperatures.[43] This effect has been attributed to the ability of the fusion peptide to decrease the intrinsic negative curvature of the lipids to the extent that they are no longer stable, but change into the more highly negatively curved HII phase.[9,44]

In the model system, the aligned bilayer phase is POPC rich and is subject to internal stress due to the presence of DOPE, while on the other hand the unoriented phase consists of lipid species in a similar ratio as observed in nature. This suggests that there is an important route for reducing the physical frustration in the bilayer system, by establishing curved bilayer structures with a higher concentration of the lipid preferring negative curvature, DOPE, predominantly in the inner layer and a higher concentration of the zero curvature preferring lipids, POPC, in the outer

layer. Since in that case POPC is forced into a suprastructure with curvature, this unoriented lipid will be subject to internal stress, implying that there is significant potential energy stored in the system.

A popular view is that membrane fusion proceeds via the formation of stalk intermediates, which lead to hemifusion.[45] The energy of the stalk intermediate depends on the lipid composition of the membranes, since different lipids tend to bend lipid monolayers in different directions, reflecting the dynamic molecular shape of the individual lipid species, referred to as "intrinsic curvature".[11,45] It is well documented that PE has a cone-like molecular shape, small head cross section and large chain cross section, and that it promotes negative spontaneous curvature.[46] It has been proposed in the past that high PE content leads to a very unstable bilayer that ruptures rather than fuses.[8] It might be expected that the presence of PE in the inner monolayers and PC in outer monolayers of fusing membranes would reduce lipid packing and promote stalk formation and membrane merger.

If a fusogenic peptide primarily interacts with lipid headgroups, then it could alter the balance of lateral stress, interfacial tension, and repulsive lateral stress, reducing the energy needed for rearrangement. If the lateral stresses and interfacial tensions are both reduced, then the repulsive lateral stresses in the mobile chain region of the bilayer become dominant, allowing the molecules to rearrange and form curved lipid cylinders. The transition region of the lipid cylinders has a tendency to grow, which may result in stalk formation and can lead to fusion. In contrast to this, when a non-fusogenic peptide is added to the lipid mixture, it supports the formation of aligned lipid bilayers or toroidal pores. This recruits more lipids to the ordered bilayer domain by reducing the relative repulsive lateral stresses within the lipids and leads to the formation positive curvature, possibly in the form of toroidal pores. Since the transition region of a toroidal pore has a tendency to minimize and is restricted to a single bilayer, this would oppose the growing of stalks involving two bilayers.

4.5 Conclusions

The membrane-fusogenic activity of simplified hydrophobic model peptides is examined to see whether it is related to their influence on a biomimetic lipid mixture. Recent results show that mixed Leu/Val sequences exhibit strong fusogenicities that are further increased by including a Gly and Pro pair.[8] At the same time, the more fusogenic peptides show a generally lower stability of their helical conformation.

Fusion involves multiple lipid rearrangements and we have investigated how different classes of peptides influence the first step of the process, thereby shifting the balance between fusogenic and non-fusogenic. The length of the peptides makes an important difference for rate of the fusion for vesicles. A peptide that can span through a bilayer appears more fusogenic than a shorter or longer one. This might be the reason why the transmembrane part of proteins is responsible for membrane fusion. The sequence of the peptide also affects the fusogenic activity. A low complexity sequence with enhanced conformational flexibility shows pronounced fusogenic behavior, which underlines the importance of the dynamics of the bio-molecules triggering fusion.

Apparently, non-fusogenic peptides quench fusion by promoting aligned bilayer structures or shrinking of bilayer defects leading to the toroidal pore type components observed in the spectra, thereby apparently provoking the formation of extended high curvature regions at low water content. In addition the biophysical studies on these peptides in biomimetic three-lipid mixtures confirm that the complex phenomenon of membrane fusion can be driven by transmembrane peptides with low complexity sequences. In line with chapter 3, the release of physical frustration within the three-lipid bilayer by inducing high curvature and phase separation across the bilayer can be the initial driving force for the membrane fusion. Finally it is tempting to conclude that peptides with optimal length and composition help lipids to overcome the thermodynamic barrier for fusion.

Many researchers, because of the complex behavior, have avoided three lipid mixtures. The data described here show that spectra collected from three lipid mixtures reproduce well and show characteristic patterns such as cylindrical or toroidal type responses across a wide range of artificial peptides interacting with the bilayers system. Although the first interpretation of the data based on the emerging simplicity in the spectra is already remarkably consistent, it can be anticipated that a further refinement of the models that are presented, can be obtained when more data also on other systems will become available in the future.

References

1. Rohrbough, J.; Broadie, K., *Nat Rev Neurosci,* **2005,** 6, 139-50.
2. Jahn, R.; Lang, T.; Sudhof, T. C., *Cell,* **2003,** 112, 519-33.
3. Peters, C.; Bayer, M. J.; Buhler, S.; Andersen, J. S.; Mann, M.; Mayer, A., *Nature,* **2001,** 409, 581-88.
4. Blumenthal, R.; Clague, M. J.; Durell, S. R.; Epand, R. M., *Chem. Rev.,* **2003,** 103, 53-69.
5. Rohde, J.; Dietrich, L.; Langosch, D.; Ungermann, C., *J. Biol. Chem.,* **2003,** 278, 1656-62.
6. Schuette, C. G.; Hatsuzawa, K.; Margittai, M.; Stein, A.; Riedel, D.; Kuster, P.; Konig, M.; Seidel, C.; Jahn, R., *Proc. Natl. Acad. Sci. U. S. A.,* **2004,** 101, 2858-63.
7. Langosch, D.; Brosig, B.; Pipkorn, R., *J. Biol. Chem.,* **2001,** 276, 32016-21.
8. Hofmann, M.; Weise, K.; Ollesch, J.; Agrawal, P.; Stalz, H.; Stelzer, W.; Hulsbergen, F.; de Groot, H.; Gerwert, K.; Reed, J.; Langosch, D., *Proc. Natl. Acad. Sci. U. S. A.,* **2004,** 101, 14776 - 81.
9. Chernomordik, L.; Chanturiya, A.; Green, J.; Zimmerberg, J., *Biophys. J.,* **1995,** 69, 922-29.
10. Siegel, D. P., *Biophys. J.,* **1999,** 76, 291-313.
11. Chernomordik, L., *Chem. Phys. Lipids,* **1996,** 81, 203-13.
12. Yang, L.; Huang, H. W., *Science,* **2002,** 297, 1877-79.
13. Opella, S. J., *Nat. Struct. Biol.,* **1997,** 4, 845-48.
14. Wildman, K. A. H.; Lee, D. K.; Ramamoorthy, A., *Biochemistry,* **2003,** 42, 6545-58.
15. Ramamoorthy, A.; Marassi, F. M.; Zasloff, M.; Opella, S. J., *J. Biomol. NMR,* **1995,** 6, 329-34.
16. Marassi, F. M.; Ramamoorthy, A.; Opella, S. J., *Proc. Natl. Acad. Sci. U. S. A.,* **1997,** 94, 8551-56.
17. Bechinger, B., *FEBS Lett.,* **2001,** 504, 161-65.
18. Bechinger, B.; Kinder, R.; Helmle, M.; Vogt, T. C. B.; Harzer, U.; S., S., *Biopolymers - Peptide Science,* **1999,** 51, 174-90.
19. Langosch, D.; Crane, J. M.; Brosig, B.; Hellwig, A.; Tamm, L. K.; Reed, J., *J. Mol. Biol.,* **2001,** 311, 709-21.
20. Rance, M.; Byrd, R. A., *J. Magn. Reson.,* **1983,** 52, 221-40.
21. Struck, D. K.; Hoekstra, D.; Pagano, R. E., *Biochemistry,* **1981,** 20, 4093-99.

22. Buffy, J. J.; McCormick, M. J.; Wi, S.; Waring, A.; Lehrer, R. I.; Hong, M., *Biochemistry,* **2004,** 43, 9800-12.
23. Pearce, J. M.; Komoroski, R. A., *Magn. Reson. Med.,* **1993,** 29, 724-31.
24. Hallock, K. J.; Lee, D. K.; Ramamoorthy, A., *Biophys. J.,* **2003,** 84, 3052-60.
25. Fenske, D. B.; Jarrell, H. C., *Biophys. J.,* **1991,** 59, 55-69.
26. Picard, F.; Paquet, M. J.; Dufourc, E. J.; Auger, M., *Biophys. J.,* **1998,** 74, 857-68.
27. Seddon, J. M., *Biochim. Biophys. Acta,* **1990,** 1031, 1-69.
28. Cantor, R. S., *J. Phys. Chem.,* **1997,** 101, 1723-25.
29. Kinnunen, P. K. J., *Chem. Phys. Lipids,* **1992,** 63, 251-58.
30. Kinnunen, P. K. J., *On the mechanism of the lamellarright-arrowhexagonal HII phase transition and the biological significance of the HII propensity*. CRC Press: Boca Raton, FL., 1996; p 153-71.
31. Ludtke, S. J.; He, K.; Heller, W. T.; Harroun, T. A.; Yang, L.; Huang, H. W., *Biochemistry,* **1996,** 35, 13723-28.
32. Janes, N., *Chem. Phys. Lipids,* **1996,** 81, 133-50.
33. Cullis, P. R.; de Kruijff, B., *Biochim. Biophys. Acta,* **1979,** 559, 399-420.
34. Brogden, K. A., *Nat Rev Microbiol,* **2005,** 3, 238-50.
35. Thompson, T. E.; Huang, C.; Litman, B. J., *Bilayers and biomembranes: compositional asymmetries induced by surface curvature*. John Wiley: New York, 1974; p 1-16.
36. Safran, S. A.; Pincus, P. A.; Andelman, D.; Mackintosh, F. C., *Phys. Rev. A,* **1991,** 43, 1071-78.
37. Tamm, L. K.; Crane, J.; Kiessling, V., *Curr. Opin. Struct. Biol.,* **2003,** 13, 453-66.
38. Tatulian, S. A.; Tamm, L. K., *Biochemistry,* **2000,** 39, 496-507.
39. Roy, R.; Laage, R.; Langosch, D., *Biochemistry,* **2004,** 43, 4964-70.
40. Doms, R. W.; Helenius, A., *J. Virol.,* **1986,** 60, 833-39.
41. Laage, R.; Rohde, J.; Brosig, B.; Langosch, D., *J. Biol. Chem.,* **2000,** 275, 17481-87.
42. Tamm, L. K.; Han, X.; Li, Y.; Lai, A. L., *Biopolymers,* **2002,** 66, 249-60.
43. Epand, R. M.; Epand, R. F., *Biochem Biophys Res Comm.,* **1994,** 202, 1420-5.
44. Siegel, D. P., *Biophys. J.,* **1993,** 65, 2124-40.
45. Gruner, S. M., *Proc. Natl. Acad. Sci. U. S. A.,* **1985,** 82, 3665-69.
46. Haque, M. E.; McIntosh, T. J.; Lentz, B. R., *Biochemistry,* **2001,** 40, 4340-48.

5

^{13}C and ^{15}N NMR of uniformly labeled fusogenic peptides incorporated in a biomimetic membrane: Additional support for the peripheral intercalation model and future outlook.

5.1 Introduction

The main target of the research described in this thesis is to contribute in understanding the membrane fusion mechanism by mimicking the natural system. Understanding the heart of membrane fusion is intrinsically related to the question how proteins and lipids communicate in space and time. Membrane fusion proceeds via stalk formation and hemifusion, which leads to fusion pore formation that allows for complete fusion. One line of evidence supporting the existence of stalk and hemifusion intermediates derives from the sensitivity of the fusion reaction to lipids of different intrinsic curvature.[1] The intrinsic curvature is defined by the ratio of the cross-sectional areas of the hydrated lipid head-group and the acyl chain moiety. This dictates the curvature of a monolayer composed of the respective lipid species. Accordingly, PC has a highly positive intrinsic curvature. It thus stabilizes positive curvature of the outer monolayer of a spherical, lipid-enclosed particle, such as a liposome or a small secretary vesicle (Chapter 3). In contrast, the negative curvature of the inner monolayer of the same particle is stabilized by lipids with negative intrinsic curvature, such as PE, diacylglycerol and phosphatidic acid or even by free fatty acids (Chapter 3). At the stalk structure and at the rim where a hemifusion

diaphragm meets the adjoining bilayers, the outer, i.e. proximal, monolayer of a fusing membrane has to adopt a more net negative curvature compared to the unfused bilayer. Thus, the fusing membrane is probably stressed at these sites. The concept of stalk formation and hemifusion rationalizes these observations since local bilayer stress can be decreased by the presence of lipids with the appropriate shape. Fusion peptides of viral fusogens are thought to catalyze membrane fusion by disturbing lipid bilayer structure and inducing curvature by peripheral intercalation with lipids.[2] The *de novo* designed peptides studied in this thesis have low complexity and can also show fusogenicity, which correlates with their structural plasticity (Chapter 2).

In this final chapter preliminary studies on the uniformly labeled peptides are performed, which contribute to converging evidence that the fusogenic peptides show structural flexibility and are peripherally intercalated at the membrane-water interface. Proton-decoupled ^{13}C, ^{15}N and proton spin diffusion heteronuclear ^{1}H–^{13}C correlation NMR experiments on oriented and unoriented samples are used to characterize the secondary structure and orientation of the peptides in some detail. For oriented samples the spectral line shapes are sensitive indicators of the rate of rotational diffusion. While rapidly rotating transmembrane peptides exhibit spectral averaging and well-defined resonances, broad spectral line shapes characterize larger immobilized complexes. The ^{15}N line shape is sensitive to the orientation of the peptide and the ^{13}C and heteronuclear experiments provide information about the secondary structure and location of peptides in vesicles.

The studies in this chapter focus on the behavior of three peptides, one previously shown to be rigid and virtually non-fusogenic, L16, one flexible and fusogenic, LV16, and the third that is highly fusogenic, LV16G8P9.[3] A mixture of brain phosphatidylethanolamine (PE), brain phospatidylserine (PS), and egg phosphatidylcholine (PC) in a 60:20:20 ratio is used to mimic the biological membrane composition of synaptic vesicles.[4] The behavior of the peptides is studied in biomimetic lipid bilayers at peptide to lipid ratios of 1:100 using different solid-state NMR techniques.

L16 : K K K W L L L L L L L L L L L L L L L L K K K

LV16 : K K K W L V L V L V L V L V L V L V L V K K K

LV16G8P9 : K K K W L V L V L V L G P V L V L V L V K K K

Although the dynamic properties of membrane-associated peptides are essential for their function,[3] the underlying conformational and configurational dynamic equilibrium complicates a detailed interpretation of the structural data obtained by solid state NMR techniques. Unambiguous analysis of these data would require detailed knowledge of the orientational state of the peptides within the sample. Proton spin diffusion gives an alternative strategy to study membrane protein topology of non-oriented bilayer samples.[5,6] In the spin-diffusion approach, dipolar couplings between protons mediate a transfer of nuclear polarization from well-defined sources. The magnetization is selected based on the mobility or other spin properties and is allowed to transfer to the desired targets in the peptide.[5]. Since the dipolar coupling is distance dependent, the rate of transfer is determined by the proximity of the sink spins to the source spins and this provides insight into how peptides can intercalate with the lipid membrane.[5] The liquid-crystalline nature of the lipid bilayer leads to high-resolution Magic Angle Spinning (MAS) ^{1}H and ^{13}C spectra.[5]

To determine the intercalation of the peptides with the membrane the considerable differences in the spin diffusion transfer rates between a rigid macromolecule and mobile lipids can be exploited. A transmembrane peptide domain provides rigid segments close to the center of the liquid-crystalline bilayer, leading to rapid spin diffusion from the protons in the lipid tails to the peptide protons.[5] In contrast, for a peptide with only surface-bound segments, the ^{1}H magnetization must first diffuse through the lipid head groups before reaching the peptide.[5] In addition, since spin diffusion in lipids is slow as a result of motionally averaged ^{1}H-^{1}H dipolar couplings, a surface-bound peptide receives little ^{1}H magnetization from remote lipid chain protons.[5]

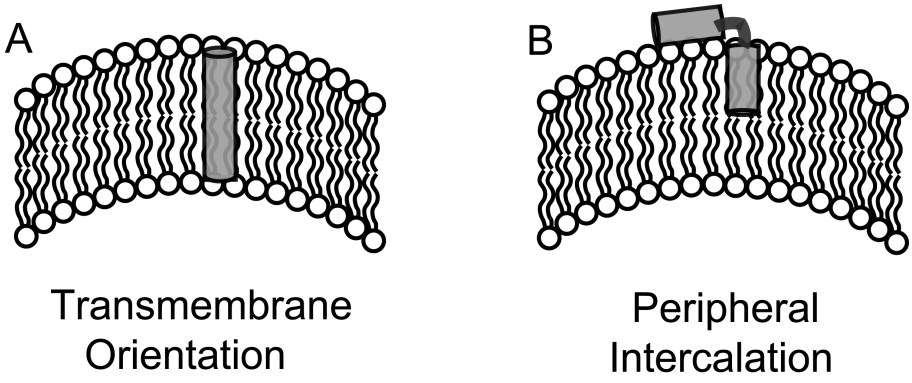

Figure 5.1: *Schematic representation of possible orientations of peptides in lipid bilayers. In case of transmembrane orientation* ***(A)*** *the peptide is buried in the bilayer while in case of peripheral intercalation* ***(B)*** *the peptide is partially inside the bilayer as well as partially interacting with the lipid head groups.*

Proton-decoupled ^{15}N solid-state NMR spectroscopy has been shown to provide information on the alignment of peptides within oriented membrane samples in a straightforward manner.[7-12] The ^{15}N chemical shift can be a good indicator of the orientation of polypeptides.[13] When ^{15}N solid-state NMR measurements are performed on monomeric polypeptides reconstituted into oriented lipid bilayers rapid lateral and rotational diffusion averages the shift anisotropy.[7] The resulting solid-state NMR signal is a direct probe of the extent of molecular alignment relative to the bilayer normal/B_0-vector and can be used to obtain orientational constraints for the molecule.[7] Upon quenching of rotational diffusion by aggregation or peptide-lipid interaction in many different alignments of the molecule with respect to the magnetic field direction, lead to broad NMR signals. Therefore, the broad NMR line shapes are indicators of slow rates of rotational diffusion and peptide aggregation in the membrane.[7]

The two possible topological models given in Figure 5.1 have been used in the past to describe the lipid disturbing behavior of fusion peptides. The fusion peptide of influenza hemagglutinin has been shown to associate laterally with membranes in a mixture of conformations, β-sheet as well as α-helix. It can assume a boomerang-shape that is thought to be critical for fusion initiation. This leads to the

peripheral intercalation model of Figure 5.1B, where the peptide lies on the bilayers and interacts with the lipid head groups, perpendicular to the bilayer normal. In comparison, in the transmembrane model peptides are oriented approximately parallel to the bilayer normal, where Lys are buried in the hydrophobic interior while the middle hydrophobic core is close to the membrane-water interface (Fig. 5.1A).[14] It will be shown below that experimental spin-diffusion build-up curves for peptides provide additional support for the transmembrane model for the non-fusogenic peptide, L16 and while the peripheral intercalation model is preferred for the fusogenic peptides LV16 and LV16G8P9.

5.2 Materials and methods

POPC, DOPS and DOPE were purchased from Avanti Polar Lipids, Birmingham, AL. Peptides were synthesized and purified according to the procedures mentioned in chapter 2. Concentrations of peptide solutions were determined via tryptophan absorbance at 294 nm in a 1:1 (v/v) mixture of TFE and dimethyl sulfoxide using an extinction coefficient of 5600 $M^{-1}cm^{-1}$.

5.2.1 Preparation of unoriented NMR samples

Liposomes were prepared from mixtures of POPC /DOPE /DOPS at a weight ratio of 3:1:1 in chloroform. Peptides were first dissolved in trifluoroethanol, dried under a stream of nitrogen to a thin film and rehydrated with a fusion buffer (25 mM Tris-HCl, pH 7.4, 150 mM NaCl, 0.1 mM EDTA, 5 mM DTT). Liposomes were formed after vortexing and freeze thawing the mixture, followed by bath sonication for 60 min while cooling with ice. The sample was centrifuged at 16000 × *g* for 20 min to remove lipid aggregates. The membrane-bound peptide sample is then transferred to a 4 mm NMR rotor. The oriented lipid bilayer samples are prepared as described in the previous chapter.

5.2.2 NMR spectroscopy

Lyophilized peptides: All experiments on peptides and unoriented samples were carried out using a Bruker AV-750 MHz spectrometer, equipped with a double channel cross polarization (CP)-MAS probe head. Peptides (5 mg) in 50% acetic acid (vol/vol) were frozen in liquid nitrogen, lyophilized, and transferred into a 4-mm MAS-NMR rotor. The 1D ^{13}C-natural abundance NMR spectra were recorded with a ^{13}C radio frequency of 188 MHz by using CP-MAS NMR spectroscopy. All data were recorded at room temperature by using a MAS spinning frequency of 12.5 kHz. The ^{13}C-carbonyl resonance of U-[^{13}C,^{15}N]-Tyr-HCl at 172.1 ppm was used as an external reference for the calibration of the isotropic ^{13}C chemical shifts.

Unoriented samples: The 1D ^{13}C and ^{1}H NMR spectra of peptides in vesicles were recorded by using CP-MAS NMR spectroscopy with a spinning frequency of 7 kHz at 277 K. The ^{13}C-carbonyl resonance of U-[^{13}C,^{15}N]-Tyr-HCl at 172.1 ppm and the ^{1}H resonance of H_2O at 4.8 ppm were used as an external reference for the calibration of the isotropic ^{13}C and ^{1}H chemical shifts, respectively.

The pulse sequence for the 2-D ^{1}H spin-diffusion experiment with ^{13}C detection is shown in Figure 5.2.[5] At the start of the sequence, four 90° pulses on the ^{13}C channel destroy residual ^{13}C magnetization. After an initial 90° pulse on the ^{1}H channel, ^{1}H magnetization from the mobile lipid segments and H_2O is selected by a T_2 filter, while the ^{1}H signals of the more rigid peptide relax due to the strong ^{1}H-^{1}H dipolar couplings. The 180° pulse in the middle of the T_2 filter refocuses the isotropic chemical shift evolution and the effect of the B_0 field inhomogeneity. Next, the lipid ^{1}H magnetization evolves under the isotropic chemical shift interaction for the t_1 period. A ^{1}H 90° pulse then stores the magnetization along the z-axis and allows it to exchange via spin diffusion for a mixing period, τ_m. After the mixing time, the ^{1}H magnetization is rotated to the CP effective field direction by $\pi/2$ and locked. A simultaneous CP pulse on the ^{13}C-channel with ramped field strengths transfers the ^{1}H magnetization to ^{13}C-spins, which are then detected during t_2.Since a short contact time of 0.5 ms was used for CP for the peptide sample, the ^{13}C signals of the

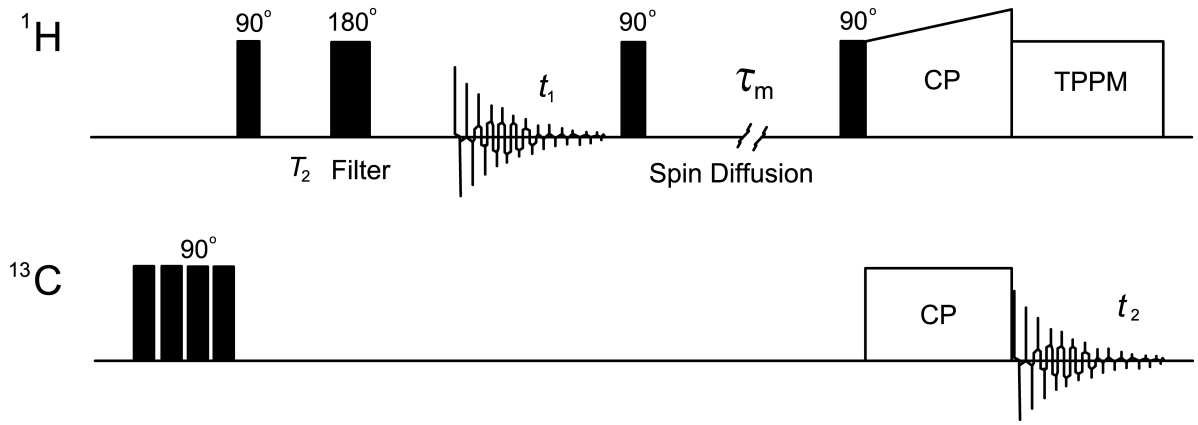

Figure 5.2: *Pulse sequence for the 2-D MAS heteronuclear correlation experiment with proton spin diffusion and ^{13}C detection. CP: cross-polarization, TPPM: two pulse phase modulation decoupling.*

mobile lipids are mostly suppressed in the spectrum. Proper function of the T_2 filter was checked with τ_m = 25 ms and only the lipids $(CH_2)_n$ and H_2O correlations are observed (data not shown). Hence with 25 ms mixing time only the magnetization from mobile lipid segments and H_2O survive while the ^{1}H signals of the more rigid peptide relax due to the strong ^{1}H-^{1}H dipolar couplings.

The 2-D ^{1}H spin-diffusion experiments were carried out using ^{1}H spin diffusion mixing times between 50 ms and 400 ms. Spinning frequencies of 7 kHz were employed and regulated to ±2 Hz by a pneumatic control unit using a standard cross polarization pulse sequence for the transfer of magnetization between ^{1}H and ^{13}C.[5] The CP contact time was 512 μs. A Goldman-Shen T_2 filter (1.96 ms) was applied to selectively excite the more mobile lipid protons.[6] Experiments were run for different spin diffusion mixing times, 50 ms $<\tau_m <$ 400 ms. The data were collected in 640 scans with a spectral width of 94 kHz. T_1 values of different lipid protons were measured in a standard inversion-recovery experiment. All PDSD measurements were performed at a temperature of 277 K. The lower temperature was chosen to optimize the signal to noise ratio.

Oriented samples: The oriented samples were inserted into a multichannel flat coil probe head and placed in a Bruker AV750 spectrometer with the membrane

normal oriented parallel or perpendicular to the magnetic field direction. Proton-decoupled 1D ^{15}N solid-state NMR spectra were recorded using a CP Hahn echo pulse sequence with a 90° pulse length of 7.8 μs, an echo delay of 40 μs, 25K scans of 1K data points, and a recycle delay of 3 s.[15] A line broadening of 10 Hz was applied before Fourier transformation. The spectra were processed without first order phase correction and calibrated to NH_4Cl at 41.5 ppm chemical shift. The NMR measurements were performed using similar conditions of pH 7.4, at a temperature of 310 K and with ~ 30 min of equilibration time in the spectrometer before recording the data. Spectra were collected over 3 hr intervals to monitor changes.

5.2.3 Data Analysis

For quantitative analysis of 2-D spin-diffusion spectra, ^1H cross sections were extracted from the 2-D spectra at the desired ^{13}C frequency. Peak intensities were recorded with respect to a first spectrum, collected with a mixing time of 50 ms. These relative peak intensities were corrected for T_1 relaxation during the mixing time by multiplication with $\exp(\tau_m/T_1)$. ^1H spin-lattice relaxation times of lipid signals were measured using a standard inversion recovery sequence.[5,6] The orientation information is extracted from the minimum distance between the peptide and the center of the bilayer; the larger this distance is, the slower is the spin diffusion.[5,6] The bilayers have an acyl chain length of about ~16 Å, a distance from the headgroup to the bilayer center of about ~ 22 Å, and a water layer thickness of about 19 Å. If a peptide is buried in the bilayer according to the transmembrane model of Figure 5.1A, then it is in close proximity of the lipid chains and away from the H_2O. In contrast, when peptides are peripherally intercalated one part is buried in the bilayer while the other part is interacting with lipid headgroups. Such peptides are in close proximity to both the ^1H of the lipid chains and the H_2O protons.

5.3 Results and Discussion

The orientational topology and secondary structure of membrane-associated peptides is an important aspect of their structure-function relationship. To assess whether the fusogenicity of the peptides is related to their structural properties, the secondary structure is studied under different conditions. To determine how the peptides fold when all solvent is removed, high-resolution ^{13}C 1D solid-state NMR data were collected from lyophilized samples, which is the starting material for the fusion assays (Fig. 5.3). The ^{13}C-carbonyl chemical shift at ~175 ppm is characteristic for an α-helix, while the signal at ~170 ppm is generally attributed to β-sheet.[16] Hence, L16 with its carbonyls resonating around 175.8 ppm predominantly forms α-helices. In contrast, LV16 shows two signals at 172.5 ppm and 171.5 ppm. This splitting indicates slightly different signals for the ^{13}C carbonyl of the alternating Leu and Val residues in a unique overall conformation. Because the chemical shift is in the upfield region, the data indicate a β-sheet conformation. The resonance at 171.3 ppm observed for LV16-G8P9 also is indicative of predominantly β-sheet. This carbonyl line is asymmetric with a downfield extension at the base into the shift range for α-helix.

The ^{13}C 1D solid-state NMR spectra of the peptides in unoriented lipid vesicles show a similar trend in the ^{13}C-carbonyl chemical shifts as for the lyophilized samples (Fig. 5.3). The ^{13}C-carbonyl chemical shift of peptide L16 is at 175.2 ppm, indicating that the peptide is in the α-helix form. The ^{13}C-carbonyl shift of peptides LV16 and LV16G8P9 is at 172.5 ppm in the upfield region, indicating a β-sheet conformation. All peptides show relatively broad signals, which indicate considerable structural disorder at the microscopic level, relative to a fully crystalline peptide preparation. The heterogeneity appears most pronounced for LV16 and LV16-G8P9, which is in line with their fusion-promoting activity. 1D ^{1}H spectra of peptides bound to the lipids are depicted in Fig. 5.4. ^{1}H chemical shifts of the different lipid protons were assigned to H_2O (4.8 ppm), $N(CH_3)_3$ (3.4 ppm), NCH_2

(2.3 ppm), CH_2CO (2.5, 2.3 and 2.1 ppm), $(CH_2)_n$ (1.3-1.6 ppm) and CH_3-ω (1.0 ppm). Due to the low concentration of peptide, the peptide proton signals are not detected.

The lipid-initiated ^1H spin-diffusion technique provides an alternative approach to obtain membrane associated peptide topology information in vesicles.[5] By exploiting the difference between the ^1H magnetization transfer rates in lipids and in peptides, information about the location of the peptides can be obtained.[5] Figures 5.5, 5.6 and 5.7 show representative 2-D ^{13}C-detected ^1H spin-diffusion datasets for the membrane-bound peptides, L16, LV 16 and LV16G8P9 respectively,

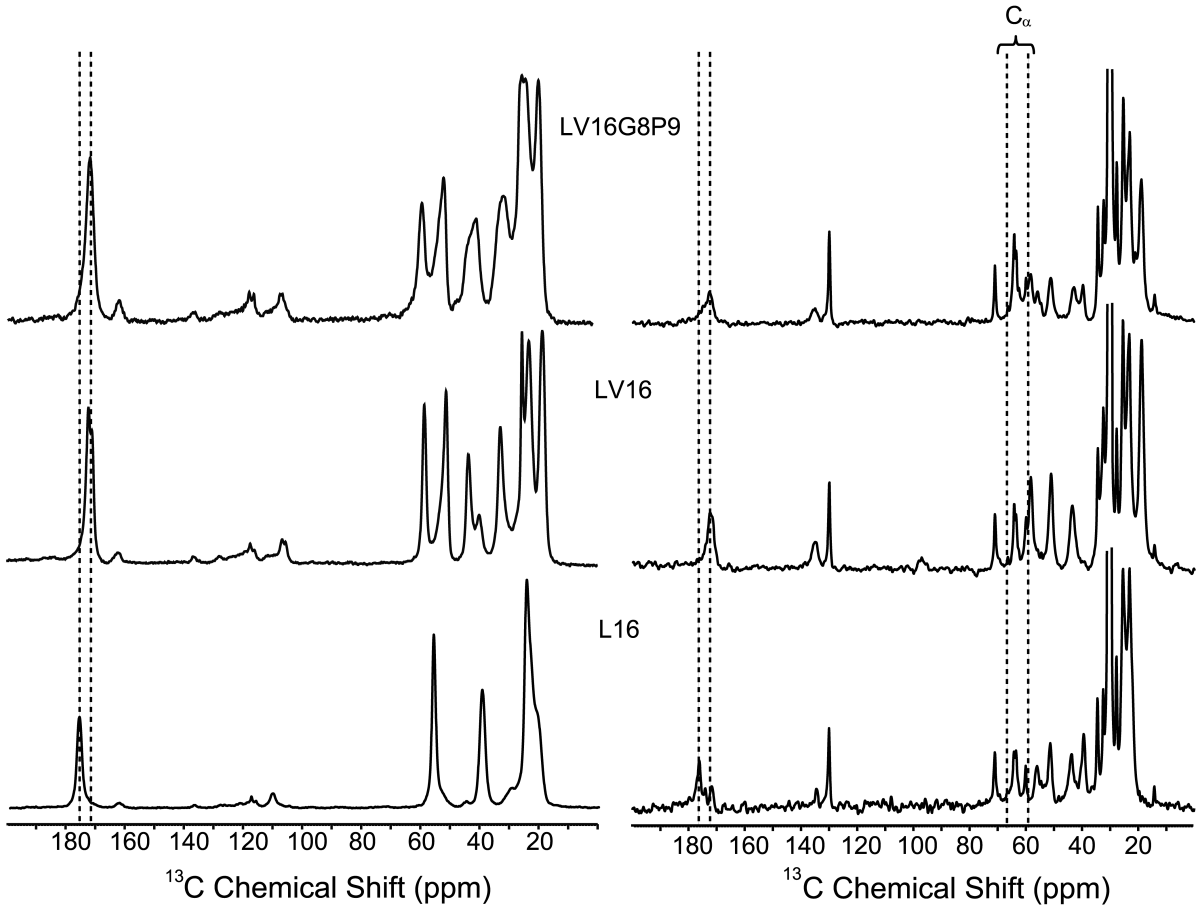

Figure 5.3: *One-dimensional ^{13}C-natural abundance CP-MAS solid-state NMR spectra of lyophilized peptides illustrating the differences in the ^{13}C-carbonyl resonances for L16, LV16 and LV16G8P9 (Left panel). One-dimensional ^{13}C CP-MAS solid-state NMR spectra of uniformly labeled peptides in a biomimetic lipid mixture (Right panel). The signals between 20 ppm and 60 ppm correspond to Cα, Cβ, as well as side-chain carbons.*

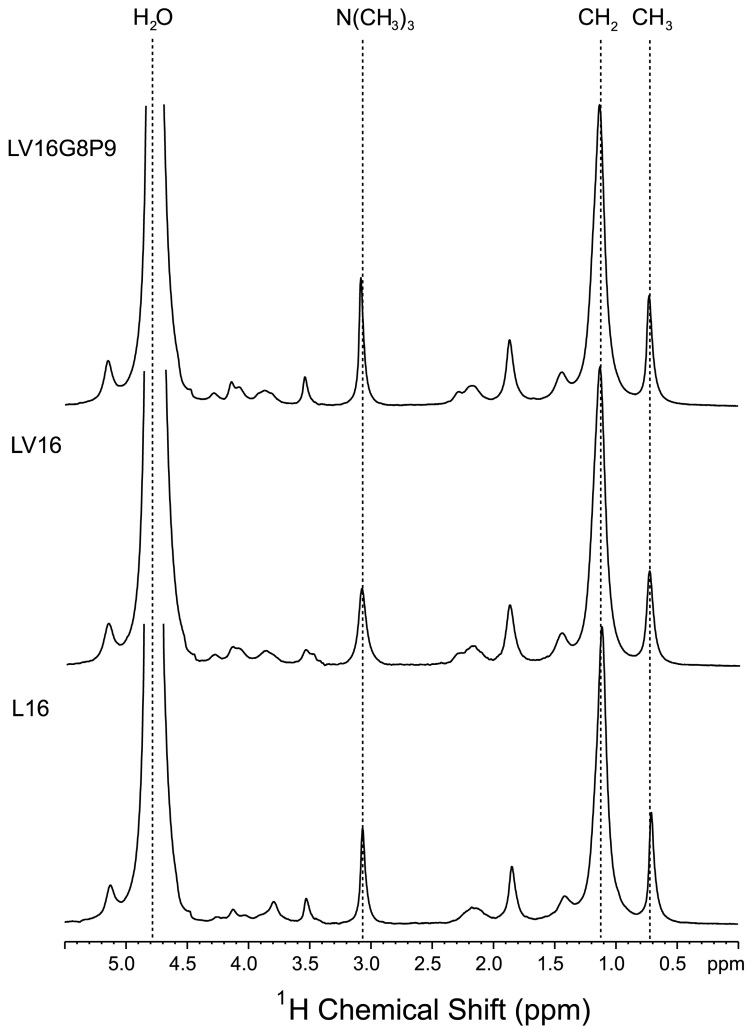

Figure 5.4: *One-dimensional ^{1}H MAS NMR spectra of uniformly labeled peptides, L16, LV16 and LV16G8P9, in biomimetic lipid mixtures. The data were recorded at 277 K with a spinning frequency of 7 kHz. The proton signals of peptides are not detected at this peptide to lipid ratio.*

obtained with a mixing time of 200 ms. The source and sink of spin diffusion are readily distinguished in the 2-D spectrum; the ^{13}C chemical shifts of the peaks mark the sinks of spin diffusion while the ^{1}H chemical shifts indicate the sources of the magnetization.[5] The ^{1}H peaks in each column indicate the origins of magnetization transfer. The strong peaks that are observed for H_2O protons are due to the correlations between water and lipid carbons, which are abundantly present in the sample. The mixing-time-dependent 2-D spin-diffusion spectra are analyzed by extracting ^{1}H cross-sections at a specific ^{13}C frequency.

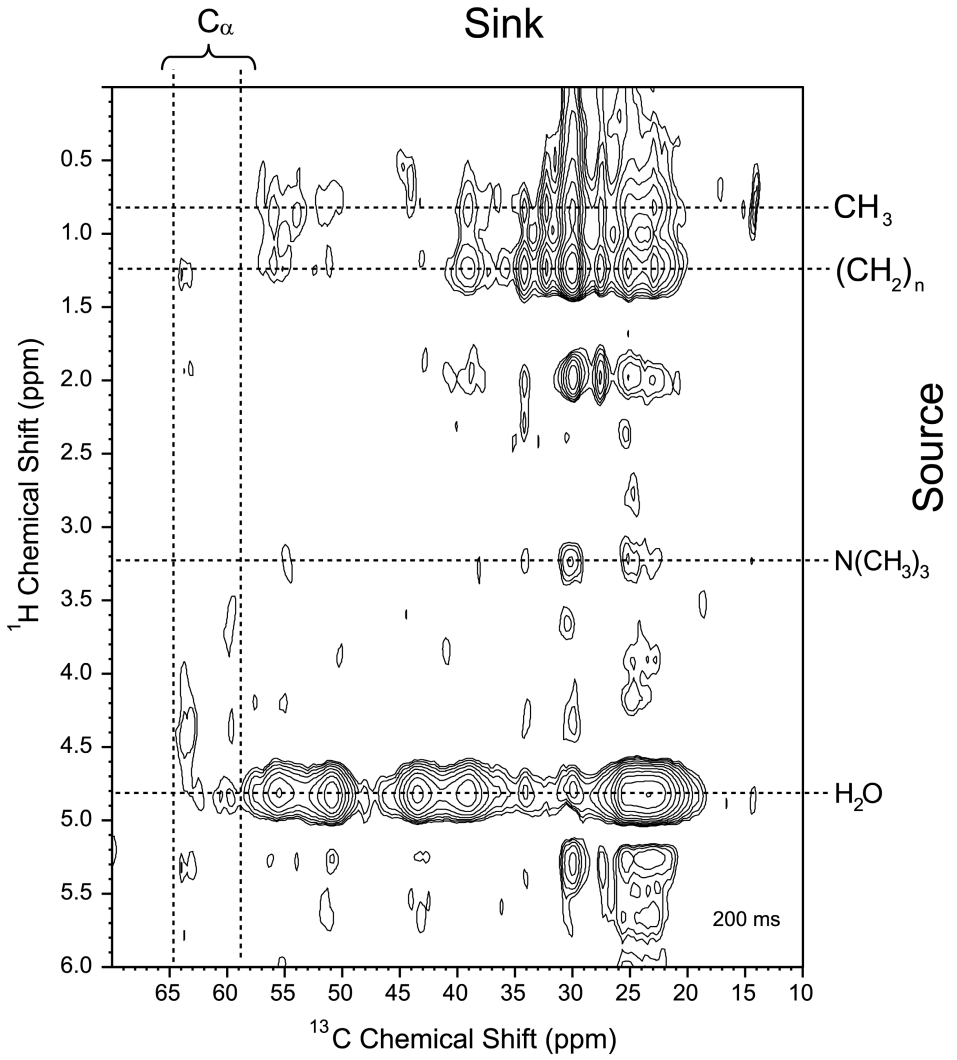

Figure 5.5: *2-D ^{13}C-detected ^{1}H spin-diffusion spectrum of the membrane bound labeled L16 with a mixing time of 200 ms. A T_2 filter time of 2 ms, a relaxation delay of 3 s, and a spinning frequency of 7 kHz were used. The spectrum was recorded at 277 K. The peptide C_α region was determined from the CP/MAS data shown in Figure 5.3.*

To determine if a peptide is intercalated into the bilayer, the cross peak intensities for spin diffusion from the lipid chain methylene protons and H_2O protons to the C_α residues in the peptides were extracted from different spin diffusion mixing times. Table 5.1 shows the normalized build up intensities for the C_α residues for the fusogenic peptides LV16 and LV16G8P9, and for the non-fusogenic peptide, L16. For all three peptides LV16G8P9, LV16 and L16 the

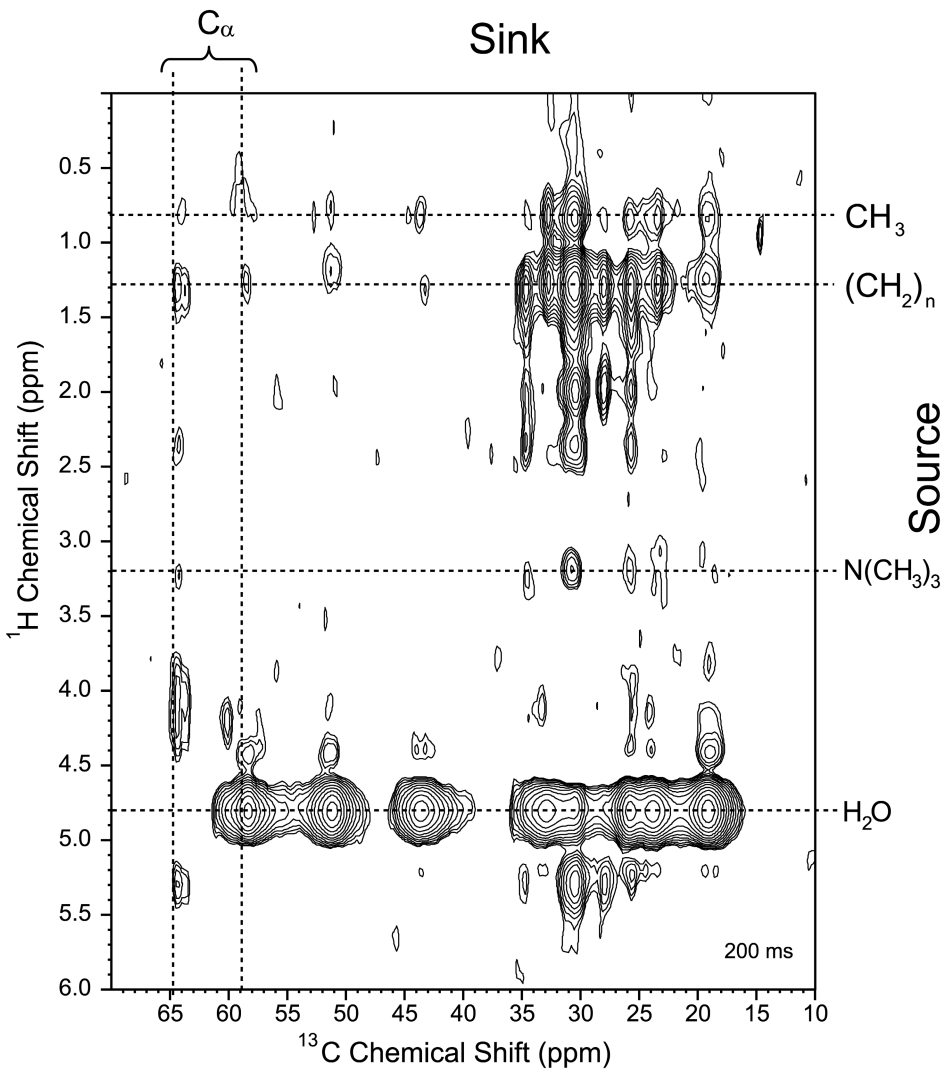

Figure 5.6: *2-D ^{13}C-detected ^{1}H spin-diffusion spectrum with a mixing time of 200 ms of the membrane bound labeled LV16. A T_2 filter time of 2 ms, a relaxation delay of 3 s, and a spinning frequency of 7 kHz were used. The spectrum was recorded at 277 K. The peptide C_α sink region is indicated with vertical dash lines.*

normalized intensities for the C_α due to spin diffusion from the $(CH_2)_n$ show a fast build up on a time scale of ~ 100 ms, corresponding with a spin diffusion gap of ~ 2 Å, as reported for other peptides.[5,6] Also the normalized build up intensities for spin diffusion from the H_2O protons for the LV16G8P9 and LV16 peptides show the fast build up characteristic for a gap of ~ 2 Å.[5,6] In contrast, the signal build up by spin diffusion from the H_2O protons into peptide L16 is slow on a time scale of 400 ms.[5,6]

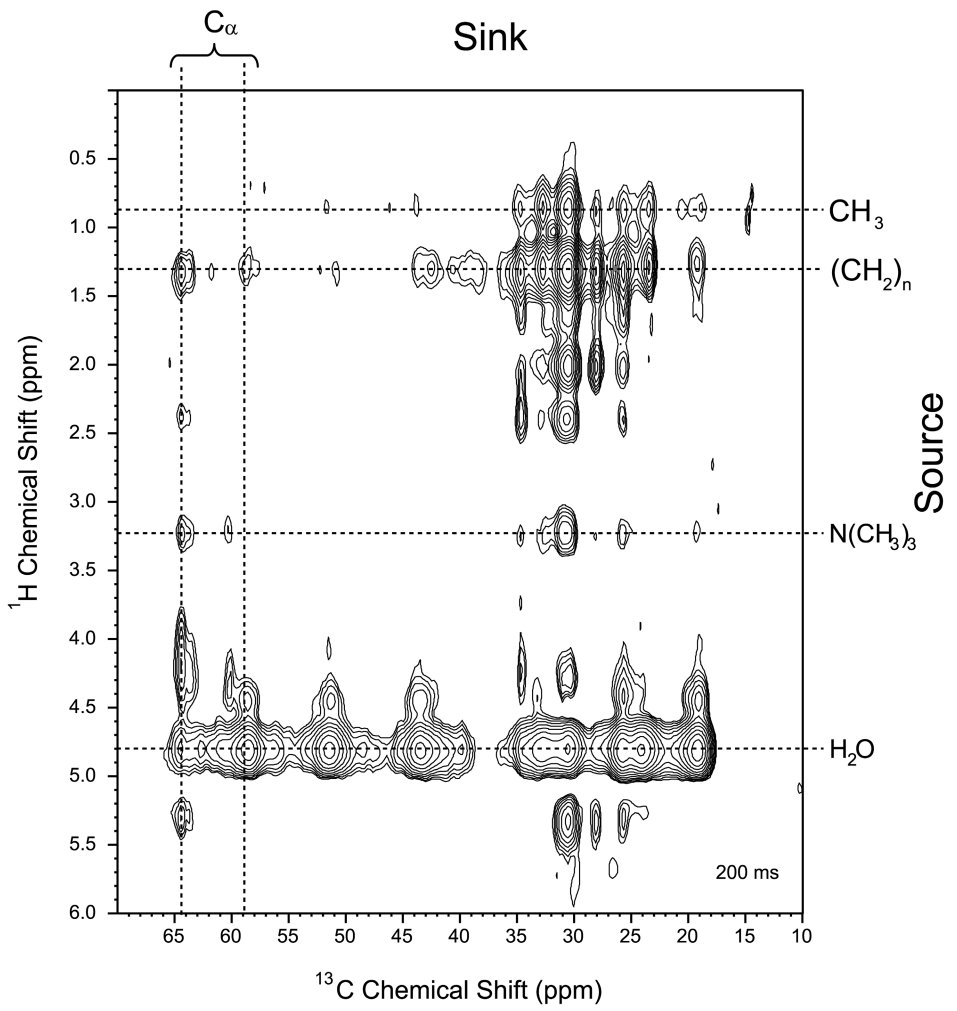

Figure 5.7: *2-D ^{13}C-detected ^{1}H spin-diffusion spectrum of the membrane bound labeled LV16G8P9 using a mixing time of 200 ms. A T_2 filter time of 2 ms, a relaxation delay of 3 s, and a spinning frequency of 7 kHz were used. The spectrum was recorded at 277 K and the peptide C_α sink region is indicated with vertical dash lines.*

As the distance increases, magnetization is transferred along the lipid chains over an increasing distance, thus resulting in slower build-up curves.[5] Model studies have shown that diffusion over the entire lipid molecule, i.e. up to ~ 16 Å corresponds with diffusion lines in the range of 400 ms. Since the rate-limiting step of the proton spin diffusion is related to distances,[5] the data indicate that the peptide L16 is closer to the protons of the lipid tails than to the H_2O. Thus, the relatively slow build-up of the H_2O signal would be in line with a peptide that is

τ_m ms	LV16G8P9		LV16		L16	
	$(CH_2)_n$	H_2O	$(CH_2)_n$	H_2O	$(CH_2)_n$	H_2O
50	0.77 ±0.12	0.76 ±0.06	0.65 ±0.12	0.78 ±0.04	0.80 ±0.11	0.63 ±0.06
100	0.95 ±0.11	0.87 ±0.07	0.79 ±0.15	0.88 ±0.05	0.99 ±0.12	0.69 ±0.05
200	0.96 ±0.12	0.92 ±0.06	0.96 ±0.12	1 ±0.07	0.95 ±0.05	0.79 ±0.06
400	1 ±0.12	1 ±0.08	1 ±0.15	0.96 ±0.07	1 ±0.08	1 ±0.05

Table 5.1: *Spin-diffusion build up for the Cα signal of LV16G8P9, LV16 and L16. The magnetization sources are $(CH_2)_n$ and H_2O. Data were corrected for ^1H T_1 relaxation. Errors represent the noise level in the 2-D spectra.*

transmembrane and inserts all the way into the core of the hydrophobic bilayer (Fig. 5.1A). In contrast, the fusogenic peptides LV16 and LV16G8P9 are probably at the membrane-water interface. The protons of the fusogenic peptides are close to both the protons of the water molecules and the protons of the lipid chains (Fig. 5.1B).

In ^{15}N NMR, different sites within a molecule are distinguished by differences in their chemical shift, which is a result of the shielding of the nucleus from the magnetic field by the surrounding electrons. The electron cloud is not symmetric in all directions around a nucleus bonded to other atoms in a molecule, and the effect of this asymmetry on the ^{15}N NMR response is described by the chemical shift anisotropy tensor, which has a particular orientation relative to the molecular frame and principal values, σ_{11}, σ_{22} and σ_{33}.

To perform solid-state NMR structural analyses using static oriented samples, peptides are reconstituted into oriented lipid bilayers and the sample is introduced into the magnet of the NMR spectrometer with the normal parallel to the magnetic field direction. With this arrangement lateral or rotational diffusion around the membrane normal averages the alignment of the peptide relative to the

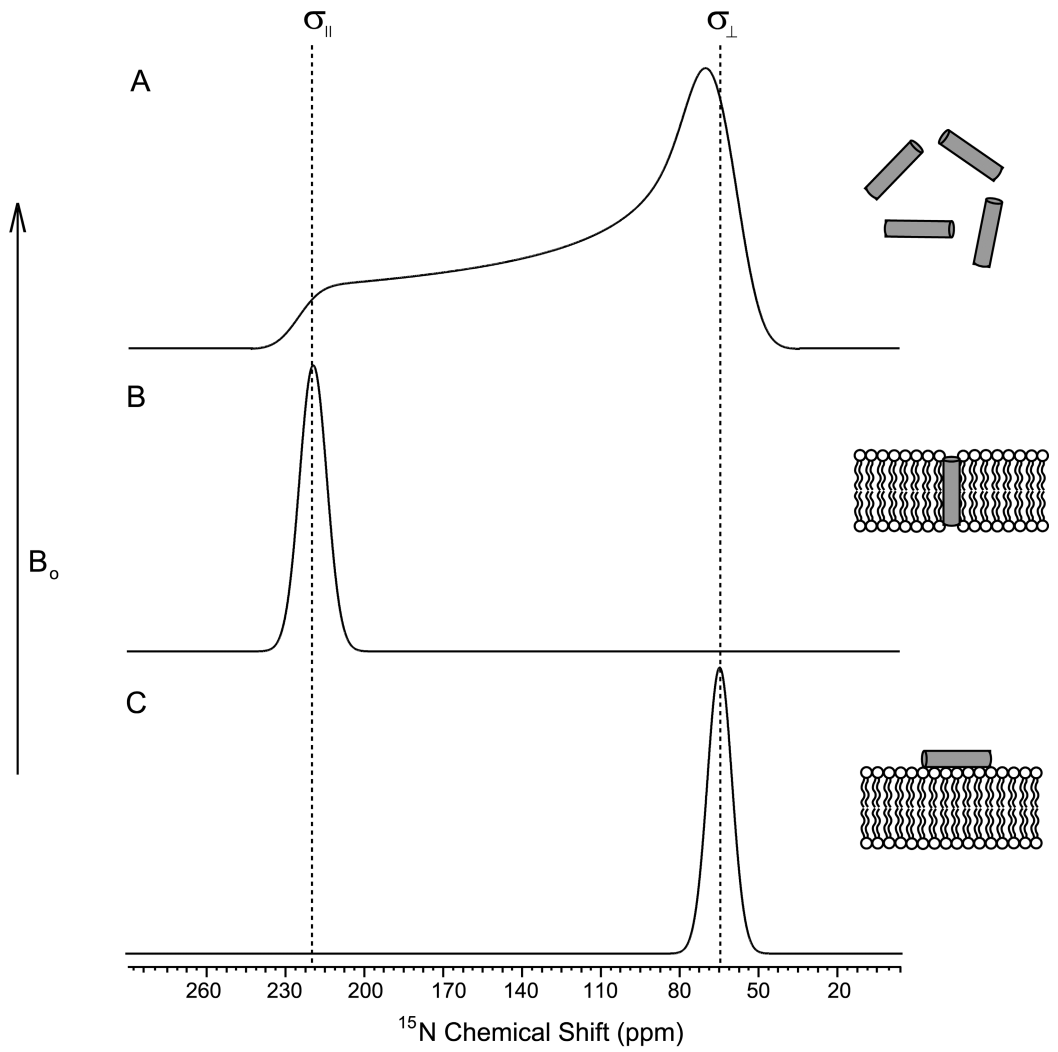

Figure 5.8: Schematic ^{15}N chemical shift spectroscopy for determination of peptide orientation. *(A) A powder pattern is observed when all orientations are present. (B) When the helix is parallel to the magnetic field, a chemical shift near σ_{33}, above 200 ppm, is observed, indicating transmembrane orientation. (C) When the helix is perpendicular to the magnetic field, a chemical shift near σ_{11} and σ_{22}, below 100 ppm, is observed upon averaging of the anisotropy by rotation.*

magnetic field direction. Therefore the resulting solid-state NMR signal reflects the molecular alignment relative to the bilayer normal and B_0-vector and this can be used to obtain orientational constraints for the molecule. However, tilting, wobbling and vibrational motions, conformational changes, or quenching of rotation or

diffusion can give incomplete averaging of the anisotropy, and this needs to be analyzed in detail for high-precision structural analyses.[17]

While the ^{15}N chemical shift of a peptide bond within a helical molecule exhibits values around 220 ppm when the helix long axis is oriented approximately parallel to the magnetic field direction, ^{15}N responses in the 60-80 ppm range are measured at perpendicular alignments (Fig. 5.8).[17] If all directions are present in a sample, such as in a solid powder, then all of the different degrees of shielding, and resulting chemical shifts, are observed as shown in Figure 5.8A. Assuming that a peptide binds and inserts into lipid bilayers with a particular orientation, then all the peptides in the aligned bilayer samples will be lined up the same way, and a single narrow peak will be observed in the ^{15}N spectrum.[17] Since σ_{33} is oriented close to the N–H bond and helix axis, a peptide α-helix with its axis parallel to the magnetic field will have a chemical shift near σ_{II}, and a peptide α-helix with its axis perpendicular to the magnetic field will have a chemical shift near $\sigma_{\perp}$ (Figs 5.8B and C).[17]

The ^{15}N solid-state NMR on macroscopically aligned bilayer samples loaded with uniformly labeled peptides with the normal parallel to B_0 shows chemical shift values covering a wide range of values within the 60-230 ppm as expected for peptide aggregates (Fig. 5.9). These NMR measurements have been performed at 310 K, *i.e.* well above the gel-to-liquid crystalline phase transition of lipids used. The broad lines in the Figure 5.9 reveal very little averaging of the shift anisotropy, since the full anisotropy is detected. The proton decoupled ^{15}N spectrum of the non-fusogenic peptides L16 in bilayers shows a powder pattern with a broad peak at 200 ppm that is intriguing, since the shift corresponds with the σ_{II} in Figure 5.8B for the signal of a monomeric transmembrane motif. When the samples are rotated by 90°, with the bilayer normal perpendicular to the magnetic field, the ^{15}N NMR spectra of the peptides show a powder pattern indicating a random distribution of orientations in the sample (Fig. 5.9, right panels).

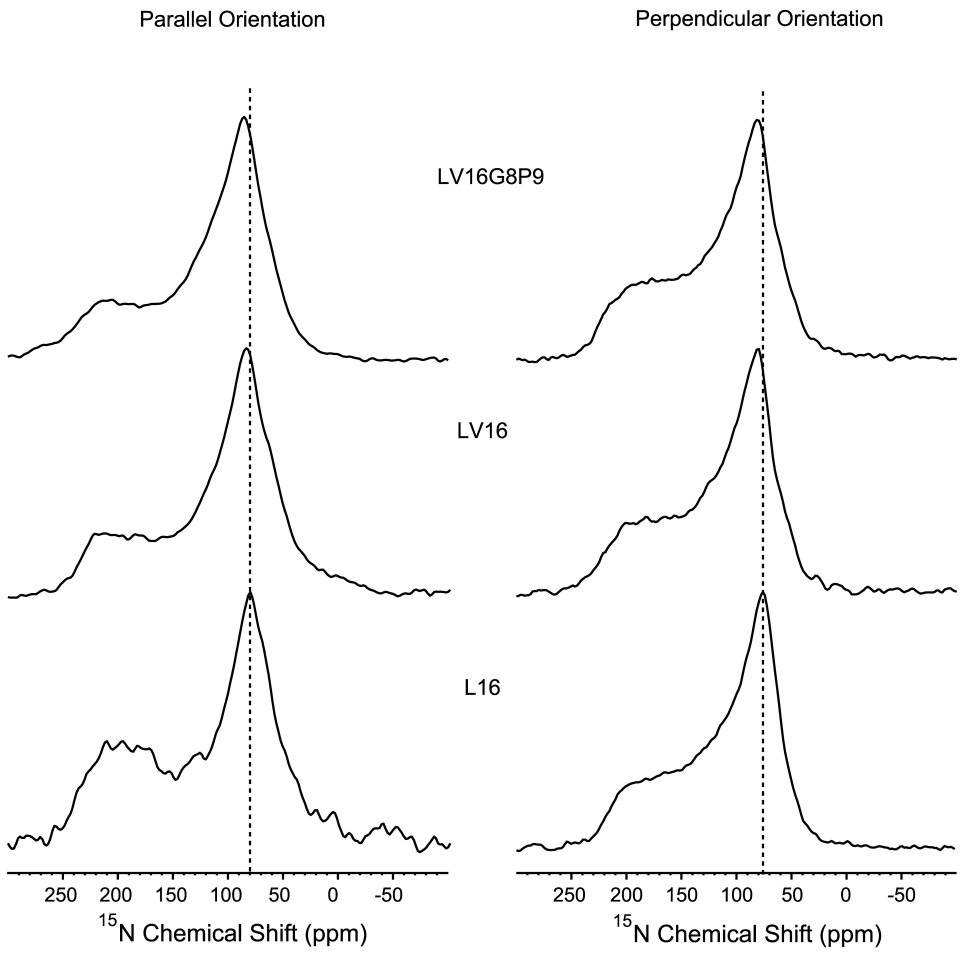

Figure 5.9: *Preliminary proton-decoupled ^{15}N spectra of L16, LV16 and LV16G8P9 reconstituted into oriented biomimetic membranes where the bilayer normal parallel or perpendicular to the magnetic field direction. The data reveal quenching of rotational diffusion for all peptides, most probably due to aggregation.*

5.4 Conclusions

According to spin-diffusion data collected from vesicles loaded with peptides, the non-fusogenic L16 favors a transmembrane topology (cf. Fig. 5.1A) while the data for the fusogenic peptides are in line with peripheral intercalation (Fig. 5.1B). Magnetization can transfer from the lipid acyl chain to the peptide, and is redistributed within the peptide. This is in global agreement with the peripheral

intercalation model for the fusogenic peptides, since it includes a membrane inserted part as well as a peptide domain interacting with the water layer. The data obtained are well in line with circular dichroism and IR measurements, which show that LV16G8P9 exists mainly in β-sheet and turns conformation in liposomes, which is also consistent with inducing curvature by peripheral association with the outer layer as depicted in Figure 5.1B.[1] The spectra given in Figure 5.9 were collected from oriented bilayer samples loaded with peptides, which is different from the vesicle preparations used in the spin diffusion experiments. It is remarkable that for the L16 peptide a marginally enhanced σ_{II} signal is observed, at the shift value expected for transmembrane peptides. Indeed an unambiguous analysis of these data would require a detailed knowledge of the aggregation state of the peptides within the sample.

The peptides incorporated in the membrane catalyze the fusion process by balancing the lipid bilayer, leading to stabilization of curved structures (Chapter 3 and 4). In addition, the structural flexibility of the core region as well as positive terminal charges are required for LV-peptide function in lipid mixing (Chapter 4). Since the fusogenic molecules interact with the lipids and influence the orientation and structural properties of the membrane, they can promote hemifusion, which then leads to the fusion. The data collected in this thesis also indicate a synergy between the interaction of the fusogenic peptide with lipid component(s) on the one hand, and interactions among lipids on the other hand, which is required for a phase change to occur (Chapter 3). In particular, the cone-shaped PE is known to favor membrane fusion, which can be attributed to its ability to support negative bilayer curvature in fusion intermediates (Chapter 3). Though the work described in this thesis it also transpires that a proper and detailed structure and functional study of bio-molecules like proteins and peptides cannot be done in a single lipid molecular environment, which might easily lead to spurious results and wrongful interpretation of data.

Future studies will show whether the fusogenicity of peptides correlates with their detailed secondary structure and conformational flexibility in a membrane

environment. If membrane defects leading to fusion pores develop at the peptide-lipid interface, pore function would depend on peptide or protein, as well as on lipids. The future will tell whether the fusion reaction moves along a well-defined pathway or involves a broad distribution of possible structural intermediates. The peptide-lipid interactions may promote outer leaflet mixing and fusion pore formation and knowledge about the location of these peptides within different lipid domains will help to understand how they do it. Peptide-peptide interactions and multimerisation of oligomeric complexes may play a role during the process of membrane fusion and this needs further investigation by suing site-specific labeling. In a potential practical application, the pH-dependent LV-peptides might prove to be useful in lipofection of eukaryotic cells. These peptides can also be used in the bio-drug delivery devices and also as smart biopolymers. The biomimetic lipid environment setup can be used as a screening tool for the peptides, proteins and other organic and bio-molecules. In conclusion, the studies discussed in this thesis show that relatively straightforward solid-state NMR experiments on systems that mimic closely the natural system can provide useful information about the complex problem of membrane fusion.

References

1. Langosch, D. *et. al.* , **Manuscript Submitted**.
2. Wasniewski, C. M.; Parkanzky, P. D.; Bodner, M. L.; Weliky, D. P., *Chem. Phys. Lipids,* **2004,** 132, 89-100.
3. Hofmann, M.; Weise, K.; Ollesch, J.; Agrawal, P.; Stalz, H.; Stelzer, W.; Hulsbergen, F.; de Groot, H.; Gerwert, K.; Reed, J.; Langosch, D., *Proc. Natl. Acad. Sci. U. S. A.,* **2004,** 101, 14776 - 14781.
4. Deutsch, J. W.; Kelly, R. B., *Biochemistry,* **1981,** 20, 378-385.
5. Huster, D.; Yao, X.; Hong, M., *J. Am. Chem. Soc.,* **2002,** 124, 874-883.
6. Raap, J.; Hollander, J.; Ovchinnikova, T. V.; Swischeva, N. V.; Skladnev, D.; Kiihne, S., *J. Biomol. NMR,* **2006,** V35, 285.
7. Aisenbrey, C.; Bechinger, B., *J. Am. Chem. Soc.,* **2004,** 126, 16676-16683.
8. Bechinger, B.; Kinder, R.; Helmle, M.; Vogt, T. C. B.; Harzer, U.; S., S., *Biopolymers - Peptide Science,* **1999,** 51, 174-190.
9. Cross, T. A., *Methods Enzymol,* **1997,** 289, 672-96.
10. Griffin, R. G., *Nat Struct Biol,* **1998,** 5 Suppl, 508-12.
11. Watts, A., *Curr Opin Biotechnol,* **1999,** 10, 48-53.
12. Davis, J. H.; Auger, M., *Prog. Nucl. Mag. Res. Sp.,* **1999,** 35, 1.
13. Bechinger, B., *Biochim. Biophys. Acta, Biomembr.,* **1999,** 1462, 157-183.
14. Hofmann, M. W.; Peplowska, K.; Rohde, J.; Poschner, B. C.; Ungermann, C.; Langosch, D., *J. Mol. Biol.,* **2006,** 364, 1048.
15. Rance, M.; Byrd, R. A., *J. Magn. Reson.,* **1983,** 52, 221-240.
16. Kameda, T.; Takeda, N.; Kuroki, S.; Kurosu, H.; Ando, S.; Ando, I.; Shoji, A.; Ozaki, T., *J. Mol. Struct.,* **1996,** 384, 17-23.
17. Burkhard Bechinger, C. S., *Concepts Magn. Reson. A,* **2003,** 18A, 130-145.

Summary

Membrane fusion is mediated by fusogenic proteins and requires restructuring of lipid bilayers. The transmembrane segments of these proteins can drive membrane fusion indicating that simple synthetic biological constructs for fusion exist and can be evaluated. The main area of the research discussed in this thesis is to understand the membrane fusion mechanism by studying a model system that mimics nature. The background of the work is described in **chapter 1**. The selection and high yield synthesis of a set of *de novo* designed synthetic peptides for use in functional investigations is described in **chapter 2**. These biomimetic peptides are isotopically enriched with ^{13}C and ^{15}N nuclei and require only 3 equivalents of amino acids for each coupling step and are prepared with a high purity, >90%. The peptides give reproducible and consistent fusion data sets that correlate well with the intended functional design characteristics, from strongly fusogenic to almost non-fusogenic.

In **chapter 3** and **chapter 4**, it is shown that small amounts of peptides incorporated in the membrane can catalyze the fusion process by massively disturbing the lipid bilayer balance and stabilizing curved bilayer structures. Using ^{31}P solid state NMR, the interactions of the *de novo* designed peptides with both a biomimetic three-lipid mixture and a single lipid system are described. The hydrophobic sequences that are made up of mixtures of helix- and sheet-promoting residues as well as helix-destabilizing residues with an optimal length of 23 amino acids are most fusogenic. This functional property is paralleled by a large degree of

cooperativity in the lipids, possibly due to phase separation across the lipid bilayer. In **chapter 5** the first studies on the uniformly labeled peptides are performed. The data contribute to converging evidence that the fusogenic peptides show some structural flexibility in the 1D ^{13}C NMR while 2D HETCOR transfer experiments indicate that they are peripherally intercalated at the membrane-water interface. Peptide-peptide interactions, multimerisation or aggregation of peptides may play a role during the process of membrane fusion and this needs further investigation.

During membrane fusion mixing of outer membrane leaflets requires lipid molecules to leave their bilayer orientation. This leads to the stalk formation, which provides a local link between both membranes. Further expansion results in a hemifusion diaphragm. It is proposed that the existence of these intermediate structures depends on the intrinsic curvature of lipids. The intrinsic curvature is defined by the ratio of the cross-sectional areas of the hydrated lipid head-group and the acyl chain moiety, which in turn determines the curvature of a monolayer of the lipid species. Accordingly, a positive intrinsic curvature of phosphatidylcholine can stabilize the outer monolayer while negative curvature of the inner monolayer can be stabilized by lipids with negative intrinsic curvature, such as phosphatidylethanolamine. At the rim where a hemifusion diaphragm meets the outer monolayer of a fusing membrane, lipid bilayers have to adopt net negative curvature compared to the remaining unfused bilayer. Such behavior is well known and well documented in the physical chemistry field and is used abundantly in the description of detergent behavior, but it is new in biological fusion. Thus fusion can indeed be stimulated by cooperative lipid behavior that is mediated by the interplay between lipid molecules with negative and positive intrinsic curvature and triggered by peptides steering the bilayer composition.

In addition, the low-complexity *de novo* designed synthetic peptides appear to induce contrasting biomimetic lipid rearrangements where the extended curvature regions can lead to the stalk formation while shrinking regions may lead to toroidal pores. From the study described in this thesis it transpires that relatively straightforward experiments on a model system that mimics the natural system can

provide useful information about the complex problem of membrane fusion while a functional study of bio-molecules performed in a single lipid molecular environment might easily lead to spurious results and the erroneous interpretation of data. It is anticipated that the first steps made in this thesis in describing a multicomponent lipid system, will be refined and improve when more data becomes available.

Samenvatting

Membraamfusie wordt geregeld door fusogene eiwitten en vereist structuurverandering van lipide bilagen. De transmembraamsegmenten van deze eiwitten kunnen membraamfusie aansturen, hetgeen erop duidt dat simpele structurele biologische constructies voor membraamfusie bestaan en dat deze verder kunnen worden ontwikkeld. Het belangrijkste onderzoeksresultaat dat in dit proefschrift wordt beschreven is het principe achter het membraamfusiemechanisme, verkregen door studie van een gesimuleerd biologisch membraamsysteem. De achtergrond van dit model wordt besproken in **hoofdstuk 1**. De selectie en synthese met hoge opbrengst van een set *de novo* ontworpen peptiden voor toepassing in dit functionele onderzoek wordt beschreven in **hoofdstuk 2**. Deze biomimetische peptiden bevatten ^{13}C en ^{15}N isotoop-verrijkte aminozuren en de synthese met hoge zuiverheid, >90%, vereist slechts 3 equivalenten van aminozuren voor iedere koppelingsstap. De peptiden vertonen reproduceerbare fusie eigenschappen, die goed correleren met de gewenste karakteristieken van een functioneel model systeem, van sterk fusogeen tot bijna niet-fusogeen.

In **hoofdstuk 3** en **4** wordt aangetoond dat kleine aantallen peptiden, die in een membraam worden geïncorporeerd, het fusieproces kunnen katalyseren door de balans in de lipide bilaag te verstoren en gekromde bilagen te stabiliseren. Met ^{31}P vastestof NMR kunnen de interacties van de *de novo* ontworpen peptides met zowel het biomimetisch drie-lipide mengsel als met het enkel-lipide systeem bepaald

worden. De hydrofobe reeksen met een lengte van 23 aminozuren die uit mengsels van α-helix- en β-sheet-initiërended residuen bestaan, alsmede α-helix-initiërende destabiliserende residuen, zijn het meest fusogeen. De fusie wordt vergemakkelijkt door de lipiden, mogelijk door fasenscheiding over de lipide bilaag. In **hoofdstuk 5** worden de eerste onderzoeksresultaten met betrekking tot de uniform gelabelde peptiden beschreven. De fusogene peptiden vertonen enige structurele flexibiliteit in de 1D-^{13}C NMR, terwijl 2D HETCOR transfer experimenten intercalatie aan het membraam-water oppervlak laten zien. Peptide-peptide interacties en aggregatie van peptiden spelen waarschijnlijk een rol tijdens het proces van membraamfusie. Dit dient verder onderzocht te worden.

Gedurende membraamfusie moeten lipide moleculen hun bilaagorientatie verstoren. Dit leidt tot vorming van een zogenaamde stengel, een lokale link tussen twee membramen. Verdere expansie resulteert in een hemifusie diafragma. Verondersteld wordt dat het bestaan van deze intermediaire structuren afhangt van de intrinsieke kromming van de lipiden. De intrinsieke kromming wordt gedefinieerd als de verhouding tussen de dwarsdoorsneden van de gehydrateerde lipide eind-groep en de lipide acyl-keten, welke op hun beurt de kromming van een monolaag van dit type lipide bepalen. Een positieve kromming zoals voor phosphatidylcholine kan de buitenste monolaag stabiliseren, terwijl negatieve kromming van de binnenste monolaag kan worden gestabiliseerd door lipiden met intrinsieke negatieve kromming, zoals phosphatidylethanolamine. Op de grens waar een hemifusie diafragma de buitenste monolaag van een fuserend membraan raakt, moeten lipide bilagen een negatieve kromming aannemen ten opzichte van de andere niet-gefuseerde bilaag. Dit gedrag is bekend, en goed beschreven in het vakgebied van de fysische chemie en wordt vaak gebruikt in de beschrijving van oppervlakte actieve stoffen, maar het is nieuw in biologische fusiestudies. Dus membraamfusie kan inderdaad worden gesimuleerd door coöperatief lipide gedrag dat geregeld wordt door de interactie tussen lipide moleculen met negatieve en positieve intrinsieke kromming, en opgestart wordt door peptides die de compositie van de bilaag sturen.

De *de novo* ontworpen synthetische model-peptiden met lage complexiteit lijken contrasterende biomimetische lipide veranderingen te veroorzaken waar stengelvorming hetzij kan leiden tot uitgebreide gebieden van kromming, hetzij tot toroidale porieën. Uit het onderzoek, beschreven in dit proefschrift blijkt dat relatief eenvoudige experimenten met een modelsysteem, dat lijkt op het natuurlijke systeem, goed inzicht kan verschaffen in het complexe probleem van membraamfusie, terwijl een functioneel onderzoek naar bio-moleculen, gedaan in een enkelvoudige moleculaire lipide omgeving, kan leiden tot onjuiste resultaten en de verkeerde interpretatie van gegevens. Naar verwachting zullen de eerste stappen, beschreven in dit proefschrift voor een multicomponent lipide systeem in de toekomst verder verfijnd en verbeterd worden.

Appendix: IGOR macros used for simulating spectra

The following macros are originally received from Dr. Ramamoorthy's lab; UMI, USA and are modified according to the IGOR pro 4.0 version as well as to simulate the various normalized NMR chemical shift spectral line-shapes, as indicated in the header of each macro. These macros are used for the simulation of the ^{31}P NMR spectra of lipid mixtures with and without peptide in chapters 3, 4 and 5.

A1.1 Macro to simulate chemical shift powder patterns

```
# MSCS UL version

// Simulates the normalized chemical shift powder pattern of a spin 1/2 nucleus with the principle CSA tensor values
// Sigma11, Sigma22, Sigma33, and broadening. The principal values must be entered in the same units; use ppm if that is the desired x-scaling for the spectrum.
// To simulate an axially symmetric powder pattern, enter the same value for 2 of the 3 CSA tensor elements.
// To simulate an oriented or isotropic peak enter the same value for all 3 of the CSA tensor elements.
Macro SimChemShift(BaseName,Sigma11, Sigma22, Sigma33, Broad, DataPoints)
	Variable DataPoints, Sigma11, Sigma22, Sigma33, Broad, Theta, Phi, SigmaL, SigmaH
	Prompt Sigma11, "Sigma11 in ppm:"
	Prompt Sigma22, "Sigma22 in ppm:"
	Prompt Sigma33, "Sigma33 in ppm:"
	Prompt Broad, "Broadening in ppm:"
	String BaseName
	Variable SigmaObs, CT, ST, SP, CP, AR, DS //CT=cos theta, ST=sin theta, etc
	Variable PhiInc=1, ThetaInc=1

	Silent 1; PauseUpdate
	If (Sigma11>Sigma33)
		SigmaL=-40.0
		SigmaH=+40.0
	Else
		SigmaL=-40.0
		SigmaH=+40.0
	Endif
	Make/O/N=(DataPoints) /D $BaseName
	SetScale /I x, SigmaL, SigmaH, $BaseName
```

```
	$BaseName=0
	DS=(SigmaH-SigmaL)/DataPoints

	// Simulate the spectrum by stepping through all theta and phi values and calculating the contribution on the spectrum from each orientation.
	Theta=0
	do
		CT=cos(Theta*pi/180)
		ST=sin(Theta*pi/180)
		Phi=0
		do
			SP=sin(Phi*pi/180)
			CP=cos(Phi*pi/180)

	SigmaObs=(Sigma11*CT*CT+Sigma22*ST*ST*SP*SP+Sigma33*ST*ST*CP*CP)
			$BaseName+=exp(-(x-SigmaObs)*(x-SigmaObs)/(2*Broad^2))*ST
			Phi+=PhiInc
		while(Phi<=90)
		Theta+=ThetaInc
		print Theta
	while(Theta<=90)
	WaveStats /Q $BaseName
	AR=Sum($BaseName)*DS
	$BaseName=($BaseName)/AR
	// $BaseName=$BaseName/V_max
End
```

A1.2 Macro to simulate spectra of cylindrical rods and the hexagonal phase

```
# MSCSC UL version

// Simulates the normalized response of a random distribution of the aligned hexagonal phase or cylindrical rods in the perpendicular to the field (glass plate perpendicular to the magnetic field).
// SigmaPara and SigmaPerp are the parallel and perpendicular edges (near 30 and -15 ppm, respectively) of the axially symmetric fluid lamelaar powder pattern.
// for parallel aligned hexagonal phase use SimChemShift with all sigma values set to (SigmaPara+SigmaPerp)/2.
// for Hexagonal phase powder pattern use SimChemShift with Sigma11=Sigma22=(SigmaPara+SigmaPerp)/2
// and Sigma33=SigmaPerp
Macro SimChemShiftCir(BaseName, SigmaPara, SigmaPerp, Broad, DataPoints)
	Variable DataPoints, SigmaPara, SigmaPerp, Broad, Theta, SigmaL, SigmaH
	Prompt SigmaPara, "Sigma Parallel in ppm:"
```

```
	Prompt SigmaPerp, "Sigma Perpendicular in ppm:"
	Prompt Broad, "Broadening in ppm:"
	String BaseName
	Variable SigmaObs, CT, ST, dTheta, AR, DS	//CT=cos theta, ST=sin theta, etc

	Silent 1; PauseUpdate
	SigmaL=-40.0
	SigmaH=+40.0
	dTheta=Pi/180
	Make/O/N=(DataPoints) /D $BaseName
	SetScale /I x, SigmaL, SigmaH, $BaseName
	$BaseName=0
	DS=80.0/DataPoints
	//The Broading is2*Broad^2 from ernst, Bodenhausen, Wokaun pg 180
	//TheHWHH equals 1.17*linebraodening
	Theta=0
	do
		CT=cos(Theta*pi/180)
		ST=sin(Theta*pi/180)

			SigmaObs=(SigmaPerp*CT*CT+SigmaPara*ST*ST)
			$BaseName+=exp(-(x-SigmaObs)*(x-SigmaObs)/(2*Broad^2))
		Theta+=1

	while(Theta<=90)
	WaveStats /Q $BaseName
	AR=Sum($BaseName)*DS
	$BaseName=($BaseName)/AR
	//$BaseName=$BaseName/V_max
End
```

A1.3 Macro to simulate the spectrum of a toroidal pore

```
# MSTP UL version

// Simulates a Toroidal Pore response in the parallel orientation (toroidal pore axis parallel to the magnetic field, bilayer normal parallel to the magnetic field)
// SigmaPara and SigmaPerp are the parallel and perpendicular edges (near 30 and -15 ppm, respectively) of the fluid lamellar powder pattern.
// PoreRad is the radius of the pore to be simulated - the distance from the central symmetry axis of the pore to the lipids.
// Llength is length of the lipid, or the monolayer thickness of the bilayer in which the pore is formed.
Macro SimToroidPara(BaseName,SigmaPara, SigmaPerp, PoreRad, Llength, Broad, DataPoints)
	String BaseName
```

```
	Variable DataPoints, SigmaPara, SigmaPerp, PoreRad, Broad, Theta, Phi, SigmaL, SigmaH
	Variable Llength, weight
	Prompt SigmaPara, "Sigma Paralle in ppm:"
	Prompt SigmaPerp, "Sigma Perpendicular in ppm:"
	Prompt PoreRad, "Pore radius in angstroms:"
	Prompt Llength, "Lipid length in angstroms:"
	Prompt Broad, "Broadening in ppm:"

	Variable SigmaObs, CT, ST, SP, CP, AR, DS, weigth  //CT=cos theta, ST=sin theta, etc
	Variable PhiInc=1, ThetaInc=1

	Silent 1; PauseUpdate
	Make/O/N=(DataPoints) /D $BaseName
	SetScale /I x, -40, 40, $BaseName
	$BaseName=0
	// DS=(SigmaH-SigmaL)/DataPoints

	Theta=0
	do
		CT=cos(Theta*pi/180)
		ST=sin(Theta*pi/180)
		SigmaObs=(SigmaPerp*ST*ST+SigmaPara*CT*CT)
		weight=Llength*(Llength+PoreRad-(Llength*ST))
		$BaseName+=exp(-(x-SigmaObs)*(x-SigmaObs)/(2*Broad^2))*weight
		Theta+=ThetaInc
		print Theta
	while(Theta<=180)
	WaveStats /Q $BaseName
	//AR=Sum($BaseName)*DS
	//$BaseName=($BaseName)/AR
	$BaseName=$BaseName/V_max
End
```

List of Abbreviations

Å	Angstrom (one Å = 0.1 nm)
1D	One-dimensional
2D	Two-dimensional
AA	amino acid
ATP	Adenosine triphosphate
Boc	*tert*-butoxycarbonyl
CD	Circular Dichroism
CSA	Chemical Shift Anisotropy
CP	Cross Polarization
Da	Dalton
DIPEA	N,N-diisopropylethylamine
DMSO	Dimethyl sulfoxide
DOPS	1,2-dioleoyl-sn-glycero-3-[phospho-L-serine]
DOPE	1,2-dioleoyl-sn-glycero-3-phosphoethanolamine
DTT	dithiothreitol
EDTA	ethylenediaminetetraacetic acid
Fmoc	9-fluorenylmethoxycarbonyl
HA	Hemagglutinin
HATU	O-(7-Azabenzotriazol-1-yl)-N,N,N',N'-tetramethyluronium hexafluorophosphate
HBTU	[2-(1 H-benzotriazol-1-yl)-1,1,3,3- etramethyluronium hexafuorophosphate]
HIV	Human Immunodeficiency Virus
IR	Infra Red
MALDI-TOF MS	Matrix Assisted Laser Desorption Ionization Time-of-flight Mass Spectrometry
MAS	Magic Angle Spinning
NBD-PE	N-(7-nitro-2,1,3-benzoxadiazol-4-yl) hexadecyl phosphatidyl-ethanolamine
NMP	N-methylpyrrolidinone
NMR	Nuclear Magnetic Resonance
NOESY	Nuclear Overhauser Enhancement Spectroscopy
NT	Neurotransmitter

PDSD	Proton Driven Spin Diffusion
POPC	1-palmitoyl-2-oleoyl-sn-glycero-3-phosphocholine
PyBOP	Benzotriazol-1-yloxytris(pyrrolidino) phosphonium hexafluoro-phosphate
r. f.	Radio Frequency
Rab	Ras in the Brain
Rh-PE	N-(lissamine rhodamin B sulfonyl) hexadecyl phosphatidyl-ethanolamine
RP-HPLC	Reversed Phase-High Performance Liquid Chromatography
SM-proteins	Sec1/Munc-18 related proteins
SNARE	Soluble NSF (N-ethylmaleimide-sensitive factor) Attachment protein Receptor
SSNMR	Solid State Nuclear Magnetic Resonance
SPPS	Solid Phase Peptide Synthesis
TFA	Tri-fluro Acetic Acid
TFE	Trifluro Ethanol
TIS	Triisopropyl Silane
TMD	Transmembrane Domain
TMS	Transmembrane Segment.
UV-vis	Ultraviolet Visible
VSV-G proteins	Vesicular Stomatitis Virus - Glycoprotein proteins

Publications

1. S P Gejji, P R Agrawal, N R Dhumal *"Ab initio structure and vibrational frequencies of lithium aromatic sulfonyl imide salts*" **Theoretical Chemistry Accounts** 107: 351–356 (2002).

2. M. W. Hofmann, K. Weise, J. Ollesch, P. Agrawal, H. Stalz, W. Stelzer, F. Hulsbergen, H. de Groot, K. Gerwert, J. Reed and D. Langosch *"De novo design of conformationally flexible transmembrane peptides driving membrane fusion*" **Proceedings of the National Academy of Sciences USA** 101: 14776-14781 (2004).

3. Prashant R. Agrawal, Mathias W. Hofmann, Nico J. Meeuwenoord, Dmitri V. Filippov, Holger Stalz, Frans Hulsbergen, Dieter Langosch, Hermen S. Overkleeft, Huub De Groot *"Solid phase synthesis and purification of a set of uniformly ^{13}C, ^{15}N labeled de novo designed membrane fusogenic peptides."* **Journal of Peptide Science** 13, 75-80, (2007).

4. Prashant Agrawal, Suzanne Kiihne, Johan Hollander, Frans Hulsbergen, Mathias Hofmann, Dieter Langosch and Huub de Groot *"Solid state NMR investigation of the interaction between biomimetic lipid bilayers and a de novo designed fusogenic peptide.*" **ChemBioChem** (in press).

5. P. R. Agrawal et. al. *"Contrasting biomimetic lipids rearrangements induced by low-complexity peptides involved in membrane fusion: extended cylindrical curvature regions versus toroidal pore signals.*" Manuscript is submitted for publication.

6. P. R. Agrawal et. al. *"^{13}C and ^{15}N NMR of uniformly labeled fusogenic peptides incorporated in a biomimetic membrane: Additional support for the peripheral intercalation model"* Manuscript in preparation.

Curriculum vitae

After finishing my education from Nagpur, I joined the Sir Parshurambhau College to enroll into the bachelor's program in Mathematics, Physics and Chemistry, and graduated with specialization in Chemistry in June 1999. The same year I joined the Department of Chemistry at the University of Pune to follow the master's program in Organic Chemistry. During this period I also worked on a 6 months research project entitled 'synthesis of β–lactum', under the guidance of Prof. Dr. B. M. Bhawal, at National Chemical Laboratory. In July 2001, I received the master's degree in Organic Chemistry. I have successfully undertaken the CSIR-UGC and GATE examinations, which are essential to become a faculty member in Indian universities. With the intention to do research I joined in the group of Prof. Dr. S. P. Gejji at the Department of Chemistry, Pune University. There I permormed QSAR studies of anti-HIV drug molecules with bioinformatics and theoretical modeling.

In August 2002, I started my PhD research at Leiden University in the workgroup of SSNMR under the supervision of Dr. Frans B. Hulsbergen and Prof. Dr. Huub J.M. de Groot. I attended the 'Science based business course: Orientation on technopreneureship and business planning', at Leiden University. The business plan written by my team "Bitter Better" was awarded in the National New Venture competition on feasibility studies, in March 2006. The research described in this thesis was presented at various meetings and conferences. This includes "NMR in Molecular Biology" (France, 2003), EENC/AMPERE-2004 (France), 21st International conference on magnetic resonance in biological systems (ICMBRS) (India, 2005), the 4th Alpine conference on solid state NMR (France, 2005), the 47P^{thP} Experimental NMR Conf., (Asilomar, USA, 2006). I won the Biotechnology-Workshop Lecture Award at Dutch Polymer Days (2005) and I orally presented my work at the plenary session at the Dutch Polymer Days (2006) in Lunteren, The Netherlands

Acknowledgement

At the end of my PhD, when I look back, I have a very good feeling. Every important work needs a beginning but to accomplish it one needs support and I would like to take this opportunity to acknowledge all those people who have contributed to the realization of my dream. Since my first day in the Netherlands Janette shared her valuable experience through many discussions and suggestions. The social and scientific interactions with past and present colleagues shaped my outlook. I am glad that I had many chances to interact, especially with Ania, Arjan, Arjan, Eugenio, Francesco, Helen, Ineke, Johan, Karthick, Michiel, Piotr, Rainier, Richard, Rob, Sacha, Samira, Thierry, Wouter and Yajie. Thank you all for the support and I wish you all the best. Few things would remember always such as, Adriaan's antique, Arjan's badminton and cooking, Arjan's big bicycle, Esha's willingness to help, Ido's cowboy Dutch politics, Niels' Disney world, Reinier's lopen, Richard's beer testing, Rob's guitar, Shipra's coffee, Swapna's sport passion. Sharing the same 'think cell' with Sylvia and her Dutch way of working and forbidden things will always be the special memory.

I am indebted to Liesbeth for her help and her efficient solving my administrative issues. I will always remember Johan Hollander, Fons Lefeber and Kees Erkelens for their technical assistance with solid state NMR and other social outings. Trudie, Paul, Arjan, Henny and John (TOA) I am grateful for your help and support.

I appreciate Geerten's help for translating my thesis summary into Dutch and his different way of working created a special memory. I had a great time with Anna, all those discussions about food, lifestyle and sports have been joyful and I really enjoyed them.

Many people have been involved in the work that I have presented in this thesis. Dr. Suzanne's valuable guidance and encouragement with sample preparation as well as NMR was extremely helpful. The discussions with her and Dr. Jan Raap were useful in visualizing overall picture of the lipids behavior. The Leiden university scientific environment allowed me to collaborate with various groups both within Leiden University and outside. Working with the biosynthesis organic chemistry group at leiden university, was very enjoyable. I learned vast amounts from Nico and Dr. Dima Filippov about the synthesis and purification of proteins and peptides and other interesting scientific topics. I had the opportunity to work on the study of membrane fusion started by Prof Dr. Dieter Langosch. I am grateful for the support of my collaborators Mathias, Jullian, Katrin,

Holger, Prof. Dr. Jennifer Reed and Prof. Dr. Klaus Gerwert in helping me to understand all the aspects of the project.

Karishma, Meenal and Nilesh you have been great friends to me, your caring and loving affection made me forget all my homesickness. Thanks for cheering me up and helping me in all the circumstances. Monica and Amol you two are great a couple and your friendship gave Bhawana and me great dreams. Andrea and Michael, you two became good friends and the time I spent with you I will always remember. Thank you all for your support and helping me out with several things during my stay in Holland. I owe thanks to all my friends in India and abroad, and all my family for being there for me. A very special thanks to Paul and Joke, who provided me a pleasant and homely environment during my starting year stay with them.

My coming to the Netherlands and taking the first step towards building a scientific career has only been possible due to the constant support from my family. I thank my sister Neeta, and brother in law Sanjay for all the love and support they have shown to me over the years. My brother Dr. Nilesh and sister in law Dr. Prachi gave their constant support and encouragement, which helped me to overcome the difficult times. Most of all, special thanks should go to Bhawana, my wife, for her unfaltering love and support over the years for understanding day-to-day ups and downs of research. Her enthusiasm was infectious and was particularly helpful when things were not quite going the way I preferred. The biggest thanks, which have been saved till last, have to go to my mom and dad whose love, support and belief in me over the years made who I am. A constant encouragement from my parents made my days bright and full of spirit. Because of your support, today I find myself finishing a PhD. Thank you mom and dad.

Leiden 1st March 2007 Prashant Agrawal